



The
University
Of
Sheffield.

Access to Electronic Thesis

Author: Suriani Shamsudin
Thesis title: The Synthesis and Characterisation of Dendritic Macromolecules for Drug Delivery Application
Qualification: PhD

This electronic thesis is protected by the Copyright, Designs and Patents Act 1988. No reproduction is permitted without consent of the author. It is also protected by the Creative Commons Licence allowing Attributions-Non-commercial-No derivatives.

If this electronic thesis has been edited by the author it will be indicated as such on the title page and in the text.

The Synthesis and Characterisation of
Dendritic Macromolecules for
Drug Delivery Application



Suriani Shamsudin

PhD Thesis

2012

The Synthesis and Characterisation of
Dendritic Macromolecules for
Drug Delivery Application

Suriani Shamsudin

A thesis submitted for the degree of
Doctor of Philosophy

Department of Chemistry,
The University of Sheffield
Sheffield S3 7HF
England

April 2012

Acknowledgement

I would like to acknowledge and extend my heartfelt gratitude to Dr Lance Twyman, who have made the completion of this thesis possible. His understanding, patience and guidance was fully appreciated throughout the time it took me to complete my research. Special thanks also goes to Melanie Hannah, Pete, Nick, Denise, Sue and Louise in managing all the orders, chemicals and equipments in the department. I would also like to thank all Twymans group and members of F floor who have gave me comfortable environment throughout these three years.

Many thanks to Mr Luo Lei for the in vitro test and discussions made for my further knowledge. Special thanks also must go to Mrs Azreena Mastor and Miss Ashley Gavin for being as a team member in synthesising the polymer.

My deepest gratitude to my husband and three children who have give me the opportunity to finish my work. Their deepest love, assistance and courage have made this thesis comes true. To my mother and family, thank you for all your duaas.

Lastly, I offer my regards and blessings to all of those who supported me in any respect during the completion of the thesis.

Abbreviations

Standard Abbreviations

^{13}C -NMR	Carbon Nuclear Magnetic Resonance Spectrometry
DMSO	Dimethyl sulfoxide
DCU	Dicyclohexylurea
DMF	Dimethylformamide
DP	Degree of polymerization
DCC	1,3-dicyclohexylcarbodiimide
D_2O	Deuterated Deuterium Oxide
EDA	Ethylenediamine
FA	Folic acid
FR	Folic receptor
FA-NHS	Folic acid ester
Folate-PEG-NH ₂	Folate-poly(ethylene glycol) bis amine
G	Generation
^1H -NMR	Proton Nuclear Magnetic Resonance Spectrometry
GPC	Gel Permeation Chromatography
IR	Infrared Spectroscopy
Mn	Number Average Molecular Weight
Mw	Weight Average Molecular Weight
HPMA	N-(2-hydroxypropyl methacrylamide)
MePEG:PDDLA	Methoxypolyethylene glycol-b-poly(D,L,-lactide)
Gly-Phe-Leu-Gly	Glycine-phenylalanine-leucine-glycine
PGLSA	Poly(glycerol succinic acid)
10 HCPT	10 hydroxycamptotecin
PHPMA	Poly N-(2-hydroxypropyl methacrylamide)
SMA	Styrene-co-maleic anhydride
PCL	Polycaprolactone
NSAID	Non steroidal anti-inflammatory drug
NHS	N-hydroxysuccinimide
NH ₂ -PEG3000-NH ₂	Poly(ethylene glycol) (PEG)3000 bis amine
PD	Polydispersity
PAMAM	Polyamido amine
PG	Polyglycidol
PEG	Poly(ethylene) glycol
PEI	Polyethyleneimine
PG-SA	Polyglycidol succinic anhydride
PG-Folate-PEG	Polyglycidol-folate-poly(ethylene glycol)
PDT	Photodynamic therapy

TCCP.....Tetracarboxyphenyl porphyrin
TRIS.....Tris(hydroxymethyl)aminomethane
UV/VisUltraviolet, Visible Light Spectrophotometry

NMR Abbreviations

s.....	singlet
d.....	doublet
t.....	triplet
q.....	quartet
dd.....	doublet of doublets
m.....	multiplet
m _i	multiplet (where <i>i</i> = multiplicity)
br.....	broad
<i>o</i> -.....	<i>ortho</i>
<i>m</i> -.....	<i>meta</i>
<i>p</i> -.....	<i>para</i>

List of Figures

- Figure 1.1: The architecture of dendrimer
- Figure 1.2: Structure of hyperbranched polymers
- Figure 1.3: Schematic of divergent synthesis
- Figure 1.4: Schematic of convergent synthesis
- Figure 1.5: Step-growth polycondensation
- Figure 1.6: Self-condensing vinyl polymerisation
- Figure 1.7: Ring-opening polymerisation
- Figure 2.1: A Cartoon of dendrimer as a delivery agent
- Figure 2.2: Cartoon of surface modification of hyperbranched polymers with PEG and FA
- Figure 3.1: Polymer architectures : A. Linear polymers, B. Hyperbranched polymers and C. Crosslinked polymers
- Figure 3.2: Ringsdorf's model of a polymer-drug conjugate
- Figure 3.3: Poly(N-(2 hydroxypropyl methacrylamide)) copolymer containing doxorubin PK1 (FCE28068)
- Figure 3.4: Three major types of micelle : (a) common block copolymer micelle, (b) drug-conjugated block copolymer micelle and (c) block ionomer complex micelle
- Figure 3.5: Block copolymer of PEG conjugated with Doxorubin drug via enzymatically degradable Gly-Phe-Leu-Gly spacer
- Figure 3.6: Encapsulated G4-PGLSA-COONa dendrimers with 10 Hydroxycamptothecin
- Figure 3.7: PAMAM-G2.5-COOH conjugated with methotrexate drug
- Figure 3.8: Conjugation of PEG to PEI: (a) a few longer PEG chain and (b) numerous shorter PEG chain
- Figure 3.9: G4 PAMAM dendrimer with PEG as the end group functionalisation
- Figure 3.10: Hyperbranched polyglycerol with a *p*-nitrophenol core
- Figure 3.11: *p*-nitrophenol
- Figure 3.12: The original ¹H NMR representing the core of the polymer
- Figure 3.13: The freshly doped *p*-nitrophenol to the polymer
- Figure 3.14: Structure of (9) naphthalene and (10) ibuprofen, (11) tetracarboxylphenyl porphyrin and (12) anti-prion drug
- Figure 3.15: UV-Vis spectra of naphthalene encapsulated with hyperbranched polymers
- Figure 3.16: Concentration of encapsulated naphthalene with a molecular weight of 4000 Da and 50000 Da
- Figure 3.17: Encapsulated naphthalene concentration with different molecular weights of hyperbranched polymer at polymer concentration of 2.00 x 10⁻⁴ M
- Figure 3.18: Encapsulated naphthalene concentration with different molecular

weights of hyperbranched polymer at polymer concentration of 4.00×10^{-4} M

- Figure 3.19: Aggregation of the hyperbranched polymers
- Figure 3.20: Increasing M_n and concentration of hyperbranched polymers with increasing concentration of encapsulated naphthalene
- Figure 3.21: A representation of polyglycerol with naphthalene within the voids
- Figure 3.22: Increased encapsulated ibuprofen concentration with increased molecular weights and concentrations of hyperbranched polymers
- Figure 3.23: Encapsulated ibuprofen concentration with different molecular weights of hyperbranched polymer at hyperbranched polymer concentration of 2.00×10^{-4} M
- Figure 3.24: Encapsulated ibuprofen concentration with different molecular weights of hyperbranched polymer at hyperbranched polymer concentration of 4.00×10^{-4} M
- Figure 3.25: Increased concentration of encapsulated ibuprofen after encapsulation with different concentrations and molecular weights of hyperbranched polymer
- Figure 3.26: Ibuprofen filled into a hyperbranched polymer
- Figure 3.27: ^1H NMR spectrum of mixing of ibuprofen with hyperbranched polymer in D_2O
- Figure 3.28: ^1H NMR spectrum of complexation of ibuprofen with hyperbranched polymers in D_2O
- Figure 3.29: Photodynamic therapy mechanism
- Figure 3.30: Schematic representation of the EPR effect
- Figure 3.31: Encapsulated TCPP concentration for molecular weight of 4000 Da and 50000 Da
- Figure 3.32: Encapsulated TCPP concentration of 2.00×10^{-4} M with different molecular weights of hyperbranched polymer
- Figure 3.33: Encapsulated TCPP concentration of 4.00×10^{-4} M with different molecular weight of hyperbranched polymer
- Figure 3.34: Increased concentration of encapsulated TCPP after encapsulation with different concentrations and molecular weights of hyperbranched polymer
- Figure 3.35: Tetracarboxyphenyl porphyrin filled in hyperbranched polymers
- Figure 3.36: Anti-prion drug used in encapsulation study
- Figure 3.37: UV spectra of anti-prion drug in methanol
- Figure 3.38: UV spectra of a hyperbranched polymer in water, an antiprion drug in methanol and encapsulation of the drug with a hyperbranched polymer
- Figure 3.39: UV spectra of a hyperbranched polymer in water, an antiprion drug in methanol and encapsulation of the drug with a hyperbranched polymer
- Figure 3.40: The EC_{50} of the drug encapsulated with hyperbranched polymers
- Figure 4.1: Anticancer drugs: Camptothecin (**12**), Cisplatin (**13**) and doxorubin

(14)

- Figure 4.2: Cartoon of dendrimers with targeting entity
- Figure 4.3: Schematic functionalisation of folic acid via a spacer with a polymer
- Figure 4.4: ^1H NMR spectrum of PG-SA in D_2O
- Figure 4.5: ^1H NMR spectrum of FA-NHS in DMSO
- Figure 4.6: ^1H NMR spectrum of PEG-FA in DMSO
- Figure 4.7: ^1H NMR spectrum of PG-PEG-FA in D_2O
- Figure 5.1: Effect of generation size in solubilisation of drugs
- Figure 5.2: Effect of polymer architecture in solubilising paclitaxel, where (a) is poly(OEGMA), (b) is five-arm star-shaped polyOEGMA and (c) are G3, G4 and G5 polyglycerol dendrimers
- Figure 5.3: PAMAM dendrimer
- Figure 5.4: The 1,4 Michael addition
- Figure 5.5: The amidation reaction
- Figure 5.6: Synthesis of PAMAM dendrimer G0.5 to G2.0 showing each Michael addition (red) and amidation step (blue)
- Figure 5.7: Synthesis of PAMAM dendrimer from G2.0 to G2.5
- Figure 5.8: ^1H NMR spectrum for G0.5 PAMAM dendrimer in MeOH
- Figure 5.9: ^1H NMR spectrum of a generation 2.5 PAMAM dendrimer
- Figure 5.10: Incomplete removal of EDA and their by-products
- Figure 5.11: Synthesis of a generation 2.5 PAMAM dendrimer into a hydroxyl terminated PAMAM dendrimer
- Figure 5.12: Molecules used in complex forming
- Figure 5.13: Increased ibuprofen solubility with increased concentration of water soluble dendrimer
- Figure 5.14: Expected model of encapsulated ibuprofen within dendrimers
- Figure 5.15: Increased solubility of TCPP with increased concentration of water soluble dendrimers
- Figure 5.16: Encapsulation of ibuprofen using water soluble hyperbranched polymers and dendrimers
- Figure 5.17: Encapsulation of TCPP using both polymers

List of Scheme

- Scheme 3.1: Synthesis of hyperbranched polymers
- Scheme 3.2: Deprotonation and ring opening mechanism of the monomer
- Scheme 3.3: Propagation of alkoxide to form hyperbranched polymers
- Scheme 3.4: Deprotonation of glycidol to form a glycidol initiator
- Scheme 3.5: The presence of water may affect the final product of polymer
- Scheme 3.6: Synthesis of tetracarboxyphenyl porphyrin
- Scheme 4.1: Synthesis of FA-NHS
- Scheme 4.2: Synthesis of Folate-PEG-NH₂
- Scheme 4.3: Synthesis of PG-SA
- Scheme 4.4: Synthesis of PG-Folate-PEG

List of Tables

Table 1.1:	Different molecular weights of polyglycidol
Table 3.2:	Physical properties of model drugs and drugs used in the encapsulation studies
Table 3.3:	Solubility of naphthalene in TRIS buffer solution with different concentrations and molecular weights of hyperbranched polymers
Table 3.4:	Amount of naphthalene encapsulated* in hyperbranched polymers
Table 3.5:	Naphthalene loading per mole of hyperbranched polymers with concentration of 1.00×10^{-4} M
Table 3.6:	Solubility of ibuprofen in TRIS buffer solution with different concentrations and molecular weights of hyperbranched polymers
Table 3.7:	Amount ibuprofen encapsulated* in the hyperbranched polymers
Table 3.8:	Ibuprofen loading per mole of hyperbranched polymers with a concentration 1.00×10^{-4} M
Table 3.9:	Solubility of tetracarboxyphenyl porphyrin in TRIS buffer solution with different concentrations and molecular weights of hyperbranched polymers
Table 3.10:	Amount of TCPP encapsulated* inside hyperbranched polymer
Table 3.11:	Tetracarboxyphenyl porphyrin loading per mole of hyperbranched polymers with concentration of 1.00×10^{-4} M
Table 5.1:	The molecular weight for G0.5 to G2.5 PAMAM dendrimers
Table 5.2:	Ibuprofen concentration in solution and encapsulated ibuprofen with dendrimer
Table 5.3:	TCPP concentration in solution and encapsulated TCPP in dendrimer

Table of contents

Chapter 1 - Introduction	1
1.1 Overview	1
1.2 Dendritic Polymers	1
1.3 Synthesis of Dendritic Polymers	3
1.3.1 Synthesis of Dendrimers	3
1.3.1.1 Divergent Approach	3
1.3.1.2 Convergent Approach	4
1.3.2 Synthesis of Hyperbranched Polymers	4
1.3.2.1 Step-Growth Polycondensation	4
1.3.2.2 Self-Condensing Vinyl Polymerisation	5
1.3.2.3 Ring-Opening Polymerisation	6
Chapter 2 - General Aims	7
Chapter 3 - Polymers and Drug Delivery Systems	11
3.1 Overview	11
3.2 Polymer Architecture and Drug Delivery	12
3.2.1 Linear Polymer for Drug Delivery	14
3.2.2 Block Copolymer and Drug Delivery	16
3.2.3 Dendritic Polymers for Drug Delivery	18
3.2.3.1 Drug Encapsulated Dendritic Polymer	18
3.2.3.2 Drug Conjugated Dendritic Polymer	19
3.3 Structure And Properties Relationship	20
3.3.1 Biocompatibility	20
3.3.2 Biodegradability	23
3.3.3 Biodistribution	24
3.4 Results and Discussion	25
3.4.1 Water Soluble Hyperbranched Polymers	25
3.4.2 Synthesis of Polyglycerol Hyperbranched Polymers	27
3.4.3 Selection of Model Drug for Encapsulation Study	34
3.4.4 Encapsulation Studies	36

3.4.4.1 General Method for Complex Formation	37
3.4.5 Encapsulation of Naphthalene with Hyperbranched Polymers	38
3.4.6 Encapsulation of Ibuprofen with Hyperbranched Polymers	47
3.4.7 Photodynamic Therapy	56
3.4.7.1 Mechanism of Photodynamic Therapy	56
3.4.7.2 Synthesis of Tetracarboxyphenyl Porphyrin (TCPP)	58
3.4.7.3 Encapsulation of TCPP with Hyperbranched Polymers	59
3.4.8 : Encapsulation of Hyperbranched Polymers with an Antiprion Drug for Prion Therapy Application	66
3.4.8.1 Prion Disease	66
3.4.8.2 Anti-prion Drug	66
3.4.8.3 Complex Formation of Antiprion Drug with Hyperbranched Polymers	67
3.4.8.4 Cytotoxicity Studies	69
 Chapter 4 - Synthesis and Characterization of Hyperbranched Polyglycidol Conjugated with Poly(ethylene) glycol and Folic acid (PG-PEG-Folate)	 72
4.1 Overview and aims	72
4.2 Results and Discussion	75
4.2.1 Synthesis and Characterization of Polyglycidol-succinic anhydride (PG-SA)	78
4.2.2 Synthesis of Folic Acid Ester (FA-NHS)	80
4.2.3 Synthesis of Folate-Polyethylene Glycol bis amine (Folate-PEG-NH ₂)	81
4.2.4 Synthesis of Polyglycidol-Folate-Poly(ethylene glycol) (PG- Folate-PEG)	82
 Chapter 5 - Comparison Between Hyperbranched Polymers and Hydroxyl Terminated PAMAM Dendrimers : Encapsulation Using TCPP and Ibuprofen	 84
5.1 Overview	84
5.2 Effect of Generation Size	85
5.3 Effect of pH	86

5.4 Effect of Core, Polymer Architecture and Surface Functionalities	86
5.5 Dendrimer Toxicity	88
5.6 Aims	90
5.7 Results and Discussion	92
5.7.1 Synthesis of PAMAM Dendrimer	92
5.7.2 Synthesis of a G0.5 to G2.5 PAMAM Dendrimer	93
5.7.3 Purification of PAMAM Dendrimer	100
5.7.4 Synthesis of PAMAM Dendrimer with 48 Hydroxyl Groups	102
5.7.5 Encapsulation of Hydrophobic Molecules with Water Soluble PAMAM Dendrimer	104
5.7.5.1. Encapsulation of Ibuprofen with Water Soluble PAMAM Dendrimer	105
5.7.5.2 Encapsulation of TCPP with Water Soluble PAMAM Dendrimer	107
5.7.6 Comparison between PAMAM Dendrimer and Hyperbranched Polymer on Solubility Enhancement of Ibuprofen and TCPP	110
Chapter 6 - Conclusion	112
Chapter 7 - Experimental	115
7.1 General Description of Chemicals and Instrumentation	115
7.2 Synthesis of Hyperbranched Polymers	116
7.2.1 General Procedures for Encapsulation Studies	118
7.2.2 Cytotoxicity Studies	119
7.3 Functionalisation of Hyperbranched Polymer with Folic Acid and PEG spacer	120
7.4 Comparison between PAMAM Dendrimer and Hyperbranched Polymer	121
Chapter 8 - References	124

Abstract

Today, drugs used in treating disease are almost all hydrophobic, which makes them unattractive for applying to patients. To overcome this problem, an amphiphilic macromolecule was designed which can deliver drugs to the specific targeted area. Therefore, this study focuses on the synthesis of water soluble hyperbranched polymers and their application in drug delivery systems.

The first part of the thesis describes the synthesis of water soluble hyperbranched polymers by the anionic-polymerisation technique, with *p*-nitrophenol as the core and glycidol as the monomer. The core is important to control the molecular weight of the hyperbranched polymer. We then produced five different molecular weights by varying the core to monomer ratio, which produced hyperbranched polymers with molecular weights of 4000 Da, 8000 Da, 12500 Da, 27000 Da and 50000 Da, and four different concentrations of each molecular weight, 1.00×10^{-4} M, 2.00×10^{-4} M, 4.00×10^{-4} M and 6.00×10^{-4} M. To investigate the performance of the hyperbranched polymers, four different hydrophobic molecules were studied. The molecules were naphthalene, ibuprofen, tetracarboxyphenyl porphyrin (TCPP) and anti-prion drug. Encapsulation studies showed the concentration of each molecule increased with an increase in molecular weight and concentration of the hyperbranched polymer

The functionalisation of folic acid on the surface of the hyperbranched polymer would enhance the effectiveness of the polymer as a drug delivery agent for targeting in cancer treatment. The above macromolecule was synthesised by conjugation with folic acid through poly (ethylene glycol) as spacer.

The final chapter of this work describes the encapsulation of two hydrophobic molecules, ibuprofen and tetracarboxyphenyl porphyrin with water soluble PAMAM dendrimers. PAMAM dendrimers from G0.5 to G2.5 were synthesised.

The results showed that more drug solubilised, the concentration of both molecules increased with an increase in dendrimer concentration. Then a comparison was made between encapsulation with water soluble hyperbranched polymers and water soluble PAMAM dendrimers. Similar molecular weight was used for both polymers of 4000 Da. For both polymers, the result demonstrated that the concentration of drug rose at 2.00×10^{-4} M and plateaued at a polymer concentration of 6.00×10^{-4} M. It was suggested the above trend was due to the aggregation of polymer.

The above studies make a valuable contribution to the development of good drug delivery systems.

Chapter 1: Introduction

1.1 Overview

Polymers are a large class of materials consisting of many small molecules that can be linked together to form long chains, thus they are known as macromolecules.¹ These macromolecules can be classified into three types: 1) linear polymers, where the molecules form long chains without branches or cross-linked structures, 2) branched polymers which consist of branched molecules, covalently attached to the main chain and 3) cross-linked polymers, which have monomers of one chain covalently bonded with monomers of other chain.¹

Over the past few decades, various attempts have been made to design new macromolecules, such as dendrimers and hyperbranched polymers. These polymers became attractive to the pharmaceutical industry due to their various applications in drug delivery systems. The above polymer is very useful because it can be synthesised in different molecular weight, polydispersity, charge and hydrophilic-hydrophobic character of the polymer which can influence drug biodistribution, clearance, biological activity and toxicity.²

1.2 Dendritic polymers

Dendritic polymers which refers to dendrimers and hyperbranched polymers, are highly branched macromolecules with a three dimensional dendritic architecture.³⁻⁴ Dendrimers are the stepwise organic synthesis approach to branch-on-branch structures. Ideally, dendrimers are spherical, defect-free and perfectly monodisperse compounds. Dendrimer synthesis, however, is usually based on tedious multistep protocols. Dendrimers are built from a starting atom, such as nitrogen, to which carbon and other elements are added by a repeating series of chemical reactions that produce a spherical branching structure. As the process repeats, successive layers are added, and the sphere can be expanded to the required size. Dendrimers consists of three components: the core

or focal point, interior layers/repetitive branch units or generations (G) which formed the dendritic units and terminal functionality at the exterior of the architecture (**Figure 1.1**).⁵

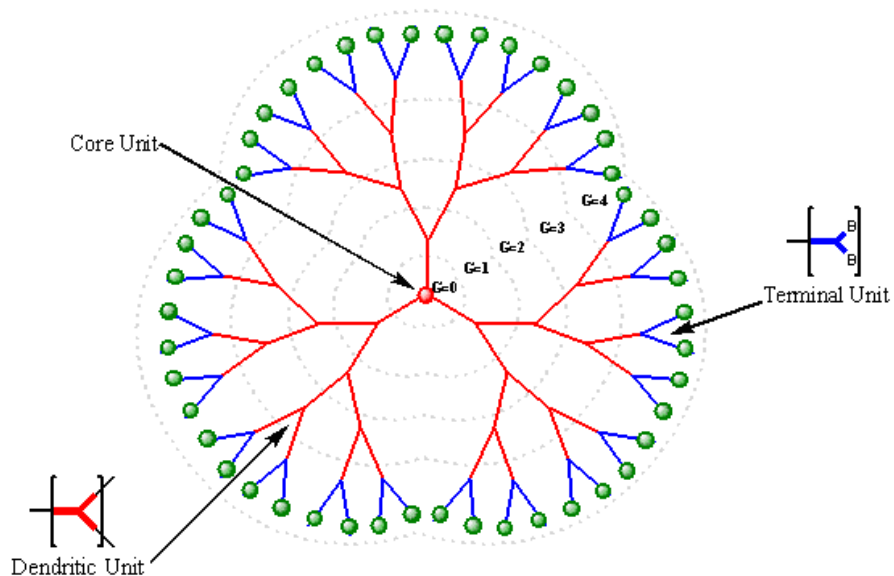


Figure 1.1: The architecture of dendrimer⁵

A second class of branched polymers is the hyperbranched polymers. In contrast to dendrimers, hyperbranched polymers are neither defect-free nor perfectly monodispersed. These polymers consist of the core, fully reacted (dendritic) and completely unreacted (linear) units and terminal units (**Figure 1.2**). Hyperbranched polymers, however, are typically obtained in a one-pot reaction and as a result can be easily prepared in large quantities.⁶⁻¹¹

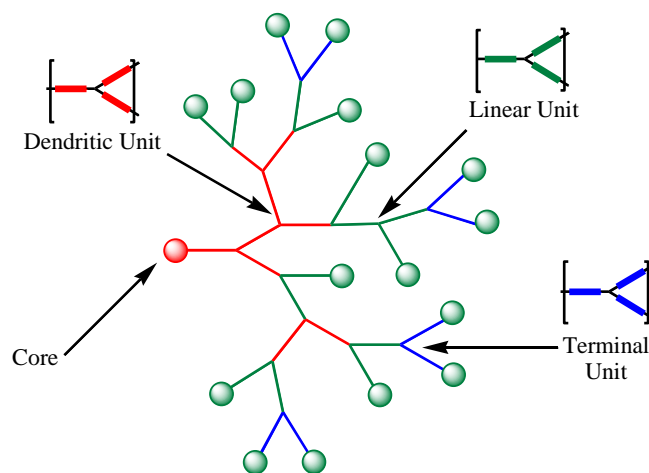


Figure 1.2: Structure of hyperbranched polymers⁵

1.3. Synthesis of dendritic polymers

1.3.1 Synthesis of dendrimers

Dendrimers are a relatively new class of macromolecules that have a three dimensional structure with a series of layered branches regularly extending from a central core. Dendrimers usually consist of three main components : a multifunctional core, branch units and surface functional groups. Two methods that have been developed to synthesise dendrimers: the divergent approaches initiated by Vögtle¹² and further applied by Newkome¹³ and Tomalia¹⁴ and the convergent method introduced by Hawker and Frachet¹⁵ and also by Miller and Neenan.¹⁶

1.3.1.1 Divergent approach

The divergent method (**Figure 1.3**) involves a stepwise layer by layer approach, which the dendrimer grows from a polyfunction core and builds up the molecule towards the periphery by the stepwise addition of successive layers of building blocks. Each of these layers is called a ‘generation’. The first generation of a dendrimer is formed by attaching the branched unit to a focal core. For the second and subsequent generations, the surface

functional group must react with the successive layers of building blocks. This reaction is repeated until the desired number of generations is obtained.¹⁷

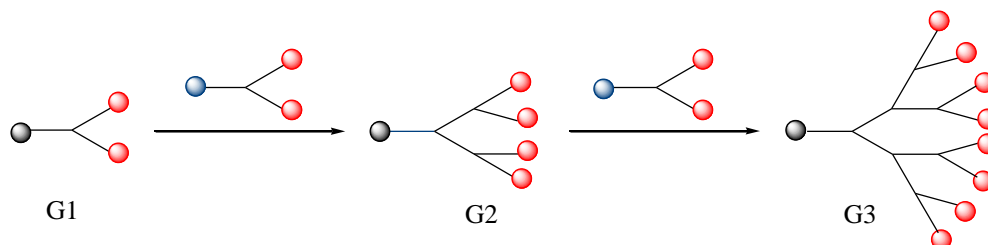


Figure 1.3: Schematic of divergent synthesis

1.3.1.2 Convergent approach

The second method, shown in **Figure 1.4** an alternative method of synthesising dendrimers. This alternative method is used to produce a more controllable dendritic architecture. The formation of the dendrimer begins at the surface functionalities of a dendrimer molecule and proceeds inwards by a step addition of branching monomers, followed by the final attachment of each branched dendritic subunit to the core.¹⁸⁻¹⁹

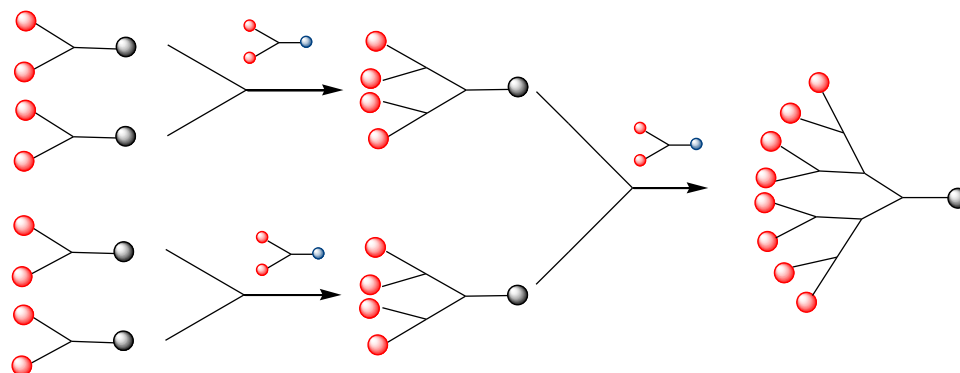


Figure 1.4: Schematic of convergent synthesis

1.3.2 Synthesis of hyperbranched polymers

Hyperbranched polymers, gained great attention after Florys in 1952 highlighted the polymerisation of AB_n monomers (where $n \geq 2$) to generate highly branched soluble polymers. Hyperbranched polymers with similar properties can be easily synthesised

via one-step reactions and therefore represent economically promising products for large-scale industrial applications. Unlike dendrimers, these hyperbranched polymers are polydisperse systems both in terms of their molecular weight characteristics and their branching factors.²⁰⁻²¹ The general synthesis of hyperbranched polymers can be divided into three specific categories: (i) step-growth polycondensation of AB_n and $A_2 + B_3$ monomers, (ii) self-condensing vinyl polymerisation of AB^* monomers and (iii) multi branching ring-opening polymerisation of latent AB_n monomers.²²

1.3.2.1 Step-growth polycondensation

Step-growth polycondensation of AB_n (where $n \geq 2$) is extensively used to synthesise hyperbranched polymers (**Figure 1.5**). The branching unit of these hyperbranched polymers is produced when each function of B from one molecule reacts with a function of A from another molecule. AB_2 type monomers are used because of their ease of preparation. A vast range of hyperbranched polymers are produced using these techniques, including polyphenylenes, polyesters, polyethers and polyamides.^{20,23} Other types of monomers such as AB_3 , AB_4 and AB_6 are also used to synthesise polyesters and polysiloxanes.

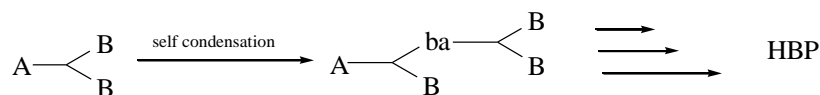


Figure 1.5: Step-growth polycondensation

1.3.2.2 Self-condensing vinyl polymerisation

The second technique uses self-condensing vinyl polymerisation and was introduced by Frechet in 1995 which involves the use of one vinyl group and one initiating moiety (AB^* monomers) to produce hyperbranched polymers (**Figure 1.6**). The activated species can be radical, a cation or a carbanion. In this process, it is preferable to use living or controlled polymerisation (SCVP) to avoid cross-linking reactions and gelation caused by dimerisation or chain transfer reactions.

Hyperbranched polystyrenes and poly (methacrylates) have been successfully synthesised by using this method.²⁰

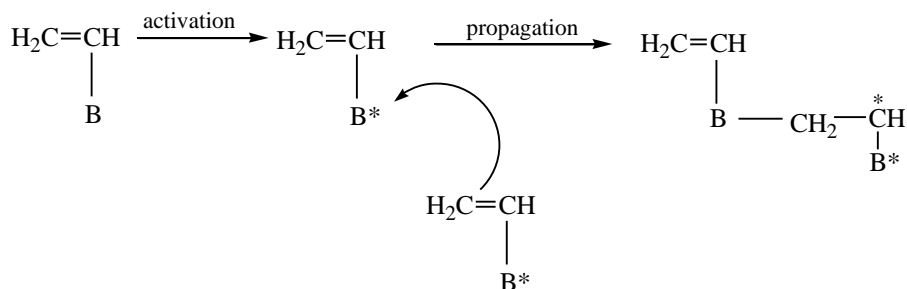


Figure 1.6: Self-condensing vinyl polymerisation

1.3.2.3 Ring-opening polymerisation

The last strategy used to produce hyperbranched polymers is the ring-opening polymerisation technique which was introduced by Suzuki in 1992 (**Figure 1.7**). The terminal function of a polymer acts as a reactive centre, where further cyclic monomers join to form a larger polymer chain through ionic propagation. Each additional monomer step produces another reactive centre. This method is used to produce hyperbranched polymers such as polyamines, polyethers and polyesters.²³⁻²⁵

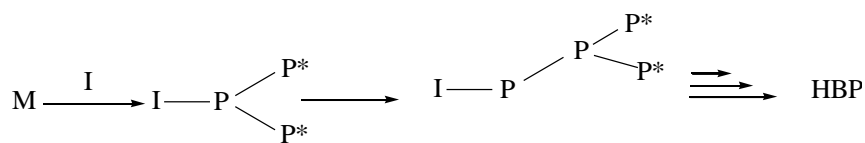


Figure 1.7: Ring-opening polymerisation

Chapter 2.0: Aims and Objectives

One of the major problems faced by the pharmaceutical industry is delivering hydrophobic drugs to a specific targeted area at a sufficient and safe dosage. Most lead drugs are either abandoned or delivered in large quantities to the cell. The uncontrolled behaviour of these drugs is due to the poor solubility of the compounds, which can result in harmful side effects. Many approaches have been envisaged, including using polymeric carriers, such as copolymers and dendritic polymers. Various types of polymer have been designed to meet the characteristics required of as drug delivery agents, including linear and block copolymers. Another class of macromolecules that has gained much attention from researchers are dendrimers. These promising candidates as drug carrier were introduced by Newkome¹³ and Frechet.¹⁵

Dendrimers are well defined controlled structures, they are monodispersed and highly branched macromolecules with a static globular construct. They offer good key characteristic of a delivery agent, such as having a multifunctional terminal surface which can modify the surface chemistry, they are water soluble and have the ability to bind drugs inside their hydrophobic cavity.¹² **Figure 2.1** showed a cartoon of dendrimer as delivery agent, especially for cancer treatment. The drug is either encapsulated inside the cavity of the dendrimer and/or simply conjugated with the functional groups on the surface of the dendrimer. However, synthesising dendrimers is difficult, time consuming and expensive.

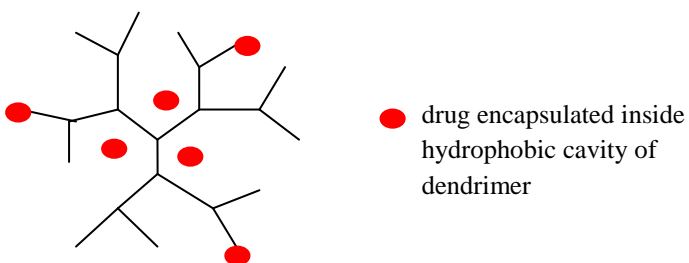


Figure 2.1: A Cartoon of dendrimer as a delivery agent

Another class of macromolecules, called hyperbranched polymers, can be used as drug delivery agents.⁴ Hyperbranched polymers are tree-like structure with a core, a branching unit and a terminal group at the surface. Hyperbranched polymers can be synthesized using existing polymerization methods and present a more cost-effective route for preparing highly branched macromolecules. These polymers are easily prepared using one-step synthesis. The ease of preparation, cost effectiveness and scale up productions makes them attractive alternatives to dendrimers for many applications.

In order to overcome the poor solubility of drugs, we proposed water soluble hyperbranched polymers as the drug delivery agent. These carriers should be water soluble in order to transport drugs in the blood stream to the specific site and be non toxic to the human body. A hyperbranched polymer was designed which consists of a *p*-nitrophenol core, a hydrophobic interior and a hydroxyl group as the surface, prepared by an anionic polymerisation technique with glycidol as the monomer. An OH group at the periphery is important to make the polymers soluble in water. The drug is encapsulated in the hydrophobic environment inside the hyperbranched polymer, thus the drug is safely trapped inside the polymer, while the outside of the polymer is soluble in water.

For dendrimers, the size increases with an increase in generation, while for hyperbranched polymers, the size is increased by varying the core to monomer ratio. In this work, we used different core to monomer ratios to increase the molecular weight of the polymers. Five different ratios, i.e. 1:5, 1:10, 1:25, 1:50 and 1:100, and four different concentrations of each polymer molecular weight, i.e. 1.00×10^{-4} M, 2.00×10^{-4} M, 4.00×10^{-4} M and 6.00×10^{-4} M were explored. An investigation of the encapsulation ability of both different sizes and concentrations of hyperbranched polymers were carried out. These water soluble hyperbranched polymer were explored as a solubilisation enhancer for selected hydrophobic molecules. The molecules used were naphthalene, tetracarboxyphenyl porphyrin, ibuprofen and an anti-prion drug. It was anticipated that the percent loading, which is the concentration of the model drug and drug used in the

encapsulation studies would increase as the concentrations and molecular weights of the hyperbranched polymer increased.

It was postulated that the model drugs and drugs were encapsulated inside the polymers through a hydrophobic effect between the hydrophobic environment and the hydrophobes. The passive release mechanism of the hydrophobes was through diffusion from the carriers.

The modification of hyperbranched polymers with other entities is a promising approach to the development of highly efficient drug carriers. The functionalisation of poly(ethylene) glycol (PEG) as a spacer allows folate to reach and bind to specific receptors of cancer cells. Without PEG spacer, the folate will be too crowded at the surface of hyperbranched polymers. **Figure 2.2** shows a cartoon of these two valuable compounds in enhancing polymers as drug delivery vehicles.

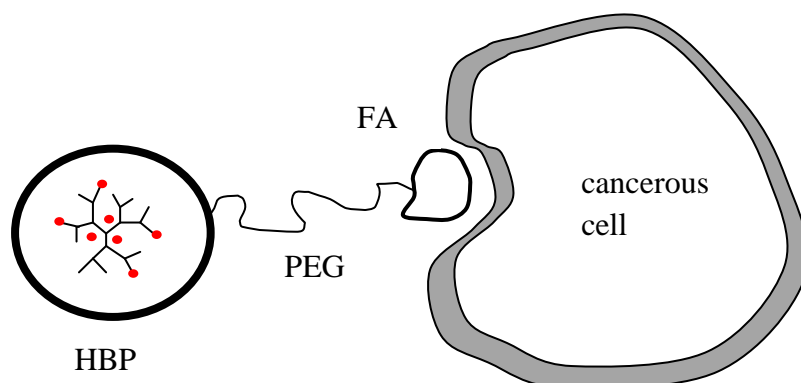


Figure 2.2 : Cartoon of surface modification of hyperbranched polymers with PEG and FA

The final part of the thesis presents a comparison of the encapsulation abilities of water soluble hyperbranched polymers and polyamidoamine (PAMAM) dendrimers. The same hyperbranched polymers were used as in the previous study. For PAMAM dendrimers, we used generation 2.5 with an amine terminated group. These amine terminated groups were substituted with a hydroxyl group to make water soluble dendrimers. Generation 2.5 PAMAM dendrimers were chosen because their molecular weight was slightly similar to that of hyperbranched polymers with a molecular weight of 4000 Da. These

water soluble dendrimers were encapsulated using ibuprofen and tetracarboxyphenyl porphyrin (TCPP). Four different concentrations were used i.e. 1.00×10^{-4} M, 2.00×10^{-4} M, 4.00×10^{-4} M and 6.00×10^{-4} M. On comparing the results it was postulated that both hyperbranched polymers and dendrimers showed same trend where the concentration increased until it plateaued at the highest concentration.

Chapter 3: Polymers and Drug Delivery Systems

3.1 Overview

The development of polymers with new chain architectures and structures has become in the past decade an intense research field in close interaction with the rapid growth of nanoscale technologies. Much effort in this area has focused on the controlled synthesis and the use of highly branched polymer architectures since new and specific properties can arise directly from the size, shape, and capacity of such nanometric-sized macromolecules.²⁶ Due to these properties, polymer chemists are actively involved in designing polymer materials for biomedical application. One field of application that has had the attention of chemists since the late 1960s is the need for advanced drug delivery systems to improve drug efficacy.²⁷

During the past few decades, a large number of drug delivery systems, mostly in the forms of microspheres, films, tablets, or implantation devices, have been designed to achieve sustained drug release by taking advantage of the peculiarities of polymers.² Today, the concept of drug delivery is not limited to prolonging the duration of drug release; instead, it applies to at least two strategies of realizing temporal and spatial distribution control in the body. Temporal control stresses the selection of predetermined kinetics of drug release during treatment, whereas spatial distribution control aims to precisely direct a drug vehicle to the desired sites of activity.²⁸⁻²⁹ For such controls, significant efforts have been devoted to explore nanotechnology based on the intersection of multiple disciplines of chemistry, biology, and engineering.

Nanotechnology focuses not only on formulating therapeutic agents in biocompatible nanocomposites but also on exploiting the distinct advantages associated with a reduced dimensional scale within 1-100 nm. Some examples of nanoscaled polymeric carriers involve polymer conjugates, polymeric micelles and polymersomes.³⁰ Because these systems often exhibit similarity in their size and structure to natural carriers such as viruses and serum lipoproteins, they offer multifaceted specific properties in drug

delivery applications. These system can be used to delivering drugs to targeted area (cellular/tissue).³⁰

3.2 Polymer architecture and drug delivery

As various nanosystems have been developed, the importance of polymer architecture-property relationships has gradually been realized and emphasized. Polymer architecture describes the shape of a single polymer molecule, which often determines its physiochemical properties² Any polymer selected for drug delivery formulation is commonly classified according to it's chemical nature such as polyester, polyanhydride, poly (amino acid), backbone stability (biodegradable, nonbiodegradable), and water solubility (hydrophobic, hydrophilic).²⁷ Polymer architectures that are relevant to drug delivery applications are presented in **Figure 3.1**.

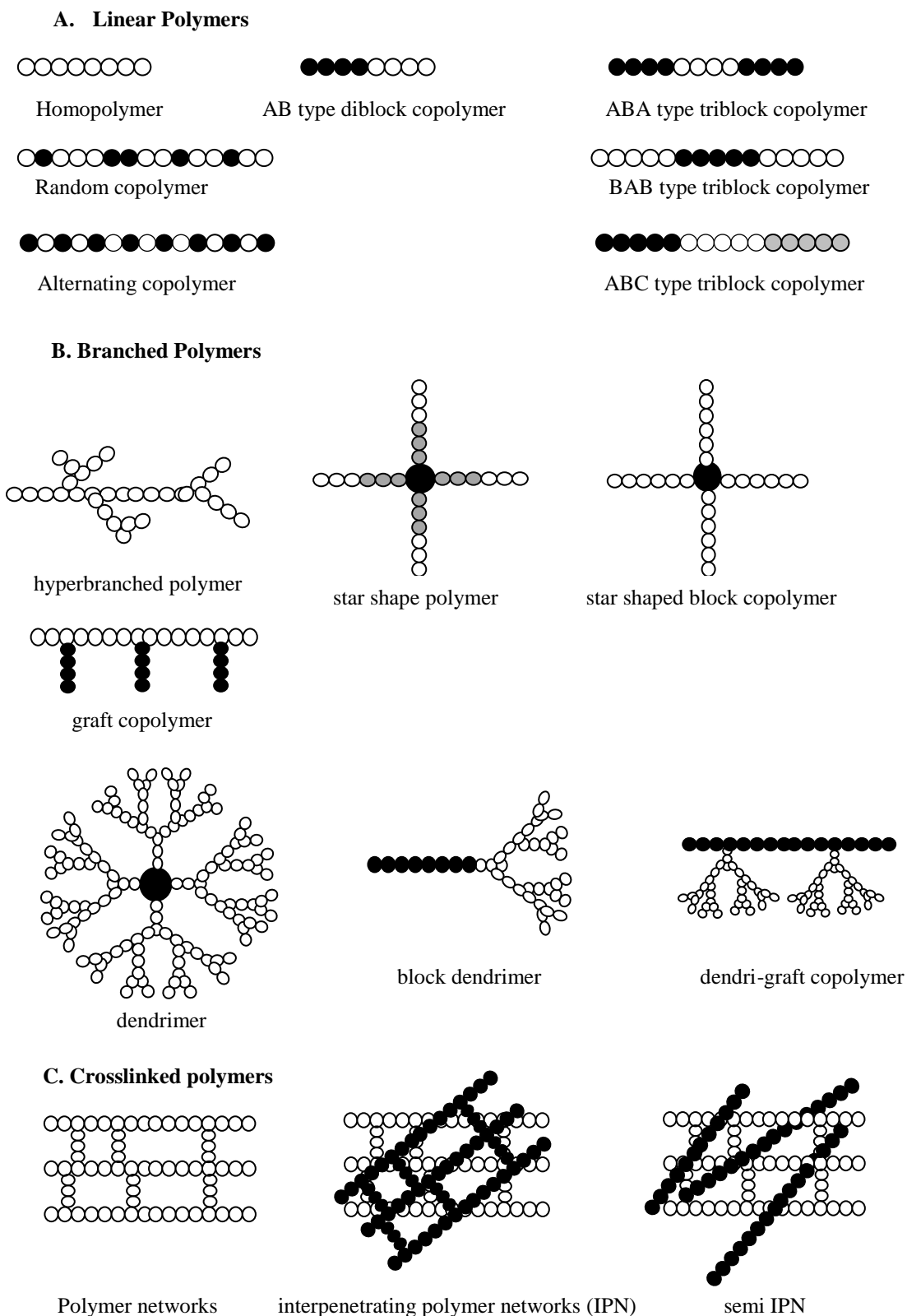


Figure 3.1: Polymer architectures : A. Linear polymers, B. Hyperbranched polymers and C. Crosslinked polymers²

Linear polymers such as polyethylene glycol (PEG) which consist of homopolymers or copolymers, have the simplest main architecture and were first reviewed for drug delivery in the early 1950s.² At this time, chemists had started to link drugs onto polymers to improve their efficiency. However, during that time, they concentrated mainly on the chemistry itself and almost any class of polymers was covalently combined with any class of drugs. The biological aspects of the design of polymeric prodrugs were hardly taken into account. In 1975, Ringsdorf proposed a model based on the combined chemistry and biology approach consisting of five main elements: polymeric backbone, drug, spacer, targeting group, and solubilizing moiety (**Figure 3.2**).^{2,31} This model is used by polymer chemists to design tailor-made polymeric carriers that can fulfil the specified requirements of drug delivery systems.

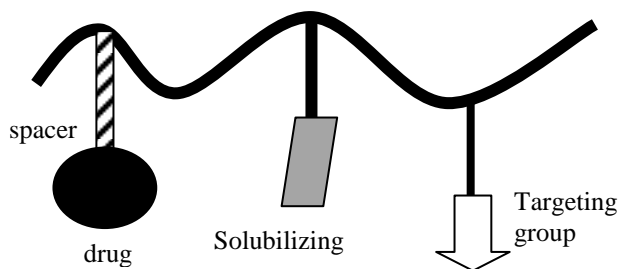


Figure 3.2: Ringsdorf's model of a polymer-drug conjugate

3.2.1 Linear polymer for drug delivery

Over the past 20 years, water soluble linear polymers have been developed for potential drug delivery. These include vinyl polymers, polysaccharides, poly(amino acids), proteins and poly(ethylene glycol) (PEG). One example of vinyl copolymers which was successfully synthesized using radical polymerisation is N-(2-hydroxypropyl methacrylamide) or HPMA. This polymer has been conjugated with the anti cancer agent doxorubin and entered phase I clinical trials as PK1 (FCE286068, **Figure 3.3**) in 1994.² Later, PK1 also reached phase II clinical trials for the treatment of breast and colon cancers.

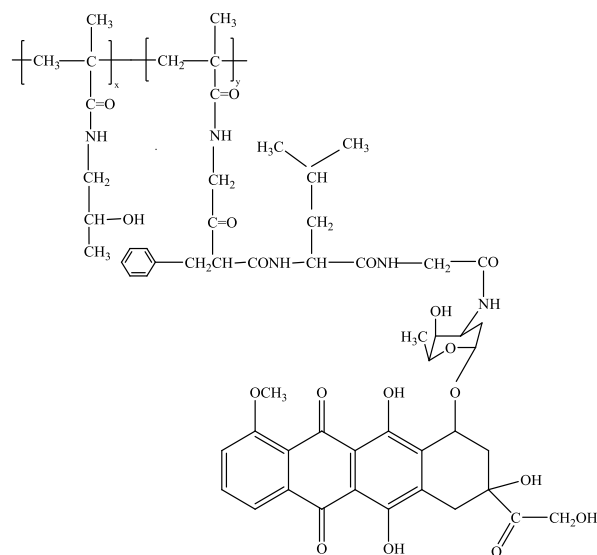


Figure 3.3: Poly(N-(2 hydroxypropyl methacrylamide)) copolymer containing doxorubin PK1 (FCE28068)

Biodistribution, immunogenicity and biological activities have proven that poly HPMA is non toxic and non immunogenic *in vivo*.³² The characteristics that should be taken into consideration in the development of a polymer as a drug carrier include molecular weight, polydispersity, charge and the hydrophilic-hydrophobic character of the polymer backbone. The latter because it can adversely effect drug biodistribution, clearance, biological activity and toxicity to the cell. A higher molecular weight of the polymer carriers was achieved by binding a drug to the polymer. As a result, this polymer drug conjugate can significantly change the biodistribution of the conjugates and also enhances the circulation times and results in better accumulation at the targeted site.³³

Drug conjugated linear polymer was first introduced to deliver drugs. The disadvantages of this architecture was increased in molecular weight will significantly increased the biodistribution of drugs because molecular weight can affect the effectiveness of the carrier. Another factor was solubility, the solubility of drug will improved when conjugated with water soluble linear polymer. However, the solubility of the polymer itself would decreased. Another class of polymer, named block copolymer can be used as delivery agent in drug delivery system and are discussed in the next section.

3.2.2 Block copolymer and drug delivery

Block copolymers consist of polymers that have two or more blocks in the main chain and can be categorized by their architectures as AB type block copolymers, ABA triblock and multiblock copolymers (**Figure 3.1**). The A unit represents the soluble block in the selected solvent and the B unit is the insoluble block. Linear amphiphilic block polymers, which consists of both hydrophilic and hydrophobic blocks in the same polymer chain, can build spherical polymeric assemblies in aqueous solution called polymeric micelles. These polymeric micelles can act as a drug carrier where the drug is conjugated to one segment of the block polymer to form the core and the other segment was PEG, which remains unmodified as a water soluble shell.^{21,31} Block copolymer have been successfully used in drug delivery to target drug to specific physiological sites such as organs, tissues or cells, to solubilise hydrophobic drugs, to increase drug stability and to control drug release.

There are three major types of micelles that contribute to drug delivery systems based on linear block copolymers: (a) common block copolymer micelles; (b) drug-conjugated block copolymer micelles; (c) block ionomer complex micelle (**Figure 3.4**).²

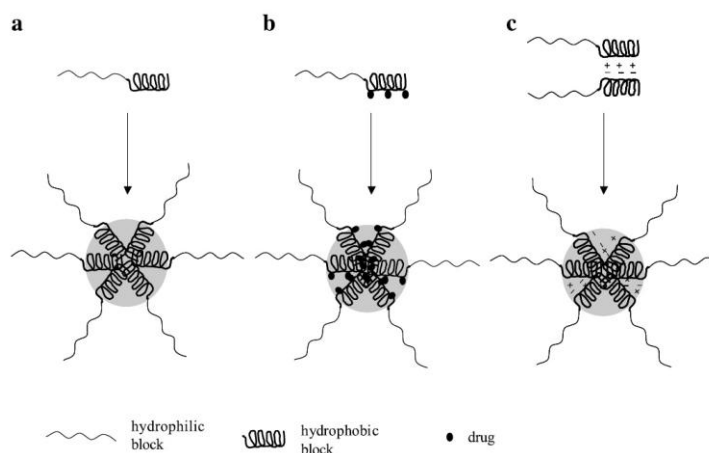


Figure 3.4: Three major types of micelle : (a) common block copolymer micelle, (b) drug-conjugated block copolymer micelle and (c) block ionomer complex micelle

Polyethylene glycol (PEG) is also an excellent biocompatible biomaterial due to its flexibility, non-toxicity and hydrophilicity. An example of this group is methoxypolyethylene glycol-b-poly(D,L-lactide) (PDDLA) (MePEG:PDDLA). This block copolymer was developed for micellar carriers of hydrophobic drugs such as paclitaxel.³⁴ This drug has been successfully incorporated into a micellar solution with up to 5% w/v of paclitaxel. Paclitaxel is an anti cancer drug that is used in chemotherapy for the treatment of lung, ovarian, breast, head and neck cancer.³⁵⁻³⁷

Drug conjugated block copolymer micelles are developed by taking advantage of the interaction between a drug and a hydrophilic block copolymer segment to build the hydrophobic polymer-drug core of micelles. An example of this type is the anti cancer polymer conjugated drug onto biodegradable block copolymers of PEG with Doxorubin attached via an enzymatically degradable glycine-phenylalanine-leucine-glycine (Gly-Phe-Leu-Gly) spacer (**Figure 3.5**).^{2,36}

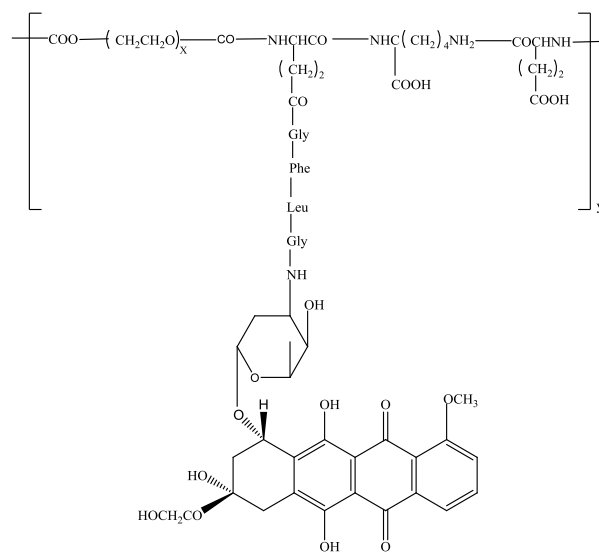


Figure 3.5: Block copolymer of PEG conjugated with Doxorubin drug via enzymatically degradable Gly-Phe-Leu-Gly spacer

This conventional micelle drug delivery has some disadvantages which were easily disassemble once the concentration falls below the critical micelle concentration. To overcome these classical micelles, we suggested static unimolecular based on dendritic or hyperbranched polymer to deliver drugs efficiently. These static unimolecular has a static structure, controlled shaped and molecular weight and furthermore has well defined surface functionalities.³⁷

3.2.3. Dendritic polymers for drug delivery

Polymer based drug delivery systems are designed to improve the pharmacokinetics and biodistribution of a drug and/or provide controlled release kinetics to the specific target. Ideal dendritic polymers should exhibit high aqueous solubility and drug loading capacity, biodegradability and low toxicity. In dendritic polymers drug delivery, a drug is either encapsulated in the interior of the polymer and/or it can be conjugated at the surface terminal to form macromolecular prodrugs.

3.2.3.1 Drug encapsulated dendritic polymer

Poly(glycerol succinic acid) dendrimers (PGLSA dendrimers) were investigated as a container for camptothecin, a group of naturally derived hydrophobic compounds with anti cancer activity. The anti cancer activity was investigated for human cancer cells such as HT 29 colon cancer, MCF-7 breast carcinoma, NCI-H460 large lung carcinoma and SF-268 astrocytoma.³⁸

To improve the solubility of the dendrimers, carboxylate (G4-PGLSA-COONa) at the peripheral groups were used and successfully encapsulated with 10 hydroxycamptotecin (10 HCPT) (**Figure 3.6**). Upon exposure to MCF-7 human breast cancer cells, the unloaded dendrimer showed no cytotoxicity while 10 HCPT encapsulated with G4-PGLSA-COONa showed significant toxicity with less than 5% of viable cells at higher concentrations (20 μ M).³⁸

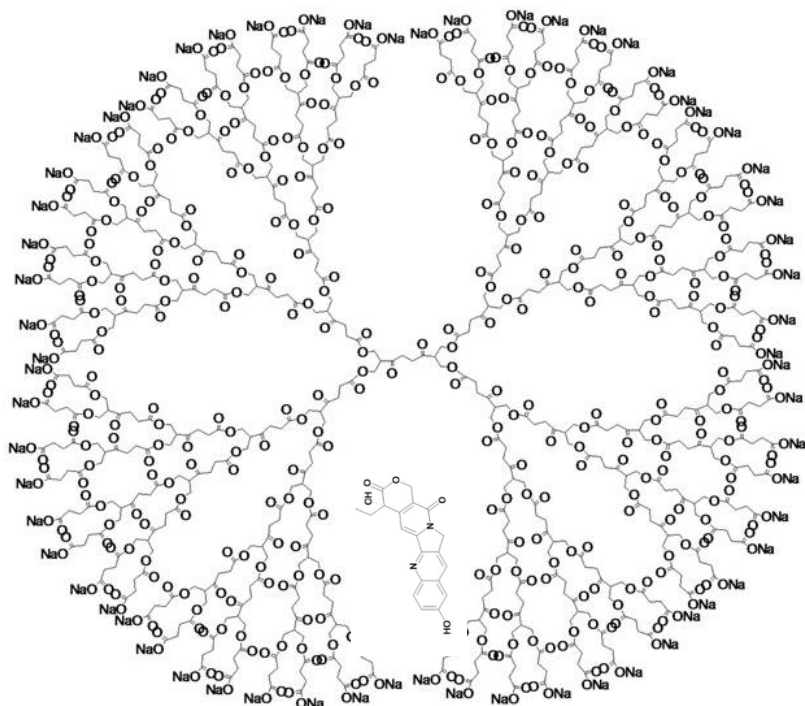


Figure 3.6: Encapsulated G4-PGLSA-COONa dendrimers with 10 Hydroxycamptothecin³⁸

3.2.3.2 Drug conjugated dendritic polymer

Dendritic drug conjugates or prodrugs consist of a drug that is chemically bound to the peripheral groups of macromolecules. There are three pathways³⁹ to create these prodrugs; i) direct conjugation of the drugs to the dendritic surface, ii) conjugation via a linker molecule and iii) drug molecules can become an integral part of the dendritic carrier and released through certain triggering events at the desired location. PAMAM-G2.5-COOH (**Figure 3.7**) and PAMAM-G3-NH₂ has been conjugated with the methotrexate drug.³⁹

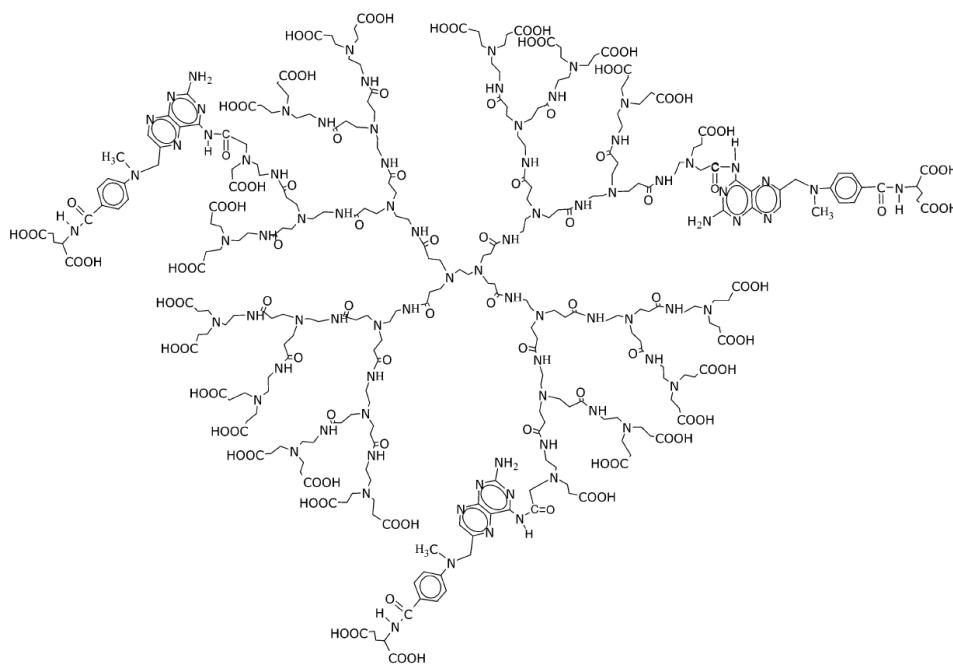


Figure 3.7: PAMAM-G2.5-COOH conjugated with methotrexate drug

3.3 Structure and properties relationship

3.3.1 Biocompatibility

A major concern when introducing a polymers into medical applications is its biocompatibility. These polymers should exhibit low toxicity and non immunogenicity to the cells. The biocompatibility of a polymer is dependent on the identity of the functional groups that are sufficiently exposed to interact with the biological tissues.^{36,40-}

⁴¹ Encapsulation of enzymatically unstable or non compatible functionalities to a highly branched polymer architectures can reduce he access to the core of a macromolecule and further minimize the undesired interactions in vivo. This is due to the highly branched polymers which can modulate the biocompatibility of polymer. For instance, polymer backbone such poly (ethylene glycol) (PEG), poly N-(2-hydroxypropyl methacrylamide) (PHPMA) and styrene-co-maleic anhydride (SMA) are biocompatible and have been extensively used in clinical studies.⁴⁰

In order to improve the water solubility and biocompatibility of polymers, PEGylation technique was introduced. This technique is widely used to improve the biological utility of small molecules, proteins, polymers, surfaces and artificial organ implants.⁴⁰ PEG grafts have been used to increase the water solubility and reduced the cytotoxicity of several linear polymers such as polycaprolactone (PCL) and poly-(N-isopropylacrylamide-co-maleic anhydride). For copolymers, which have the similar weight ratios of branched polyethyleneimine (PEI) and PEG, a shorter chain of PEG is better than a single larger PEG distributed throughout the structure to improve the biocompatibility of the polymer (**Figure 3.8**). This is due to shorter PEG chains reduced cytotoxicity effectively than fewer longer PEG. Other factors that should be considered to minimize the cytotoxicity of these copolymers include reducing the number of primary amines or the larger weight percentage of linkers.

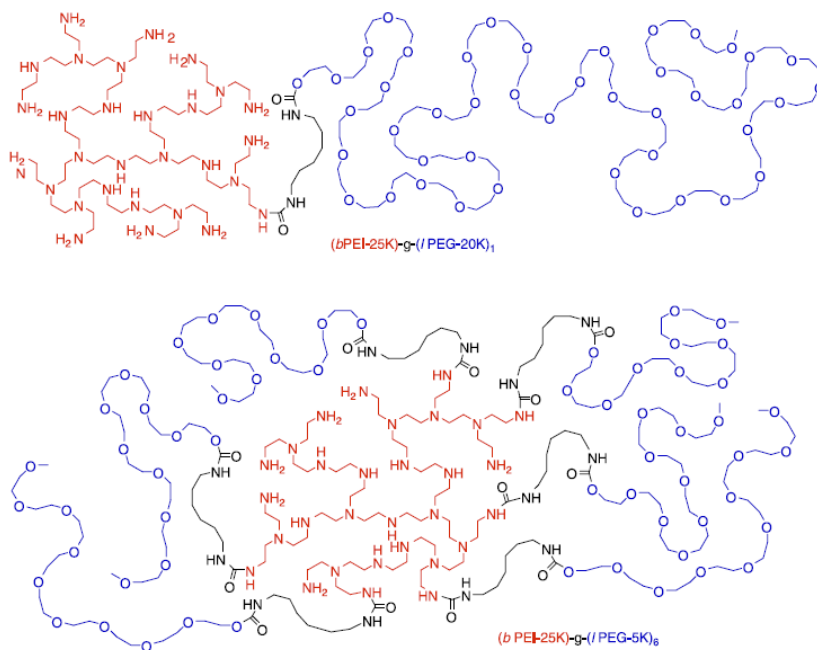


Figure 3.8: Conjugation of PEG to PEI: (a) a few longer PEG chain and (b) numerous shorter PEG chain

The surface of the copolymers should also have high solubility in an aqueous medium. For amino-terminated poly(amidoamine) (PAMAM), a cationic surface destabilizes the cell membrane and instigates cell lysis. Furthermore, the cytotoxicity of the amino terminated dendrimer is generation dependant with higher generation dendrimers being the most toxic.³⁶ Other factors that contribute to the toxicity of amino-terminated dendrimers include the type of amine functionalities being used as primary amines are more toxic than secondary amines. However, the cytotoxicity of a cationic dendrimer can be improved by conjugation with comparable end groups such as PEG (**Figure 3.9**).⁴⁰⁻⁴¹

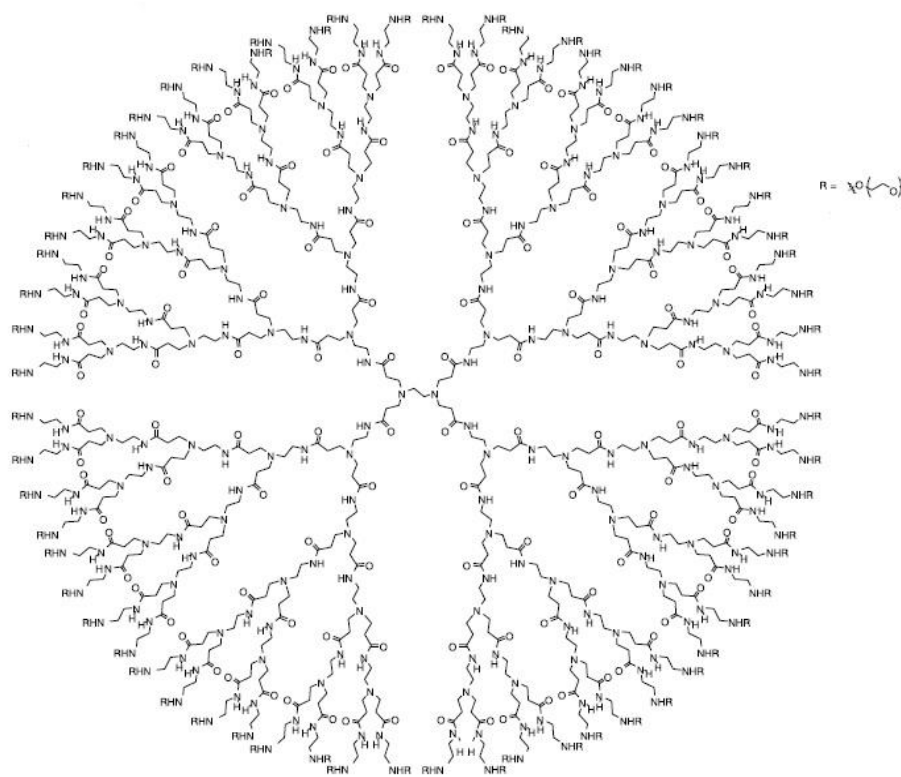


Figure 3.9: G4 PAMAM dendrimer with PEG as the end group functionalisation⁴⁰

Anionic surface functionalities show lower cytotoxicity compared to cationic dendrimers. Lower generation PAMAM dendrimers possessing carboxylate surface group are neither haemotoxic or cytotoxic at wide range of concentrations.⁸ Dendrimers

containing an aromatic polyether core and anionic carboxylated surface groups show significant haemolytic activity in rat blood cells after 24 hours. The aromatic interior of the dendrimer may cause haemolysis through hydrophobic membrane contact. However, the influence of the dendrimer core diminishes with increasing dendrimer generation and rigidity of the dendritic branches that form the shell around the core. The rigidity of the shells encapsulates the core unit and prevents interaction between the core and the surface segments.⁴²⁻⁴⁴

3.3.2 Biodegradability

Biodegradability is an important factor for a macromolecule being used in biomedical applications.⁴⁰ Higher molecular weight polymers show promising properties as a delivery component but larger molecule (more than 40 kDa) can accumulate in the body and caused undesired side effects. The incorporation of biodegradable linkages is vital for the cleavage and clearance of the polymeric carriers. Natural polymers such as polysaccharides and polypeptides are suitable candidates for biodegradable materials. Polysaccharides such as cellulose, dextran, hyaluronic acid, chitin and chitosan are employed for drug delivery due to their characteristics such as ease of functionalisation, efficient enzymatic degradation and relatively low immunogenicity.⁴⁰

Synthetic polyester such as poly(glycolic acid), poly(lactic) acid and poly(caprolactone) are stable for short periods yet degradable over long periods into small molecules components via enzymatic or hydrolytic cleavage. Other synthetic polymers that have been investigated for biodegradable materials including poly(amides) and poly(orthoesters).⁴⁰

3.3.3 Biodistribution

The synthetic polymer drug carrier designed for drug delivery depends solely on its size and surface functionalities. Ideally, the carrier must have minimal non-specific interactions and accumulate at the desired receptor. However, the polymer drug carrier will also interact with sites throughout the body. Therefore, it is important to design a drug carrier that has a optimum capability of accumulating at the desired site and causing minimum toxicity to other cells.⁴⁵ The critical factor in controlling biodistribution is to increase the blood circulation time. Increased blood circulation means that the macromolecule drug conjugate is in the bloodstream and can interact with the desired targeted site. A higher molecular weight can prolong the circulation time, but it can also interact with other healthy organs.⁴⁰

The preferential delivery of drugs to the specific site is the crucial factor for an effective macromolecular therapeutic. The polymer carrier should be designed to enable sufficient exposure to the specific targeting site while minimising accumulations in other parts of the body.^{40,45}

3.4 Results and discussion

3.4.1 Water soluble hyperbranched polymers

At present, people are often faced with the pressures of life, which causes them to take medication to relieve pain. Among the most common drugs taken is ibuprofen. The main problem of ibuprofen or other hydrophobic drugs is that they have poor solubility, and are not easily absorbed into the bloodstream. Consequently, most lead drugs are either abandoned or delivered in large quantities to the cell. Many approaches have been envisaged including using polymeric carriers, such as copolymers, polymer aggregates and dendritic polymers. One promising delivery agent is the dendritic polymer (dendrimers and hyperbranched polymers).

Dendrimers, are highly branched macromolecules, that are monodisperse, possess a globular shape and have large numbers of controllable surface functionalities. Even though this carrier has perfect characteristics, they are not easy to synthesise. Their synthesis is time consuming, which makes it very expensive. Another issue raised is their toxicity to the human body. For example, amine-terminated polyamidoamine (PAMAM) dendrimers, have significant toxicity to human intestinal adenocarcinoma cells. Another concern is cytotoxicity, which is found to be generation dependant, with higher generation dendrimers being most toxic to the human body.³⁶

In contrast, hyperbranched polymers are spherical, branched macromolecules possessing a specific architecture, the key scheme of which includes the core, the interior branching units and the terminal end groups. These polymers are easy to synthesise using a one step reaction. These polymers are currently attracting much attention from the pharmaceutical industry as dendritic carriers in drug solubilisation and delivery applications. To produce a hyperbranched polymer suitable for the applications described above, a polymer is needed that is non-toxic to humans and readily dissolves

in water. So, a hyperbranched polymer with a hydroxyl terminal group was prepared, as a solubilisation enhancer for hydrophobic drugs.

Initially, *p*-nitrophenol was chosen as a core because it consists of an aromatic structure and an OH group. Aromatic structure is important because it can be easily detected by NMR. The molecular weight of hyperbranched polymers can be calculated using this aromatic signal in NMR. The calculation will be described later in this chapter. The OH group is easily deprotonated by a base to form a phenoxide before further propagation with the monomer (glycidol). This commercially available monomer is a reactive hydroxy epoxide which represents a latent AB₂ monomer (wherein the B groups of the monomer are only activated for polymerisation after the preceding reaction of the A group)⁴⁶⁻⁴⁸ that can be further polymerised to hyperbranched polyethers with numerous hydroxyl terminal groups. These macromolecules possess a hydrophobic interior and hydrophilic OH groups at the periphery.⁴⁸ A representative structure is shown below in

Figure 3.10.

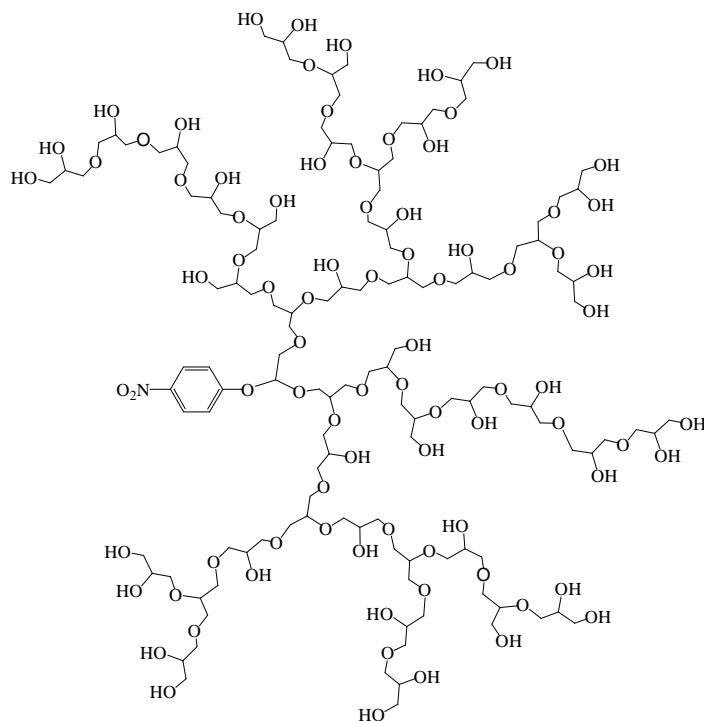


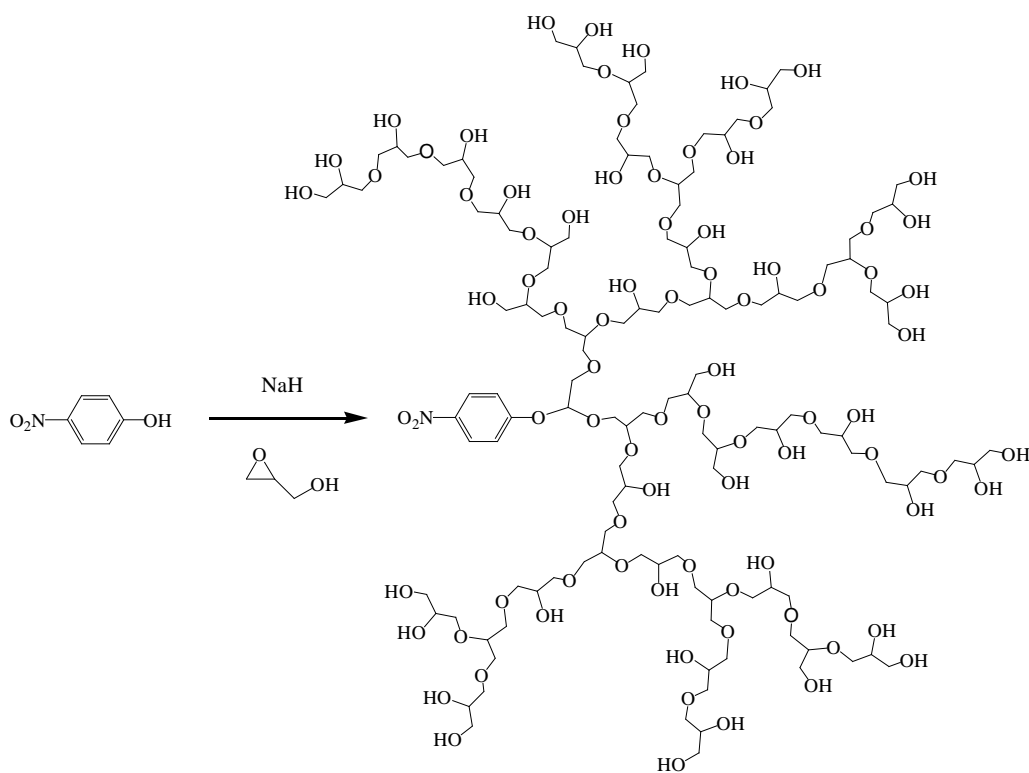
Figure 3.10: Hyperbranched polyglycerol with a *p*-nitrophenol core

In the first part of this work, hyperbranched polymers of controlled molecular weight were synthesised. Further investigation was carried out into the ability of these polymers to solubilise four different UV active species. These compounds were naphthalene, as a model hydrophobic compound and ibuprofen, a commercial non-steroidal anti-inflammatory drug (NSAID), used widely in the treatment of pain and fever. Another compound used was tetracarboxyphenyl porphyrin (TCPP), which is used as a photosensitizer in photodynamic therapy. The final drug was an anti-prion drug, used to treat mad cow disease.

3.4.2 Synthesis of polyglycerol hyperbranched polymers

Hyperbranched polymers can be synthesised with or without a core. Hyperbranched polymers synthesised without a core will lead to an uncontrolled molecular weight of polymer. In this study, *p*-nitrophenol was chosen as the core to control the molecular weight of the polymers. Hyperbranched polymers were synthesised with different core to monomer ratios, which led to a several polymer molecular weights. Various polymer molecular weights allowed investigation of the effect of molecular weight on the encapsulation and release of drugs.

Initially, synthesis was carried out using a *p*-nitrophenol core and glycidol as the monomer, with a core/monomer mixture (1:5) mole ratio (**Scheme 1**). All glassware was thoroughly cleaned and dried in an oven. The polymer was synthesised using diethylene glycol dimethyl ether as the solvent. The synthesis was carried out in a nitrogen environment. The reaction started with the addition of the core to solvent in a three neck round bottom flask. The mixture was heated to 50 °C until the entire core was dissolved. The temperature was raised to 90 °C prior to the addition of NaH. Glycidol was then added slowly over 12 hours using a syringe pump. Slow monomer addition was crucial to minimise secondary polymerisation that can occur without the initiator or core.⁴⁷ The mechanisms are discussed later in this chapter.



Scheme 1: Synthesis of hyperbranched polymers

The prepared polymer was dissolved in methanol before being precipitated in acetone to remove unreacted monomer or small oligomers. This step was repeated twice and the final product was dried overnight in a vacuum oven at 30 °C. The product was a brown viscous polymer with 40% yield. Confirmation of the polymer structure was done using ¹H NMR. The spectrum showed aromatic protons characteristic of the *p*-nitrophenol core at 8.16 and 7.05 ppm. This represents H_a and H_b in the core molecule in **Figure 3.11**. H_a was the more deshielded due to its position near the electron-withdrawing group, NO₂.

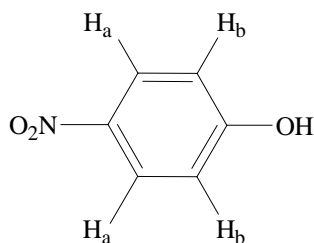


Figure 3.11: *p*-nitrophenol

To confirm that the core was totally incorporated inside the polymer rather than simply mixed, another experiment was carried out. To the synthesised polymer, fresh *p*-nitrophenol was added and physically mixed before the ¹H NMR spectrum was reacquired. **Figure 3.12** shows the original ¹H NMR spectra from a previous sample, and **Figure 3.13** shows the freshly doped *p*-nitrophenol to the sample. **Figure 3.12** shows that there were an additional two doublets at 8.14 and 6.85 ppm respectively, which is attributed to the two new peaks of freshly doped *p*-nitrophenol. This confirmed that the core molecule was chemically incorporated into the polymer structure. A broad peak in the range of 2.35 to 4.05 ppm was attributed to the remaining protons in multiple proton environments within the polymer, which were CH, CH₂ and OH groups.

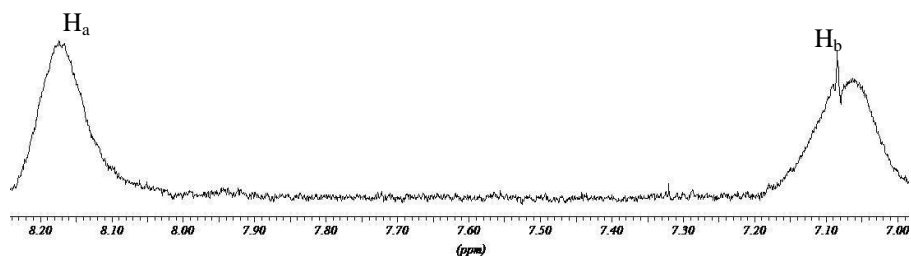


Figure 3.12: The original ¹H NMR representing the core of the polymer

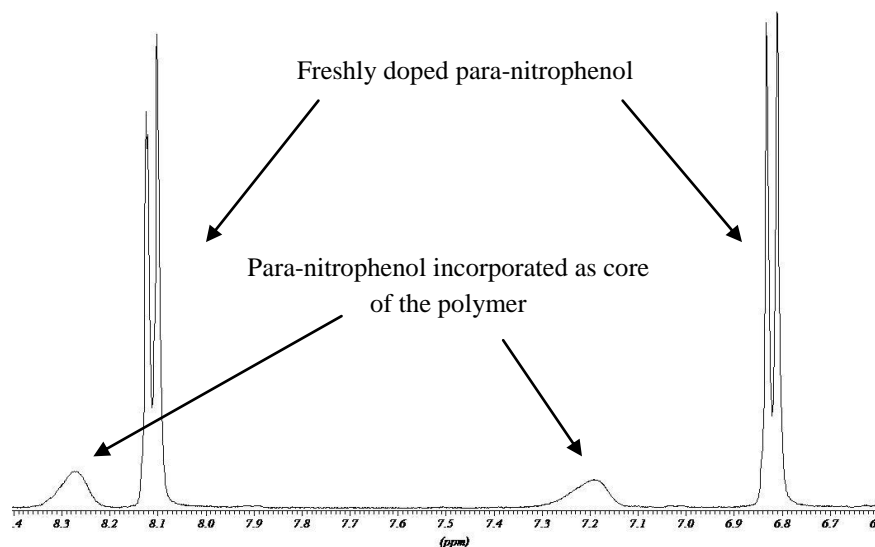


Figure 3.13: The freshly doped *p*-nitrophenol to the polymer

To prove that the hyperbranched polymers were fully synthesised, further characterisation using FTIR was performed. The FTIR result revealed a broad OH peak at 3420 cm^{-1} , CH_2 at 2873 cm^{-1} and a carbonyl peak at 1643 cm^{-1} . The molecular weight (M_n) from GPC was 4000. A solubility test showed that these hyperbranched polymers were easily dissolved in water.

In this work, several attempts were made to polymerise hyperbranched polymers with different molecular weights. This can be achieved by varying the core to monomer ratio. For example, the first trial was to polymerise a hyperbranched polymer using a 1:5 mole ratio, and the expected molecular weight was 500 Da. The expected molecular weight was calculated by multiplying the molar mass of glycidol (74.08 gmol^{-1}) by 5 and adding the molar mass of the *p*-nitrophenol core (139.11 gmol^{-1}). The core should be totally dissolved in the solvent. Ideally, when polymerisation occurred, it was expected that one molecule of the core would be incorporated with one molecule of the polymer.

From the aqueous GPC result, the calculated molecular weight (M_n) was around 4000 Da relative to linear PEG-PEO with a polydispersity of 1.85 in an aqueous solution. This

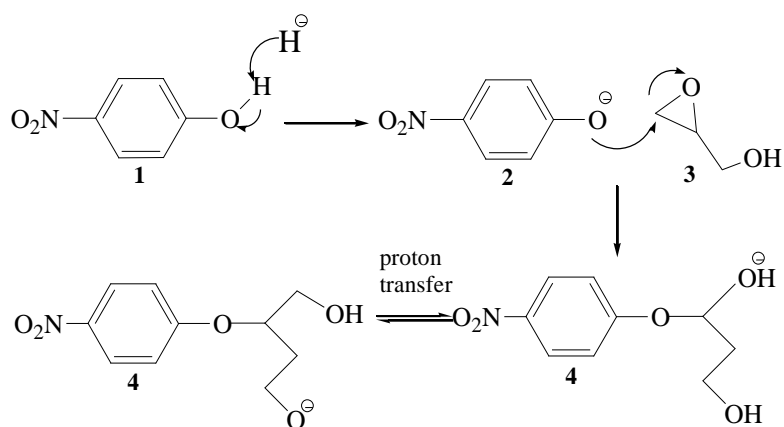
is much higher than the calculated molecular weight. Therefore, it could be argued here that the core is doing nothing. However, the polydispersity suggested otherwise. If this polymerisation was carried out without a core, the polydispersity could be around 10.

From the ^1H NMR spectra, when the core peak was integrated relative to the broad peak of the polymer backbone, the calculated molecular weight was around 7000 Da. The difference between these two values is discussed here. When the core and monomer began polymerisation, some core molecules were incorporated well into the polymer molecule and others were not. But GPC cannot differentiate between the polymers with or without a core. As a result, it calculated all the polymers as bulk. Another contributing factor was the way that the GPC was calibrated. The GPC was calibrated against linear polystyrene and underestimated the M_n of the dendritic molecules.⁴⁹ This is because the branched structure of the dendritic molecules gave a compact configuration compared to linear molecules of the same molecular weight. For these reason, GPC provided a minimum value of M_n , (M_n^{min}).

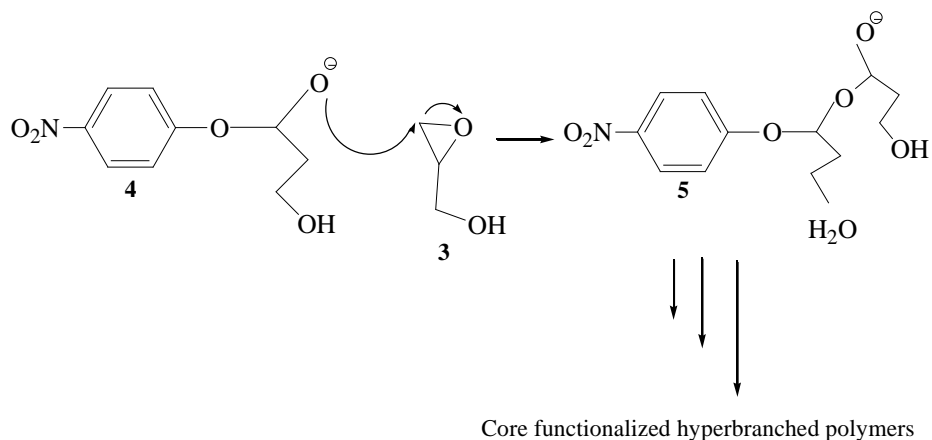
In contrast to ^1H NMR, M_n was calculated by integrating the *p*-nitrophenol core peak at $\delta_{\text{H}} = 8.16$ ppm with the abundance of proton peaks from the polymer backbone, with δ_{H} in the range of 2.35 to 4.05 ppm (not shown). From this integration, the calculated M_n was 7000 Da. This value was higher than GPC due to ^1H NMR calculations based on the assumption that each polymer molecule contained a core molecule. Thus, the M_n from the ^1H NMR calculations will always be high and represents the maximum value, (M_n^{max}).

Earlier discussion mentioned that the core to monomer ratio used was 1:5. It was predicted that the molecular weight is 500 Da. However, results from the GPC and NMR were different from the directly calculated molecular weight. The following discussion is about the mechanism involved in the synthesis of hyperbranched polymers. The mechanism of hyperbranched polymers polymerised using a *p*-nitrophenol core and

glycidol as the monomer is shown below. It involves two steps: initiation of the core and propagation of the monomer. For the first step, the reaction was initiated by deprotonation of the core **1** by sodium hydride before the slow addition of glycidol monomer was started. The anionic core, called phenoxide **2**, was then reacted with glycidol **3** by a ring-opening mechanism to form an alkoxide **4** (**Scheme 2**). The next step was the propagation of the monomer to form a new alkoxide **5** before further propagation to form hyperbranched polymers (**Scheme 3**).



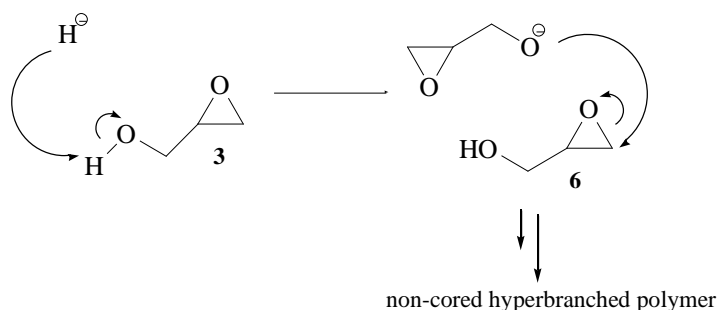
Scheme 2 : Deprotonation and ring opening mechanism of the monomer



Scheme 3 : Propagation of alkoxide to form hyperbranched polymers

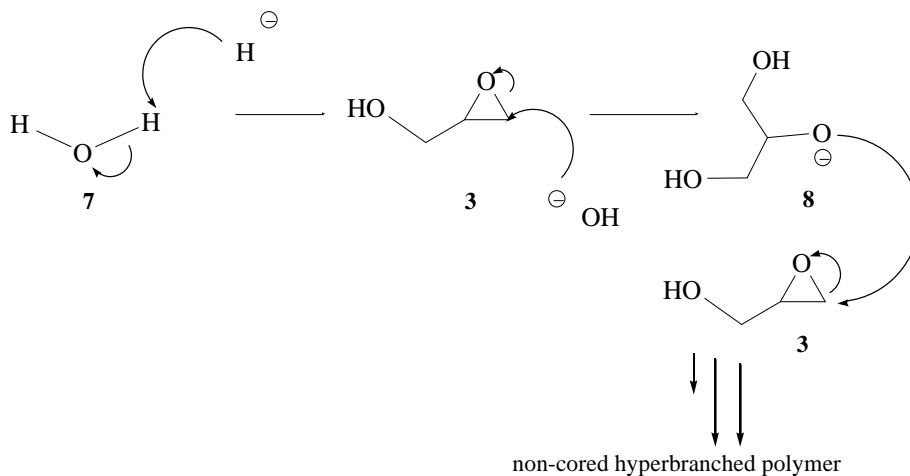
However, the above route did not always occur. Sodium hydride is a strong base, and if any remains after initiation, it can also deprotonate glycidol **3** and form a glycidol

initiator **6**, which is depicted in **Scheme 4** below. When this happens, a non-cored polymer is produced.



Scheme 4 : Deprotonation of glycidol to form a glycidol initiator

Another deviation from normal polymerisation can occur if, water **7** is present in the reaction. It can form a hydroxide ion that further reacts with glycidol **3**, which leads to the formation of anion **8** (**Scheme 5**). Again, a non-cored polymer is produced.



Scheme 5: The presence of water may affect the final product of polymer

After the first attempts to polymerise hyperbranched polymers with a 1:5 ratio had succeeded, it was attempted to polymerise the same hyperbranched polymers with different core to monomer ratios. The selected ratios were 1:10, 1: 25, 1:50 and 1:100. For this work, precise control of molecular weight was required (for example, a 1:5 ratio

actually gave a molecular weight of 500). The investigation was to determine the ratio of monomer could affect the molecular weight, i.e. more monomer will increase the molecular weight. The spectroscopy results showed that the polymers exhibited the same characteristic peaks as before. The GPC results showed that the molecular weight of the polymers range from low to medium to high, as shown in **Table 3.1**. As predicted, the estimated molecular weights for all the ratios were different from those calculated by GPC and NMR, as described earlier.

Table 3.1: Different molecular weights of polyglycidol

Polymer ratio	Estimated molecular weight*	Molecular weight by GPC	Molecular weight by NMR	Polydispersity
1:5	500	4000	7000	1.8
1:10	900	8500	8500	2.0
1:25	2000	12500	13000	2.3
1:50	4000	27500	2130000	3.5
1:100	7500	50000	**	6.0

**based on core to monomer ratio*

***molecular weight could not be determined as of the peak were barely visible and could not be accurately integrated relative to the polymer*

The table above shows that hyperbranched polymers with different molecular weights were successfully synthesised. These different molecular weights were used to investigate the performance of the polymers in drug delivery.

3.4.3 Selection of model drug for encapsulation study

Initially, the study was started using a very simple molecule, which was readily available in our lab. After this attempt succeeded, we then used a model drug and drug (naphthalene, tetracarboxyphenyl porphyrin and ibuprofen) with some solubility and finally, a real drug was used to assess the efficiency of the polymers.

In this work, several compounds were chosen and encapsulated with the synthesised hyperbranched polymers. The selected compound should be at least partially soluble in aqueous solution and be UV active. Naphthalene was used to start with, as it is readily

available in our lab. Naphthalene (**9**) is a compound that consists of two benzene rings fused together and shows some solubility in water. The second compound which was a model drug, ibuprofen (**10**), has a carboxylic functional group and shows some solubility in water. These two compounds are available commercially.

The third compound was from the porphyrin group. This group has aromatic heterocycles with pyrrole groups. They are a highly conjugated system and have an intense peak in the visible region. The type of porphyrin used was tetracarboxyphenyl porphyrin (TCPP) (**10**) which exhibits some solubility in water. Having studied the compounds, it was desirable to investigate with a real drug. The final drug used was an anti-prion drug (**11**) which was synthesised by another group in the department (**Figure 3.14**). This drug does not dissolve in water. **Table 3.2** represents the physical properties of all molecules used for this study.

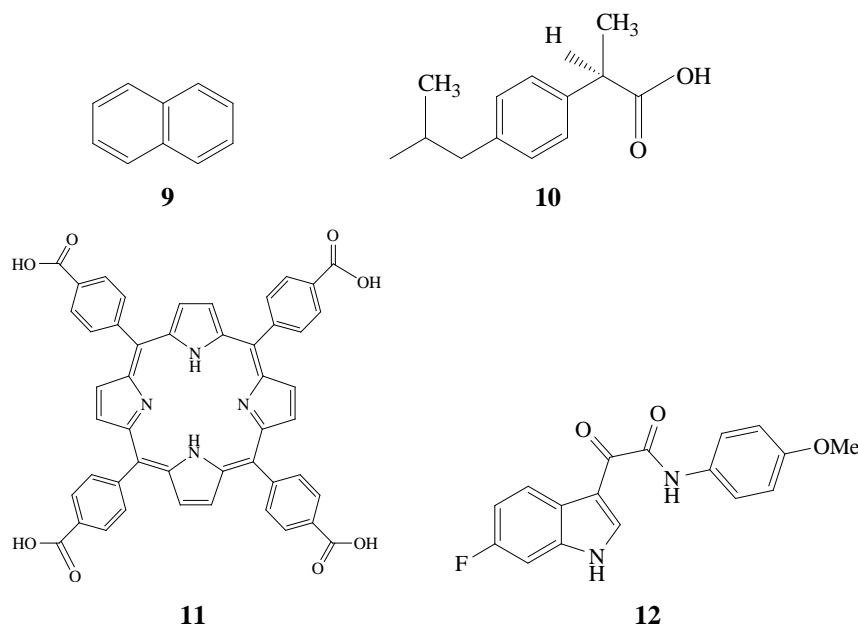


Figure 3.14: Structure of (**9**) naphthalene and (**10**) ibuprofen, (**11**) tetracarboxyphenyl porphyrin and (**12**) anti-prion drug

Table 3.2: Physical properties of model drugs and drugs used in the encapsulation studies

	Naphthalene	Ibuprofen	Tetracarboxyphenyl porphyrin	Antiprion drug
Molecular weight (g mol ⁻¹)	128.17	206.28	854.33	312.30
Empirical formula	C ₁₀ H ₈	C ₁₃ H ₁₈ O ₂	C ₄₈ H ₃₁ N ₄ O ₈	C ₁₇ H ₁₃ FN ₂ O ₃
Characteristic wavelengths (nm)	219	222	415	350
Solubility* (x 10 ⁻⁴ M)	0.58	2.68	0.72	Not soluble in water

**The solubility was determined using the same experimental method and condition and no effort made to maximise it*

3.4.4 Encapsulation studies

Five types of hyperbranched polymers with different molecular weights, as previously described were synthesised by varying the core to monomer ratio using the method shown in **Scheme 1**. The five different molecular weights (Mn) synthesised were 4000 Da, 8500 Da, 12500 Da, 27500 Da and 50000 Da.

In order to select the right concentration ranges to use in this study, a series of experiments were performed. For example, if the range was too small, the concentration of polymer rose with increased concentration of guest molecule. After several attempts, four different concentrations of each polymer, i.e. 1.00 x 10⁻⁴ M, 2.00 x 10⁻⁴ M, 4.00 x 10⁻⁴ M and 6.00 x 10⁻⁴ M were prepared to explore the maximum loading of the model drug (TCPP and naphthalene) and other drugs (ibuprofen and anti-prion) used in this study.

The selected guest molecules under study were naphthalene, ibuprofen and tetracarboxyphenyl porphyrin (TCPP). The studies were carried out in a buffer solution at pH 7.4 and room temperature. The buffer solution used was tris(hydroxymethyl) aminomethane (TRIS) with 0.1 M and pH 7.4. The result obtained from these

experiments indicated the behaviour and interaction between the polymer and guest molecules.

As a control, the complexation experiment was repeated without the hyperbranched polymers. The excess model drugs and drug were dissolved in water and filtered. The solution was then assessed by UV-Vis spectrophotometer. The concentration was determined by dividing the absorbance with each individual extinction coefficient (ϵ) of model drugs and drug. The ϵ value was determined from Beer-Lambert plot. All values were higher than we determined because the data were obtained using experiments specially designed to maximise solubility (sonication, heating, etc.). In our work, we made an effort to collect all datas using the same experimental conditions (without heating and at room temperature). It was believed these method is more reasonable as it used the same method and equipment to record all datas and make them comparable.

3.4.4.1 General method for complex formation

As mentioned earlier, water soluble hyperbranched polymers were successfully synthesised with different molecular weights ranging from 4000 to 50000 Da. To establish the validity of the technique, a hyperbranched polymer with a molecular weight of 8500 Da was used. If successful, this would be followed by encapsulation with different molecular weights and concentrations. Several methods were used to performed the encapsulation. The first attempt was to mix the guest molecule and polymer in water. Even though the polymer dissolved easily in water, the guest molecule was hard to dissolve. A co-precipitation⁴⁶ method was then used.

The method involved the dissolution of a water soluble hyperbranched polymer and model drug/drug separately in methanol. This was to ensure that the crystal lattice of both substances was collapsed fully.⁴⁶ The methanol was then removed in vacuo to give the hyperbranched polymer/drug co-precipitate. This step was followed by the addition of buffer solution at 0.1M and pH 7.4, and the solution was filtered to remove

undissolved guest molecules. Drug concentrations for all prepared samples were assessed using a UV-Vis spectrophotometer.

3.4.5 Encapsulation of naphthalene with hyperbranched polymers

The first attempt to investigate the ability of hyperbranched polymers to solubilise a hydrophobic molecule was done using naphthalene, which has a UV chromophore at $\lambda_{\text{max}} = 219$ nm in methanol and has low solubility in water at 30.00 mg/L (2.34×10^{-4} M). Naphthalene is a hydrophobic compound and the structure consists of two fused benzene rings with a molecular weight of 128.17 g/mol.

For the first attempt, a hyperbranched polymer (10.00 mg) with a molecular weight of 8500 Da and 10.00 mg of naphthalene was used. Both were dissolved in 10 ml methanol in two different vials. After both were dissolved, they were physically mixed and all solvents was removed using a rotary evaporator. Finally, 10 ml water was added and the undissolved solid was filtered. The solution was assessed using a UV-Vis spectrophotometer at its characteristic wavelength. When naphthalene was incorporated into hyperbranched polymers, the solubility of naphthalene increased from 33.58 to 45.37 mg/L (**Figure 3.15**).

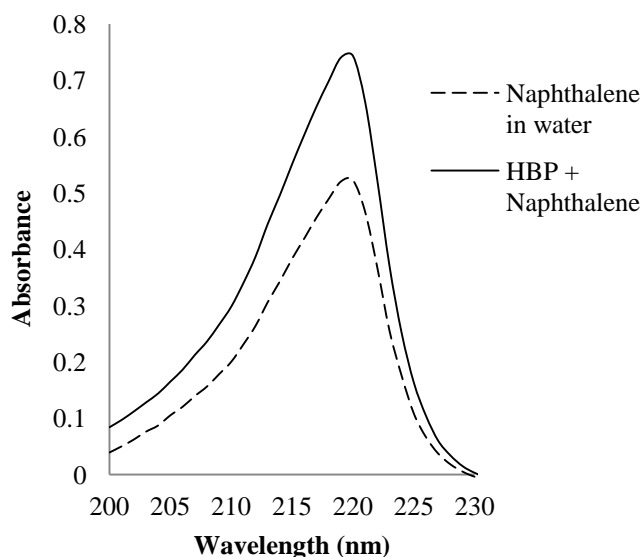


Figure 3.15: UV-Vis spectra of naphthalene encapsulated with hyperbranched polymers

Further investigation were conducted using different concentrations and different molecular weights. For example, to prepare a sample with a concentration of 1.00×10^{-4} M, 8.00 mg of hyperbranched polymer with a molecular weight of 4000 was dissolved in 10 ml methanol. An excess of naphthalane was also dissolved in 10 ml methanol. Both solution were physically mixed. All solvent was removed using a rotary evaporator. Buffer solution was added and finally all undissolved solid was filtered. All the prepared samples were measured by UV-Vis spectrophotometer.

The absorbance was too strong; therefore, dilution was needed in order to achieve an absorbance of less than 1. All samples were diluted 20 fold. The final concentration value of all samples was determined by dividing the absorbance by the extinction coefficient (ϵ) of naphthalene and multiplying by the number of dilutions. This extinction coefficient value was determined graphically from a Beer-Lambert plot as $41945 \text{ M}^{-1}\text{cm}^{-1}$. This plot was prepared using naphthalene dissolved in methanol. The reason that methanol was used instead of water was that naphthalene does not dissolve easily in water, while methanol has the same polarity as water and inside the

hyperbranched polymer. This allowed us to make a comparison with any encapsulated product. The concentration of naphthalene after encapsulation in a series of hyperbranched polymers of different molecular weights and concentrations are shown in **Table 3.3**.

Table 3.3: Solubility of naphthalene in TRIS buffer solution with different concentrations and molecular weights of hyperbranched polymers

Mn	[Naphthalene] x 10 ⁻⁴ M			
	1.00 x 10 ⁻⁴ M	2.00 x 10 ⁻⁴ M	4.00 x 10 ⁻⁴ M	6.00 x 10 ⁻⁴ M
Without polymer	0.58	0.58	0.58	0.58
4000	1.20	1.30	1.86	2.26
8500	1.59	1.98	2.11	2.36
12500	1.79	2.44	2.56	2.90
27500	2.70	3.23	3.47	4.48
50000	2.91	3.94	4.49	6.28

As a control, the complexation experiment was repeated without the hyperbranched polymers as discussed in **Section 3.4.4**. The solution was assessed by UV-Vis spectrophotometer, and the calculated naphthalene concentration was 0.58 x 10⁻⁴ M, while as previously described (page 39), the maximum solubility of naphthalene has been recorded as high as 2.34 x 10⁻⁴ M.

The amount of naphthalene encapsulated inside the hyperbranched polymer was calculated by taking the result from **Table 3.3** and subtracting 0.58 x 10⁻⁴ M from it, and all values are tabulated in **Table 3.4** below.

Table 3.4: Amount of naphthalene encapsulated* in hyperbranched polymers

Mn	[Naphthalene] x 10 ⁻⁴ M			
	1.00 x 10 ⁻⁴ M	2.00 x 10 ⁻⁴ M	4.00 x 10 ⁻⁴ M	6.00 x 10 ⁻⁴ M
Without polymer	0.00	0.00	0.00	0.00
4000	0.62	0.72	1.28	1.66
8500	1.01	1.40	1.53	1.78
12500	1.21	1.86	1.98	2.32
27500	2.12	2.65	2.89	3.90
50000	2.33	3.36	3.91	5.70

*concentration after solubility of free naphthalene taken into account

Overall, the results showed that the solubility of naphthalene increased after encapsulation with hyperbranched polymers. The solubility also increased with increasing molecular weight of the hyperbranched polymers. For example, for a molecular weight of 4000 Da, at polymer concentration of 1.00 x 10⁻⁴ M, the concentration is 0.62 x 10⁻⁴ M and it increased to 2.33 x 10⁻⁴ M for molecular weight of 50000 Da. Similar trend applied to polymer concentration of 6.00 x 10⁻⁴ M, the naphthalene solubility increased from 1.66 x 10⁻⁴ M at polymer molecular weight of 4000 Da to 5.70 x 10⁻⁴ M at 50000 Da.

The increased polymer concentration also increased the solubility of naphthalene which was from 0.62 x 10⁻⁴ M at polymer concentration of 1.00 x 10⁻⁴ M to 1.66 x 10⁻⁴ M at polymer concentration of 6.00 x 10⁻⁴ M. If there is a linear relationship between polymer concentration and solubility of naphthalene, we should see the naphthalene concentration doubled at polymer concentration of 2.00 x 10⁻⁴ M, but this is not the case, which is clearly shown in **Figure 3.16**.

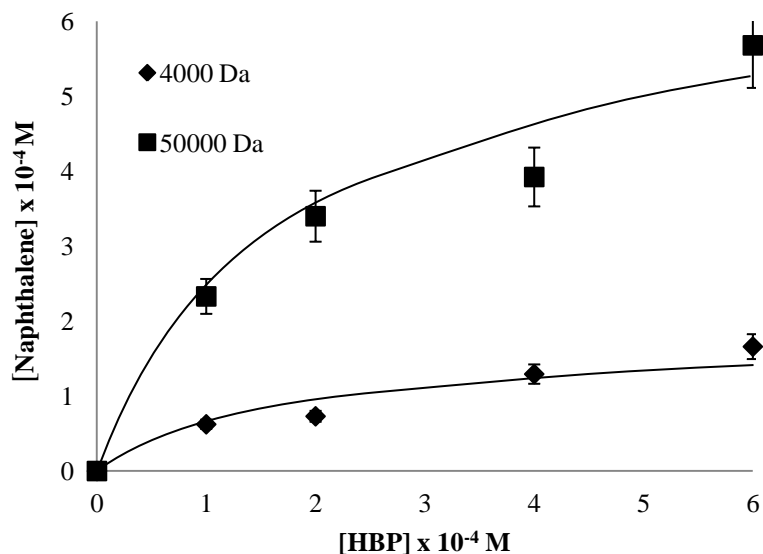


Figure 3.16: Concentration of encapsulated naphthalene with a molecular weight of 4000 Da and 50000 Da

From the graph, it was clearly demonstrated that the polymer with molecular weight of 4000 Da, the solubility of naphthalene increased up to polymer concentration of 2.00×10^{-4} M, and it starts to flattened at polymer concentration of 6.00×10^{-4} M. The graph also showed that not much increased of naphthalene solubility at polymer concentration of 4.00×10^{-4} M and 6.00×10^{-4} M which were 1.28×10^{-4} M and 1.66×10^{-4} M respectively. This shows the polymer concentration of more than 4.00×10^{-4} M was not required.

For polymer with molecular weight of 50000 Da, it was anticipated more solubilisation effect for bigger molecule, but it was not the case. At polymer concentration of 2.00×10^{-4} M, the solubility of naphthalene was 3.36×10^{-4} M and at polymer concentration of 4.00×10^{-4} M, the model drug solubility was only 3.91×10^{-4} M and at polymer concentration of 6.00×10^{-4} M, the solubility of naphthalene was only 5.70×10^{-4} M. This indicates that the polymer concentration exceeding than 4.00×10^{-4} M is not required.

After discussing the effects of increasing concentrations of naphthalene with concentration of polymer, the discussion continued with the relation between two hyperbranched polymer concentrations, which were 2.00×10^{-4} M and 4.00×10^{-4} M with different molecular weights of the polymer. An investigation was made to determine whether an increase of the polymer molecular weight really affects the solubility of naphthalene. **Figure 3.17** shows the relation between naphthalene concentration and different polymer molecular weights at hyperbranched polymer concentration of 2.00×10^{-4} M.

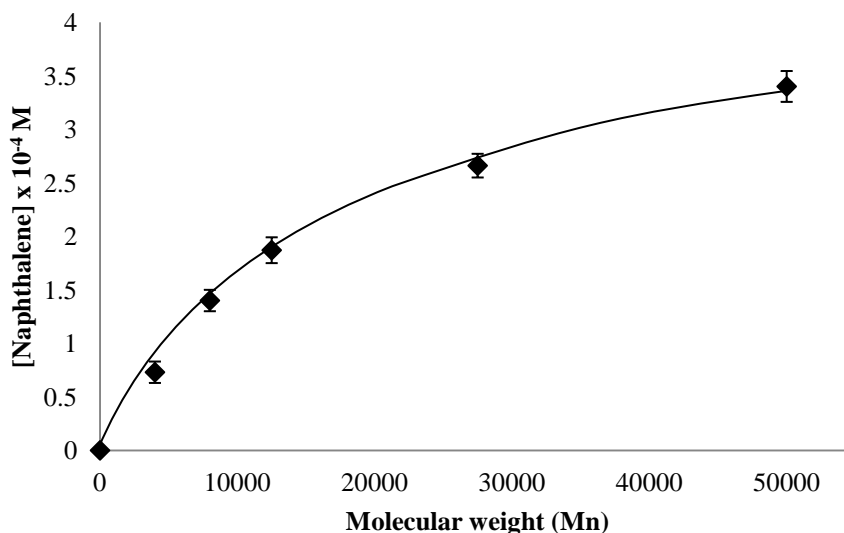


Figure 3.17: Encapsulated naphthalene concentration with different molecular weights of hyperbranched polymer at polymer concentration of 2.00×10^{-4} M

For polymer with a molecular weight of 4000 Da, the naphthalene concentration was 0.72×10^{-4} M and it doubled at molecular weight of 8500 Da. However, at polymer molecular weight of 12500 Da, the naphthalene concentration was only 1.86×10^{-4} M, and at polymer molecular weight of 50000 Da, the naphthalene concentration was 3.36×10^{-4} M. The naphthalene concentration increased until polymer molecular weight of 8500 Da and plateaued at polymer molecular weight of 50000 Da.

Figure 3.18 shows the effect of increase of polymer molecular weight with naphthalene concentration at polymer concentration of 4.00×10^{-4} M. For polymer molecular weight of 4000 Da, the solubility of naphthalene was 1.28×10^{-4} M and at polymer molecular weight of 8500 Da, the solubility increased to 1.53×10^{-4} M.

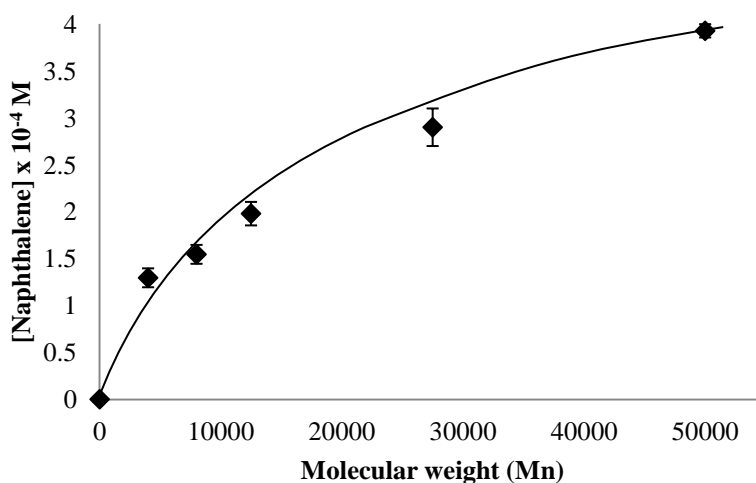


Figure 3.18: Encapsulated naphthalene concentration with different molecular weights of hyperbranched polymer at polymer concentration of 4.00×10^{-4} M

At polymer molecular weight of 12500 Da, the naphthalene concentration rose to 1.98×10^{-4} M. However, there was not much increased of naphthalene concentration when the molecular weight of the polymer increased until 50000 Da. From the above two graphs (**Figure 3.17** and **Figure 3.18**), it was clearly shown that the polymer molecular weight of more than 12500 Da gives less solubilisation effect for naphthalene.

It was anticipated that the above situation might be due to the aggregation of the polymers and steric effect which prevent the guest molecules solubilised inside the hydrophobic voids of the polymers (**Figure 3.19**).

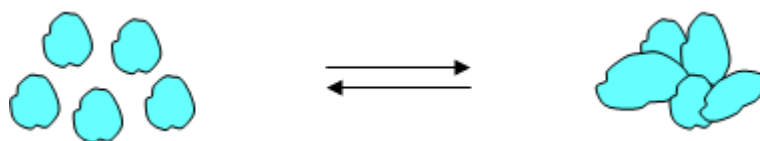


Figure 3.19: Aggregation of the hyperbranched polymers

A better view of the solubilisation behaviour for all samples are shown in **Figure 3.20**. It can be seen from the bar graph, that before encapsulation, the solubility of naphthalene is zero (after free solubility of naphthalene taken into account), and increases drastically after encapsulation with the host molecule. For example, for a host molecular weight of 8500 Da and concentration of 1.00×10^{-4} M, the concentration of naphthalene increased to 1.01×10^{-4} M. The concentration rose gradually to a host concentration of 6.00×10^{-4} M. This trend also applies to the increasing concentration of guest molecule with the increasing molecular weights of the host.

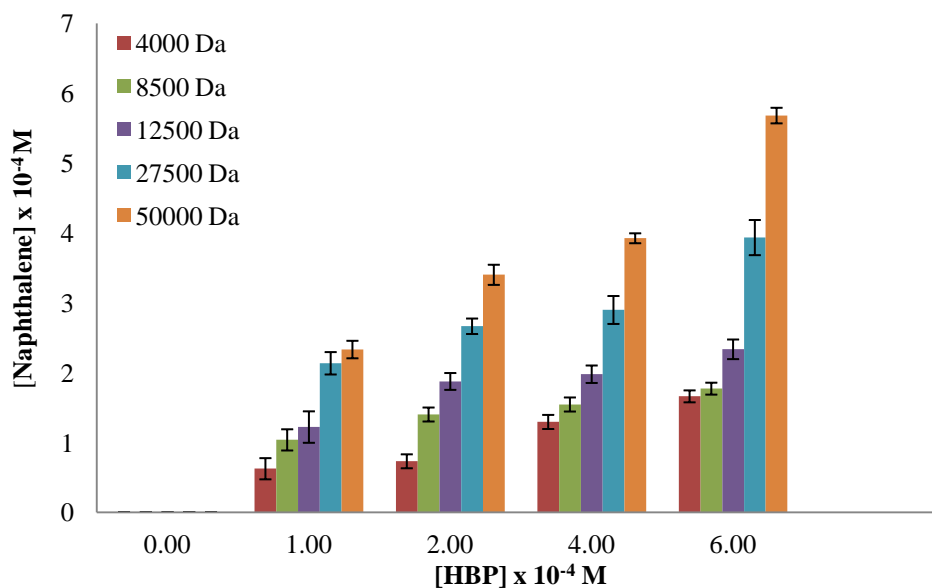


Figure 3.20: Increasing Mn and concentration of hyperbranched polymers with increasing concentration of encapsulated naphthalene

The data obtained show that these hyperbranched polymers have the ability to encapsulate guest molecules within their hydrophobic voids. A higher molecular weight resulted in higher loading of naphthalene. The loading per mole of polymer was calculated by dividing the concentration of naphthalene by the concentration of polymer. Different molecular weight resulted in different loading of guest molecule, for example, hyperbranched polymers with a concentration of 1.00×10^{-4} M, as shown in **Table 3.5**. Every mole of polymer with Mn 4000 Da can only encapsulate 1 mole of naphthalene. The number of moles of naphthalene increased to 2 for Mn 50000 Da. This shows that increasing molecular weight will increase the loading per mole of naphthalene in hyperbranched polymers.

Table 3.5: Naphthalene loading per mole of hyperbranched polymers with concentration of 1.00×10^{-4} M

Mn	Absorption	[Naphthalene] ($\times 10^{-4}$)M	Loading
4000	0.1298	0.62	1
8500	0.2117	1.01	1
12500	0.2539	1.21	1
27500	0.4499	2.12	2
50000	0.4910	2.33	2

Figure 3.21 shows part of a polymer with a molecular weight of 3000 g mol^{-1} . From this theoretical diagram, it can be seen that the polymer can be filled with around ten molecules of naphthalene. However, **Table 3.5** shows that only one naphthalene molecule was encapsulated in the polymer. For a larger Mn of polymer, the results showed that only two naphthalene molecules were trapped inside the hyperbranched polymers. This may be due to the physical property of naphthalene, a very hydrophobic molecule with two fused benzene rings, which only permit a small number of these molecules to be trapped in the cavities of the hyperbranched polymers. Other possibility

is the steric effect of the polymers which allows small amount of naphthalene trapped inside its' cavities.

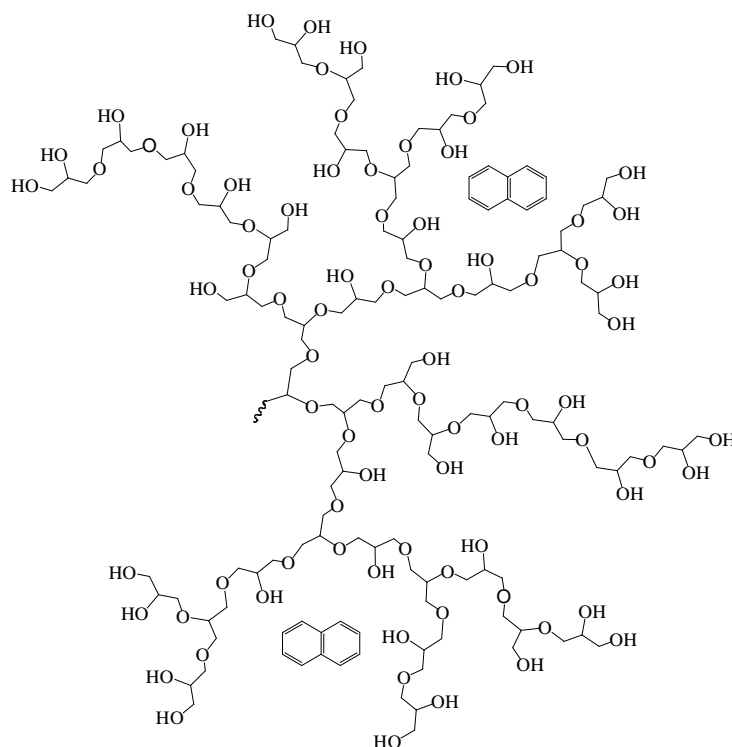


Figure 3.21: A representation of polyglycerol with naphthalene within the voids

3.4.6 Encapsulation of ibuprofen with hyperbranched polymers

The second molecule used to investigate the ability of hyperbranched polymers to solubilise hydrophobic moieties is ibuprofen. Ibuprofen is a non-steroidal anti-inflammatory drug widely used for pain and fever treatment. This drug has a molecular weight of $206.28 \text{ g mol}^{-1}$ and is detected at $\lambda_{\text{max}} = 222 \text{ nm}$. It has a polar and ionisable carboxylic acid functional group which gives it partial solubility in water (less than $4.80 \times 10^{-3} \text{ M}$). Although this drug is widely used in modern medicine, ibuprofen is not free of disadvantages. One of its side effects is aggravation of the stomach lining, leading to stomach ulceration and bleeding. Encapsulation of ibuprofen with these potential hyperbranched polymers may reduced the risk of side effects when administered into the human body.

Encapsulation using ibuprofen was carried out using the same method as discussed in **Section 3.4.4.1** (page 38). The absorbance peak was too strong as absorbance needs to be observable by UV, and therefore was diluted 50 fold and the absorbance was assessed at its characteristic wavelength. The initial concentration was calculated by dividing the actual absorbance by the extinction coefficient (ϵ) of ibuprofen. The extinction coefficient value was obtained graphically from a Beer Lambert plot as $8387.5 \text{ M}^{-1} \text{ cm}^{-1}$. It was then multiplied by 50 to get the concentration as shown in **Table 3.6** below.

Table 3.6: Solubility of ibuprofen in TRIS buffer solution with different concentrations and molecular weights of hyperbranched polymers

Mn	[Ibuprofen] x 10 ⁻⁴ M			
	1.00 x 10 ⁻⁴ M	2.00 x 10 ⁻⁴ M	4.00 x 10 ⁻⁴ M	6.00 x 10 ⁻⁴ M
Without polymer	2.68	2.68	2.68	2.68
4000	7.98	8.75	9.20	10.39
8500	8.08	9.60	11.24	12.57
12500	8.83	10.35	15.63	18.63
27500	10.13	12.77	18.80	21.25
50000	15.56	16.97	21.89	23.14

To calculate the exact amount of ibuprofen encapsulated in the hyperbranched polymers, a complexion without the hyperbranched polymers was prepared. Excess ibuprofen was dissolved in water and filtered. The solution was measured using UV and the value obtained was $2.68 \times 10^{-4} \text{ M}$. This amount was calculated by taking the result from **Table 3.6** and subtracting $2.68 \times 10^{-4} \text{ M}$ from it and the new data is shown in **Table 3.7** below.

Table 3.7: Amount ibuprofen encapsulated* in the hyperbranched polymers

Mn	[Ibuprofen] x 10 ⁻⁴ M			
	1.00 x 10 ⁻⁴ M	2.00 x 10 ⁻⁴ M	4.00 x 10 ⁻⁴ M	6.00 x 10 ⁻⁴ M
Without polymer	0.00	0.00	0.00	0.00
4000	5.30	6.07	6.53	7.71
8500	6.07	7.00	8.56	9.89
12500	6.15	7.67	12.95	12.95
27500	7.45	10.09	16.12	18.57
50000	12.88	14.29	19.21	20.46

*Concentration after free ibuprofen solubility taken into account

From the above table, it can be seen that the concentration of ibuprofen increased with increasing concentrations and molecular weights of the polymer. For a better view of the discussions, we chose hyperbranched polymers with a molecular weight of 4000 Da and 50000 Da, as shown in **Figure 3.22**.

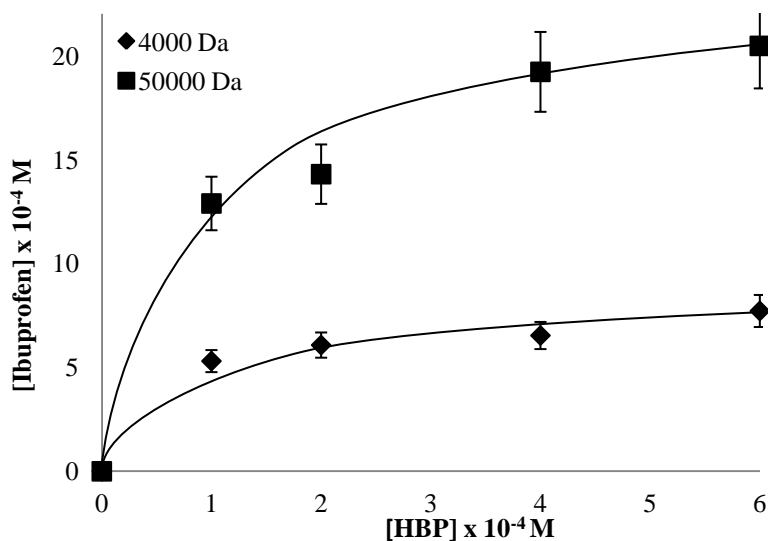


Figure 3.22: Increased encapsulated ibuprofen concentration with increased molecular weights and concentrations of hyperbranched polymers

For hyperbranched polymers with a molecular weight of 4000 Da, the concentration of ibuprofen rose after encapsulation with a hyperbranched polymer with a concentration of 2.00×10^{-4} M and after this point, there was not much increased in ibuprofen concentration. The same pattern was also detected for a hyperbranched polymer with a molecular weight of 50000 Da. If we look carefully, the trendline increased gradually at polymer concentration of 2.00×10^{-4} M and plateaued at 6.00×10^{-4} M. It was clearly shown that polymer concentration of more than 4.00×10^{-4} M is not required.

To investigate the maximum polymer molecular weight for solubilising ibuprofen, a graph of encapsulated ibuprofen concentration versus different polymer molecular weights is plotted as shown in **Figure 3.23**.

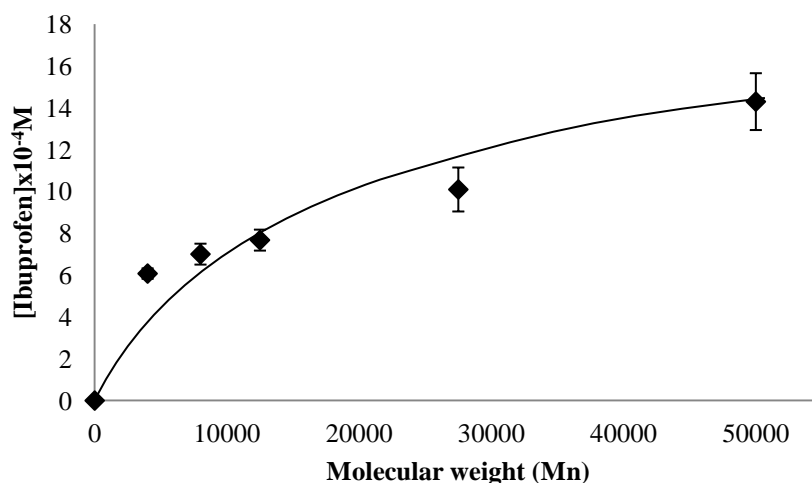


Figure 3.23: Encapsulated ibuprofen concentration with different molecular weights of hyperbranched polymer at hyperbranched polymer concentration of 2.00×10^{-4} M

The above graph demonstrated the relation between encapsulated ibuprofen concentration with different polymer molecular weights at hyperbranched polymer concentration of 2.00×10^{-4} M. At polymer molecular weight of 4000 Da, the ibuprofen concentration was 6.07×10^{-4} M and it rose to 7.67×10^{-4} M at polymer molecular

weight of 12500 Da. After polymer molecular weight of 12500 Da, there was no significant increased in ibuprofen concentration.

Figure 3.24 showed the encapsulated ibuprofen concentration with different molecular weights of hyperbranched polymer at polymer concentration of 4.00×10^{-4} M. The graph shows the same trend as previous graph, where, the ibuprofen concentration increased to 12.95×10^{-4} M at polymer molecular weight of 12500 Da and not much increased in ibuprofen concentration (19.21×10^{-4} M) at polymer molecular weight of 50000 Da. It was postulated that the polymers experienced an aggregation and become more significant at higher molecular weight.

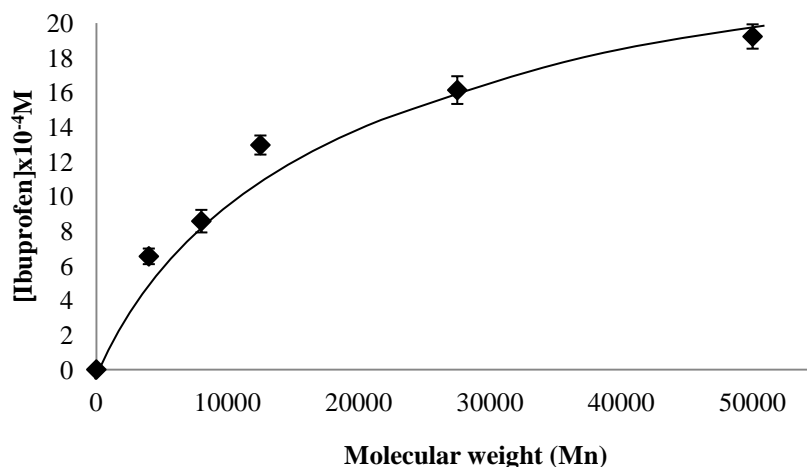


Figure 3.24: Encapsulated ibuprofen concentration with different molecular weights of hyperbranched polymer at hyperbranched polymer concentration of 4.00×10^{-4} M

Illustration of the behaviour of the solubilisation effect on different polymer concentrations and molecular weights are shown in **Figure 3.25**. The concentration of encapsulated ibuprofen increased with increasing polymer concentration and molecular weight. From the bar graph below, for a hyperbranched polymer with a molecular weight of 4000 Da, the lowest concentration of ibuprofen was 5.30×10^{-4} M and the highest concentration was 7.71×10^{-4} M. If we take the highest molecular weight of

50000 Da, the highest concentration of ibuprofen was 20.46×10^{-4} M. This could be due to the formation of hydrogen bonds between the carboxylic group of ibuprofen and the interior of the polymers.

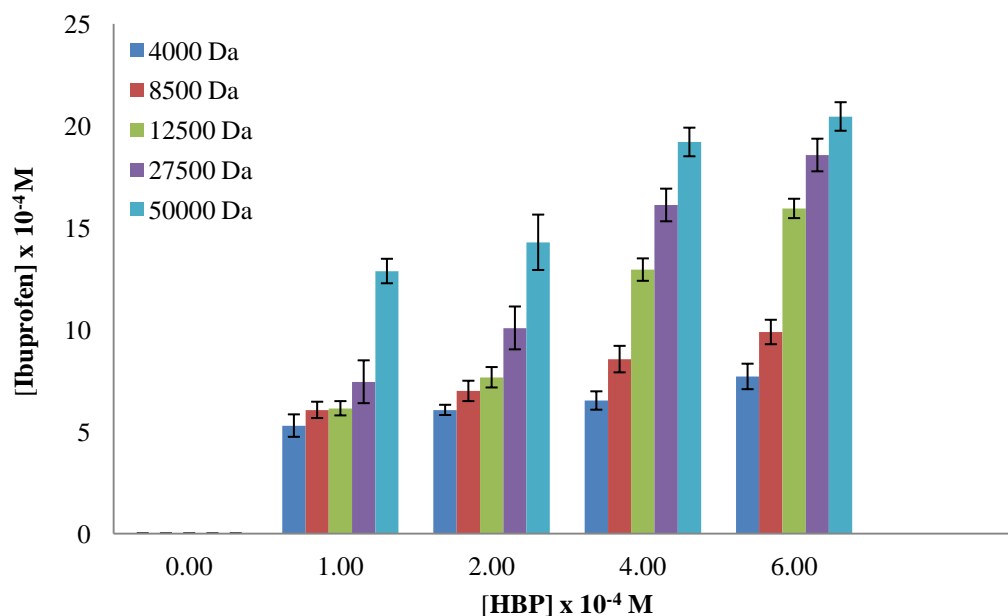


Figure 3.25: Increased concentration of encapsulated ibuprofen after encapsulation with different concentrations and molecular weights of hyperbranched polymer

As previously discussed, the concentration of ibuprofen increased gradually and plateaued at a polymer concentration of 6.00×10^{-4} M. From the results, the loading of ibuprofen per mole of polymers can be calculated. The loading was defined by dividing the concentration of ibuprofen with the concentration of polymer. **Table 3.8** below shows the loading of ibuprofen if only 1.00×10^{-4} M polymers were consumed. The loading increased with an increase in molecular weights of the hyperbranched polymers.

Table 3.8: Ibuprofen loading per mole of hyperbranched polymers with a concentration 1.00×10^{-4} M

Mn	Absorption	[Ibuprofen] ($\times 10^{-4}$) M	Loading
4000	0.1338	5.30	5
8500	0.1355	6.07	6
12500	0.1482	6.15	6
27500	0.1700	7.45	7
50000	0.2611	12.88	13

The encapsulation of ibuprofen within the cavities of the hyperbranched polymers is illustrated below in **Figure 3.26**. This figure reveals only a part of the hyperbranched polymers to show the entrapment of ibuprofen. From **Table 3.8**, the loading of ibuprofen per mole of polymer was 5 for the lowest molecular weight, increasing to 13 for polymers with a molecular weight of 50000 Da. More ibuprofen was trapped in the cavities of the hyperbranched polymers due to the formation of hydrogen bonds between the interior of the hyperbranched polymers and the carboxylic groups of ibuprofen.

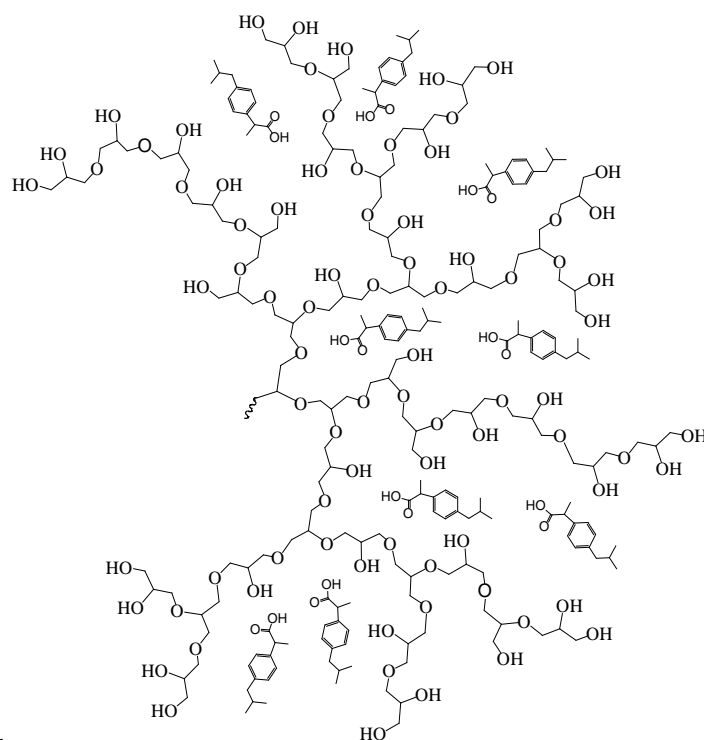


Figure 3.26: Ibuprofen filled into a hyperbranched polymer

As ibuprofen has some solubility in water therefore the signal can be detected by the NMR instrument, so this technique was used to prove the complex formation within the hydrophobic voids of hyperbranched polymers. **Figure 3.27** shows the spectrum of a simple mix of ibuprofen and hyperbranched polymers, and **Figure 3.28** reveals the spectrum of ibuprofen after being encapsulated within the polymers.

In **Figure 3.27**, the broad peak from 4.00 to 3.25 ppm can be attributed to the hyperbranched polymer backbone whereas the peaks at 2.32, 1.23 and 0.71 ppm refer to ibuprofen peaks. Significantly, the ibuprofen intensity peaks increased around 20 % when the drug formed a complex with the hyperbranched polymer. The concentration of ibuprofen rose from 2.68×10^{-4} M to 3.12×10^{-4} M with polymer concentration of 1.00×10^{-4} M. This is shown in **Figure 3.28**. The hyperbranched polymer peak was normalised,

so that the peak are the same size. Therefore, any increases in ibuprofen peaks are due to the increased in ibuprofen solubility.

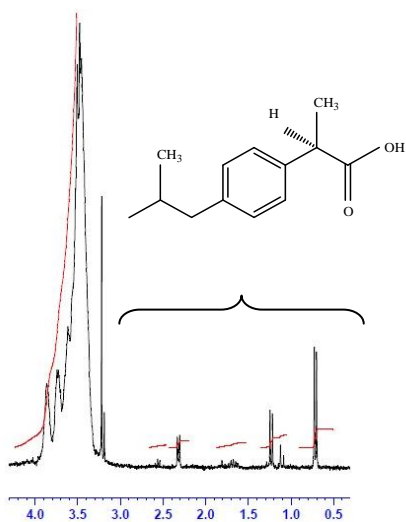


Figure 3.27: ¹H NMR spectrum of mixing of ibuprofen with hyperbranched polymer in D₂O

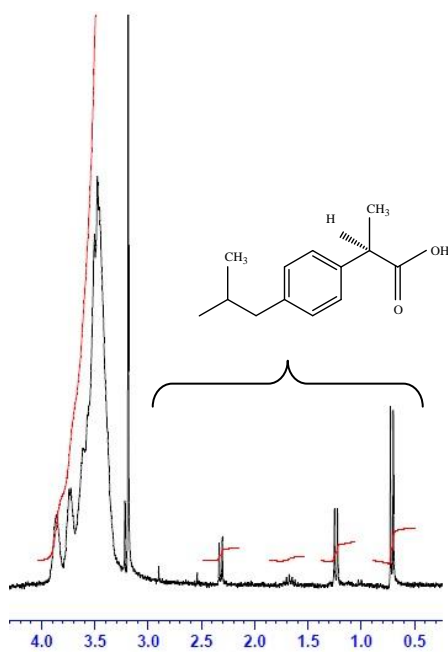


Figure 3.28: ¹H NMR spectrum of complexation of ibuprofen with hyperbranched polymers in D₂O

In conjunction with UV studies that hyperbranched polymers can enhance the solubility of ibuprofen. From this promising data, further investigation was carried out using a bigger molecule, from the porphyrin group, i.e. tetracarboxyphenyl porphyrin (TCPP). TCPP was encapsulated with the hyperbranched polymers. This model drug has been studied extensively in the application of cancer treatment.

3.4.7 Photodynamic therapy

Photodynamic therapy (PDT) is a promising clinical tumour treatment, especially for the treatment of digestive tract, skin, bladder, respiratory and head and neck cancers. PDT is based on the induction of cell death by the administration of special drugs known as photosensitisers (PS) which selectively accumulate in the tumour tissue, followed by subsequent exposure to light of an appropriate wavelength and the presence of oxygen.⁵¹⁻⁵³ The advantages of PDT compared to conventional methods are that it has very low systemic toxicity, PS is only activated in the presence of light, it has the ability to selectively destroy the tumours and PDT can be used alone or in combination with other therapeutic modalities such as chemotherapy, radiotherapy, immunotherapy or surgery.⁵⁴ However, the rest of the body must be protected from light (unless the PS only accumulates in the tumour).

3.4.7.1 Mechanism of photodynamic therapy

The main factors that plays an important role in PDT are the photosensitisers, the radical singlet oxygen ($^1\text{O}_2$) and the delivery of light source. The basic routes by which the combination of photosensitizer (PS), light and O_2 are delivered are shown in **Figure 3.29**. A ground state of PS contains two electrons of opposite spins at a low energy molecular level, known as the singlet state (S_0). This non-excitation state of PS absorbs visible light (photons) and shifts to an electronically excited singlet state (S_1). This state is short lived and loses its energy by emitting fluorescent light. The excited singlet state PS may also undergo a process known as intersystem crossing, where the excited

electron converts to a long-lived triplet excitation state (T1) and its energy is dissipated by emitting phosphorescent light.

The PS in a triplet excitation state can undergo two types of reaction. Firstly, PS reacts directly with molecules to form various species of hydrogen atom or an electron, or generates radicals that interact with the oxygen atom to produce a reactive oxygen species (ROS), which are toxic to all cells. In the other reaction, PS transfers its energy directly to the ground state molecular oxygen to form an excited state singlet oxygen (1O_2).⁵¹⁻⁵⁹ The latter reaction is an important indicator of successful PDT.

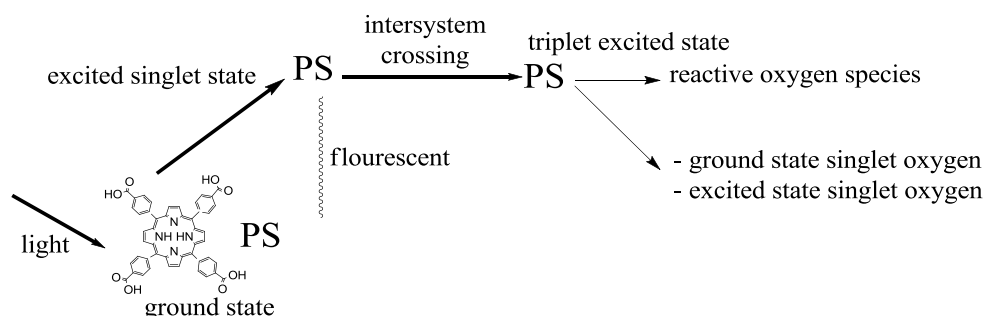


Figure 3.29: Photodynamic therapy mechanism

In the early stages of the PDT experiment, the photosensitisers used were haematoporphyrin (HP) and its derivative (HPD) which is a mixture of mono-, di- and oligomers of porphyrin. A photosensitizer suitable for PDT should have several characteristics including chemical purity, selectivity for tumour cells, chemical and physical stability, a short time interval between administration and maximum accumulation within tumour tissues, activation of wavelengths with optimal tissue penetration and be easily removed from the body. The four main classes of photosensitisers are porphyrin derivatives, chlorins, phthalocyanines and porphycenes.⁵¹ These photosensitisers are directly administered into the body and ideally they accumulate in the affected cancerous area.

However, this is not always the case. A mechanism known to help with accumulations of molecules within tumors is the enhanced permeability and retention (EPR) effect. The EPR effect is a phenomenon whereby a certain size of a molecule, especially big molecules such as macromolecules and nanoparticles, tend to accumulate in tumour tissue. These occur when tumour cells undergo aggregation and new blood vessels are produced to fulfil oxygen and nutrient demands from the tumour cell. This new blood vessel has an irregular in shape and openings at the cell surface. These big molecules are not easily removed and they are retained in the tumour.⁶⁰⁻⁶³ **Figure 3.30** illustrates the EPR effect.

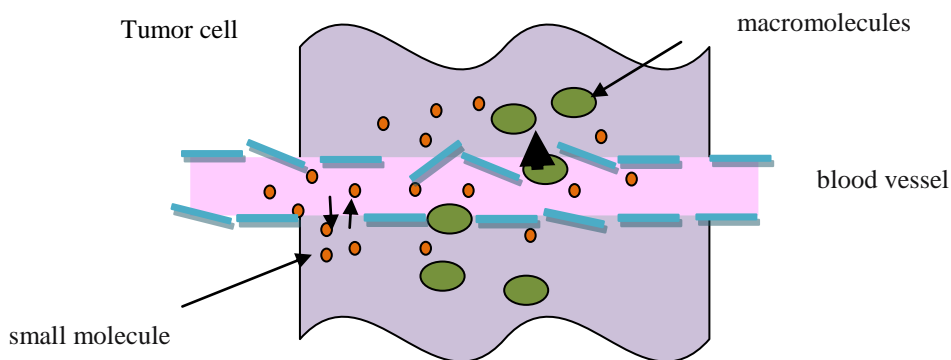


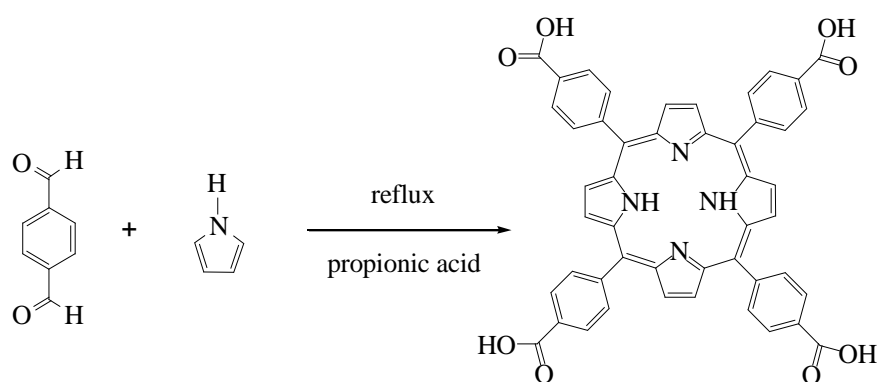
Figure 3.30: Schematic representation of the EPR effect

The following discussion will point out the importance of this effect in designing a big drug delivery system, which consists of a porphyrin derivative and is encapsulated within hyperbranched polymers with different molecular weights.

3.4.5.2 Synthesis of tetracarboxyphenyl porphyrin (TCPP)

Tetracarboxyphenyl porphyrin (TCPP) (**Scheme 6**) was synthesized by refluxing 4-carboxy benzaldehyde and pyrrole in propionic acid. The black slurry mixture was filtered and then washed with refluxing dichloromethane. The product obtained was a deep purple crystal. Confirmation of the product was achieved using ^1H NMR, UV-vis

spectrometer, mass spectrometer and CHN analysis. A singlet was observed at 8.86 ppm and was assigned to the pyrrolic β -protons. A quartet peak was seen around 8.23 ppm and was attributed to the 16 phenyl protons. The highly shielded -NH protons were seen at -2.95 ppm. A singlet peak at 13.32 ppm was due to the 4 protons attached to the carboxylic group. Mass spectrometry showed the exact molecular ion with M/z of 791. UV-Vis spectrophotometry revealed characteristic peaks at $\lambda_{\text{max}} = 412, 512, 546, 588$ and 645 nm.



Scheme 6 : Synthesis of tetracarboxyphenyl porphyrin

3.4.7.3 Encapsulation of tetracarboxyphenyl porphyrin with hyperbranched polymers

The third model drug used was tetracarboxyphenyl porphyrin. This model drug has a molecular weight of 791.44 gmol^{-1} and was synthesised successfully using chemicals available in the laboratory. Encapsulation of tetracarboxyphenyl porphyrin was done using four different polymer concentrations and five different molecular weights. The complexes were added to TRIS buffer at pH 7.4 at 0.1 M. The absorbance of all solutions was recorded using a UV-vis spectrophotometer. A strong porphyrin peak was detected at $\lambda_{\text{max}} = 415 \text{ nm}$. The purple red colour of porphyrin can be seen by the naked eye, and several dilutions were needed to reduce the concentration and ascertain the correct absorbance for the sample. For hyperbranched polymers with molecular weights of 4000 Da and 8500 Da, dilutions were made 100 fold. For polymers with molecular

weights of 12500 Da, 27500 Da and 50000 Da, 200 fold dilutions were performed to record the suitable spectra.

TCPP concentration was determined by dividing the absorbance from raw UV data by the standard extinction coefficient (ϵ) of TCPP which was calculated as $3.30 \times 10^5 \text{ M}^{-1} \text{ cm}^{-1}$. This value was then multiplied by the number of dilutions made to determine the concentration of TCPP. The values of different concentrations and molecular weights are tabulated in **Table 3.9**.

Table 3.9: Solubility of tetracarboxyphenyl porphyrin in TRIS buffer solution with different concentrations and molecular weights of hyperbranched polymers

Mn	[Tetracarboxyphenyl porphyrin] x 10 ⁻⁴ M			
	1.00 x 10 ⁻⁴ M	2.00 x 10 ⁻⁴ M	4.00 x 10 ⁻⁴ M	6.00 x 10 ⁻⁴ M
Without polymer	0.72	0.72	0.72	0.72
4000	2.09	2.61	3.44	3.61
8500	2.43	3.21	3.60	3.79
12500	3.48	5.19	8.32	9.92
27500	4.69	7.92	9.12	10.17
50000	5.73	9.04	10.55	11.65

As a control, the solubility of TCPP in water was determined by dissolving an excess amount of TCPP in water. All undissolved TCPP was filtered. The solution was measured using UV and the absorbance was divided by the extinction coefficient constant; the value was $0.72 \times 10^{-4} \text{ M}$. The amount of TCPP encapsulated in the hyperbranched polymer (**Table 3.9**) was subtracted with $0.72 \times 10^{-4} \text{ M}$; the data is shown below in **Table 3.10**.

Table 3.10: Amount of TCPP encapsulated* inside hyperbranched polymer

Mn	[Tetracarboxyphenyl porphyrin] x 10 ⁻⁴ M			
	1.00 x 10 ⁻⁴ M	2.00 x 10 ⁻⁴ M	4.00 x 10 ⁻⁴ M	6.00 x 10 ⁻⁴ M
Without polymer	0.00	0.00	0.00	0.00
4000	1.39	1.91	2.74	2.91
8500	1.73	2.51	2.90	3.09
12500	2.78	4.49	7.62	9.22
27500	3.99	7.22	8.42	9.47
50000	5.03	8.34	9.85	10.95

*Concentration after free TCPP taken into account

The results showed that the concentration of TCPP increased with increased concentration of hyperbranched polymers. The behaviour of these encapsulation experiments is depicted in **Figure 3.31**. For hyperbranched polymers with a molecular weight of 4000 Da, TCPP concentration increased up to a polymer concentration of 2.00 x 10⁻⁴ M and became plateaued at a polymer concentration of 6.00 x 10⁻⁴ M. The same pattern applied to a polymer with a molecular weight of 50000 Da.

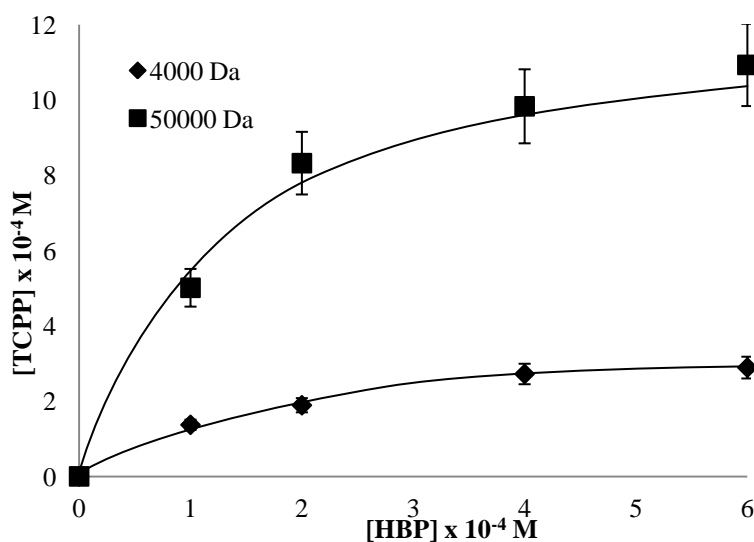


Figure 3.31: Encapsulated TCPP concentration for molecular weight of 4000 Da and 50000 Da

A closer look at the above graph showed that there was not much increased in TCPP concentration above polymer concentration of 4.00×10^{-4} M. To investigate the effect of the polymer molecular weight in solubilising TCPP, a graph between TCPP concentration with different polymer molecular weights at hyperbranched polymer concentration of 2.00×10^{-4} M and 4.00×10^{-4} M were plotted in **Figure 3.32** and **Figure 3.33** respectively.

Figure 3.32 showed the TCPP concentration was 1.91×10^{-4} M at polymer molecular weight of 4000 Da and it increased to 4.49×10^{-4} M at polymer molecular weight of 12500 Da. Further increased in polymer molecular weight did not make any significant changes in TCPP concentration.

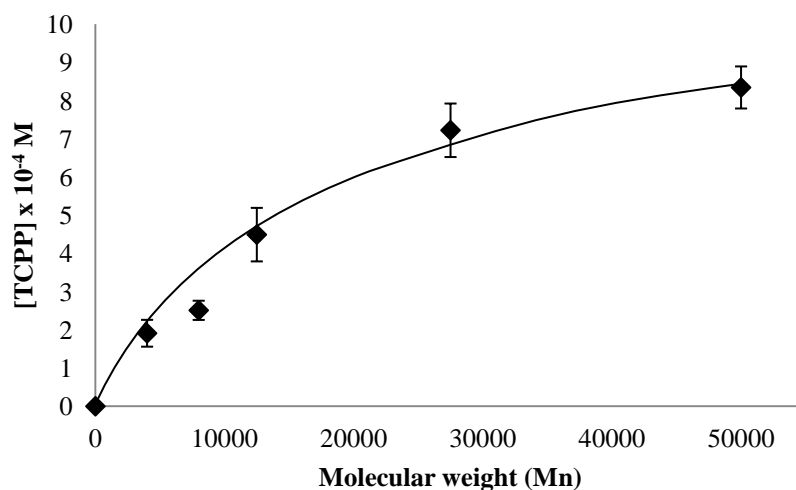


Figure 3.32: Encapsulated TCPP concentration of 2.00×10^{-4} M with different molecular weights of hyperbranched polymer

Figure 3.33 demonstrated encapsulated TCPP concentration at various polymer molecular weights at hyperbranched polymer concentration of 4.00×10^{-4} M. The same trend was observed, where TCPP concentration increased to 7.62×10^{-4} M at polymer molecular weight of 12500 Da, and only a small increment of TCPP concentration at 50000 Da.

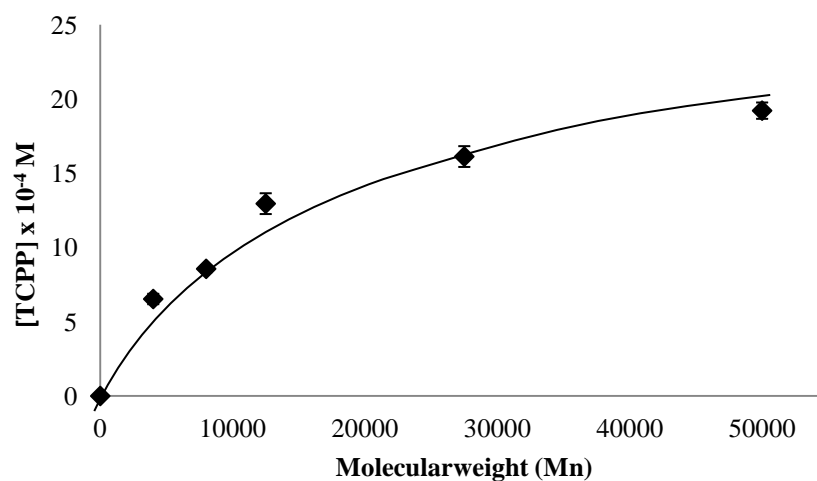


Figure 3.33: Encapsulated TCPP concentration of 4.00×10^{-4} M with different molecular weight of hyperbranched polymer

From the above observation, for both hyperbranched polymer concentrations used (2.00×10^{-4} M and 4.00×10^{-4} M), the polymer molecular weight of above 12500 Da did not showed any significant difference in solubilising TCPP. This trend might be due to aggregation of polymers at higher concentration.

Further evidence for these results is depicted in **Figure 3.34**. It can be seen in the bar graph, that TCPP concentration increased after encapsulation with each molecular weights used in these studies. TCPP concentration also increased with increased polymer concentration. Let's take a closer look at polymers concentration of 1.00×10^{-4} M and 6.00×10^{-4} M with different molecular weights. For a polymer concentration of 1.00×10^{-4} M and a molecular weight of 4000 Da, TCPP concentration was 1.39×10^{-4} M and this almost tripled at a molecular weight of 50000 Da, at 5.03×10^{-4} M. The same pattern applied to a polymer concentration of 6.00×10^{-4} M and a molecular weight of 4000 Da: TCPP concentration was 2.91×10^{-4} M and increased to 10.95×10^{-4} M at 50000 Da. From these observations, it was concluded that higher molecular weights give higher concentrations of TCPP.

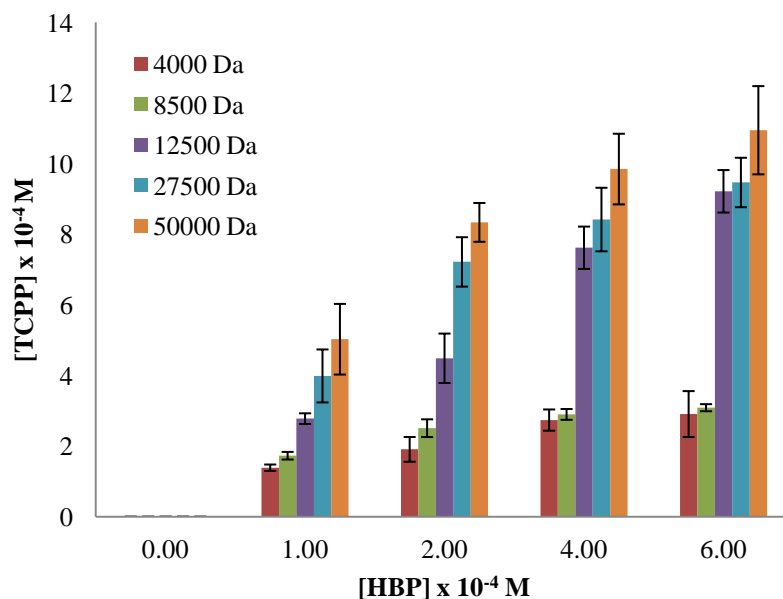


Figure 3.34: Increased concentration of encapsulated TCPP after encapsulation with different concentrations and molecular weights of hyperbranched polymer

Even though the concentration increased with increased molecular weight of the hyperbranched polymers, there was no real changes from a molecular weight of 12500 Da to 50000 Da. They reached a limit at 12500 Da and 12500 Da could be the best molecular weight to encapsulate TCPP. There was not much increased for 50000 Da with respect to solubility, but this might be useful in the delivery systems, as size is important factor in the EPR effect.

In order to calculate the TCPP loading per mole of polymer, one polymer with a concentration of 1.00×10^{-4} M was selected. Loading per mole of TCPP in polymers was obtained by dividing the TCPP concentration after encapsulation with the polymer concentration. For this purpose, hyperbranched polymers with a concentration of 1.00×10^{-4} M were used as the model of calculation. All values are shown in **Table 3.11**.

Table 3.11: Tetracarboxyphenyl porphyrin loading per mole of hyperbranched polymers with concentration of 1.00×10^{-4} M

Mn	Absorption	[TCPP] ($\times 10^{-4}$)M	Loading
4000	0.6918	1.39	1
8500	0.8019	1.73	2
12500	0.5755	2.78	4
27500	0.7741	3.99	4
50000	0.9454	5.03	5

The results show that, only one mole of porphyrin was encapsulated within the cavities of the polymer at 4000 Da. At a molecular weight of 50000 Da, only five moles of TCPP can be accommodated in the polymer dendritic box. This value is quite reasonable, because TCPP is a big molecule and has carboxylic groups attached to the main molecule. The carboxylic group may interact with the interior of the polymers. Other possibility is the steric effect between the polymer and TCPP. **Figure 3.35** represents a portion of a hyperbranched polymers filled with some porphyrin molecules, which indicates that the numbers obtained in **Table 4.9** are realistic.

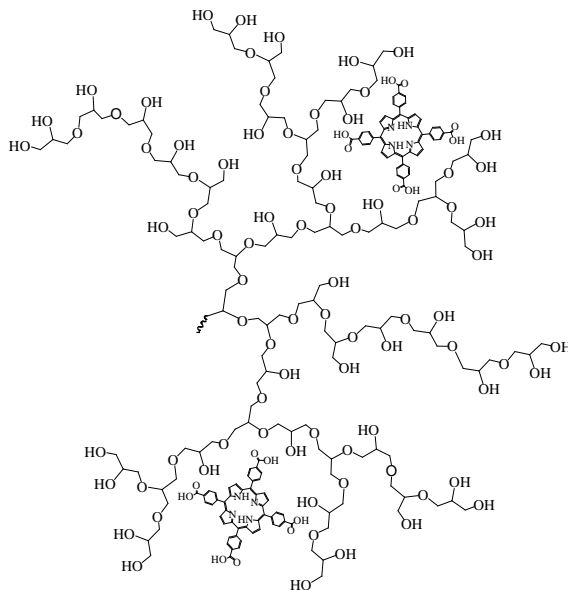


Figure 3.35: Tetracarboxyphenyl porphyrin filled in hyperbranched polymers

A further investigation was done using a real drug to combat prion disease. This drug was synthesized by other group in the department (Dr Chen's group) Therefore, the following discussion is about encapsulation of the anti-prion drug with hyperbranched polymers.

3.4.8: Encapsulation of hyperbranched polymers with an anti-prion drug for prion therapy application

3.4.8.1 Prion Disease

Prion diseases, also known as transmissible spongiform encephalopathies (TSEs), are a group of animal and human brain diseases.⁶⁴ TSEs in humans include Creutzfeldt-Jakob disease (CJD), kuru, Gerstmann-Straussler-Scheinker Syndrome (GSS), fatal familial insomnia (FFI) and new variant JCD (nvCJD). These diseases are predominantly inherited by 10% of sufferers, and less than 1% are acquired by infection. The disease also affects sheep and goats, cats, pumas and cheetahs.⁶⁴ All prion diseases are progressive, fatal and presently incurable. Prion disease is associated with the accumulation of prion protein in the brain.⁶⁵⁻⁶⁶ Prions are infectious agents, composed of misfolded protein. When this happens, protein aggregates and has a toxic effect on the adjacent protein.

3.4.8.2 Anti-prion drug

After unsuccessful attempts to make collaboration with other university to evaluate the performance of our hyperbranched polymer. It was found that the evaluation was not what we required. Therefore a collaboration with Dr Chen's group in our department. This group eventually synthesised drugs for prion disease. The anti-prion drug is shown below in **Figure 3.36**.

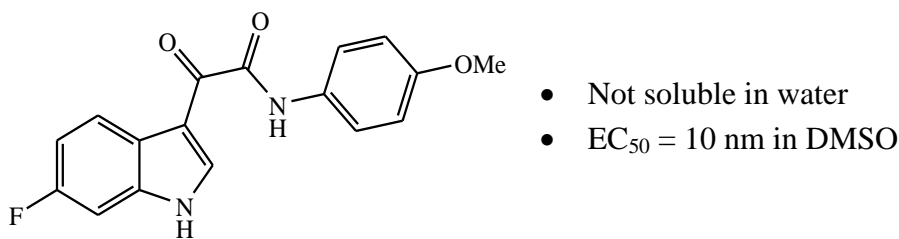


Figure 3.36: Anti-prion drug used in encapsulation study

The drug synthesis was a good anti-prion drug but is insoluble in water. Therefore, we proposed to encapsulate this drug with our hyperbranched polymers. The following discussions is about our investigation of the performance of hyperbranched polymers in complex formation with the anti-prion drug.

3.4.8.2 Complex formation of anti-prion drug with hyperbranched polymers

The previous drugs and models were encapsulated using different molecular weights and concentrations. However, for prion therapy studies, only one polymer was selected hyperbranched polymers with a molecular weight of 12500 Da. This polymer was chosen because previous results showed that hyperbranched polymers with a molecular weight of 12500 Da give the best encapsulation outcome. This anti-prion drug does not dissolve in water. Therefore, to evaluate the characteristic peak of the drug, excess drug was dissolved in methanol and filtered to separate the undissolved drug. The solution was measured using a UV-Vis spectrophotometer, and the peak was at 335 nm, as shown in **Figure 3.37**. Methanol was used as the solvent because it has a similar polarity as water.

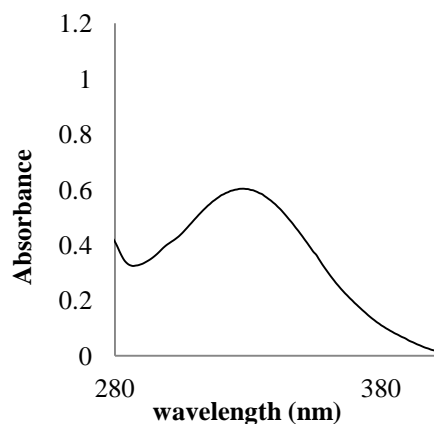


Figure 3.37: UV spectra of anti-prion drug in methanol

The anti-prion drug used is completely insoluble in water: therefore, it was interesting to explore how this hyperbranched polymer could effectively encapsulate the drug. Both drug and polymer were dissolved separately in methanol. Both solution were then physically mixed and all solvents removed in vacuo to form co-precipitation. Water was then added and finally the solution was filtered to remove any undissolved drug. The active compound in the sample was detected using a UV-Vis spectrophotometer. The spectrum is shown in **Figure 3.38**.

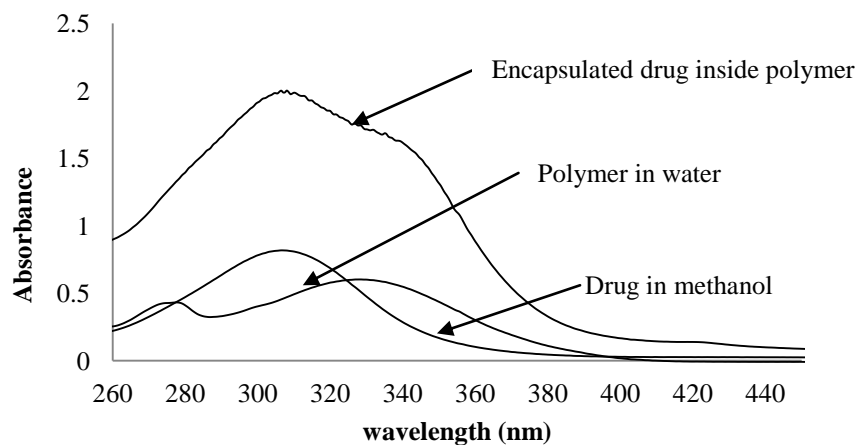


Figure 3.38: UV spectra of a hyperbranched polymer in water, an antiprion drug in methanol and encapsulation of the drug with a hyperbranched polymer

The hyperbranched polymer peak was detected at 310 nm. A shoulder peak was clearly observed in the encapsulated spectra at 330 nm. The concentration of encapsulated drug can be calculated by dividing the absorbance of the drug by the standard extinction coefficient (ϵ) of the drug. The standard extinction coefficient of the drug was determined using a Beer Lambert plot which and was $19155 \text{ M}^{-1}\text{cm}^{-1}$. After calculation, the concentration of the drug increased to $9.02 \times 10^{-5} \text{ M}$. The concentration of polymers used in these study was $3.42 \times 10^{-4} \text{ M}$. This was clearly proof, that hyperbranched polymers can solubilised hydrophobic molecules inside their hydrophobic voids. Loading per mole of drug that can be encapsulated inside the polymers was obtained by dividing the polymer concentration by the drug concentration. From the calculation, only 0.27 mole of drug was encapsulated inside the hyperbranched polymers.

3.4.8.3 Cytotoxicity Studies

This study was carried out with the collaboration of Mr Luo Lei, a member from Dr Chen's group. To determine whether these hyperbranched polymers can behave as a delivering agent, a cytotoxicity test was carried out. This test was done using MTT assay against a cultured scrapie mouse brain cell. The MTT assay is based on the ability of a mitochondrial dehydrogenation enzyme in viable cells to cleave the tetrazolium rings of the pale yellow MTT and form formazon crystals with a purple colour.⁶⁷ Therefore, the number of surviving cells is directly proportionate to the level of the formed formazon. The MTT assay of all hyperbranched polymers with three different concentrations, 100 μM , 500 μM and 1000 μM , are depicted in **Figure 3.39**. As shown in the bar chart, all polymers were not toxic against the scrapie mouse brain (SMB) cell.

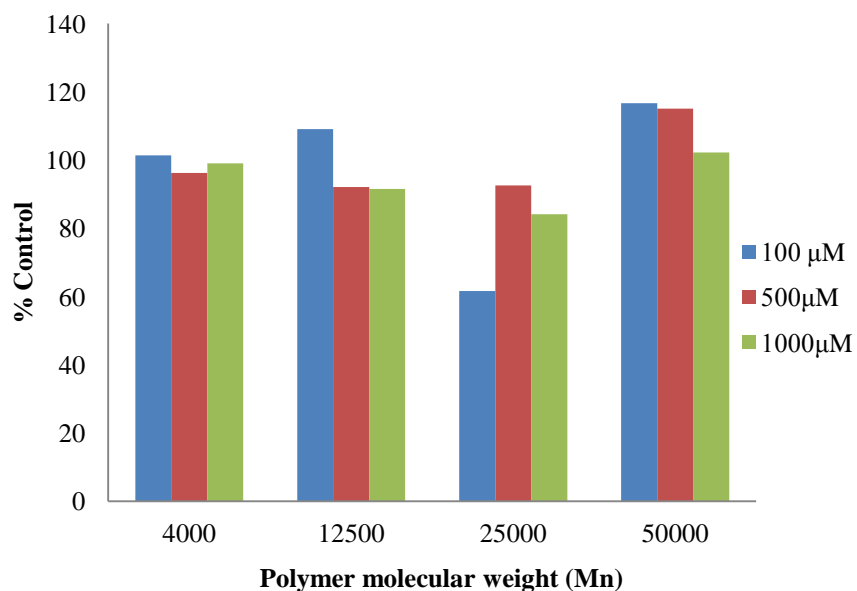


Figure 3.39: UV spectra of a hyperbranched polymer in water, an antiprion drug in methanol and encapsulation of the drug with a hyperbranched polymer

EC₅₀ of a drug denotes as measurement of the concentration of drug which gives 50% of the maximum response.⁶⁸ Even though the EC₅₀ of the drug against the SMB cell is 10 nm, it is in DMSO, whereas the EC₅₀ of the drug encapsulated in the hyperbranched polymer is 0.693 μM, but it is in water (**Figure 3.40**). From this preliminary studies, it is concluded that hyperbranched polymers have the ability to bind drugs inside their hydrophobic voids. We proposed that the mechanism of solubility enhancement is due to the hydrophobic interaction between the drug and moieties inside the hyperbranched polymers.

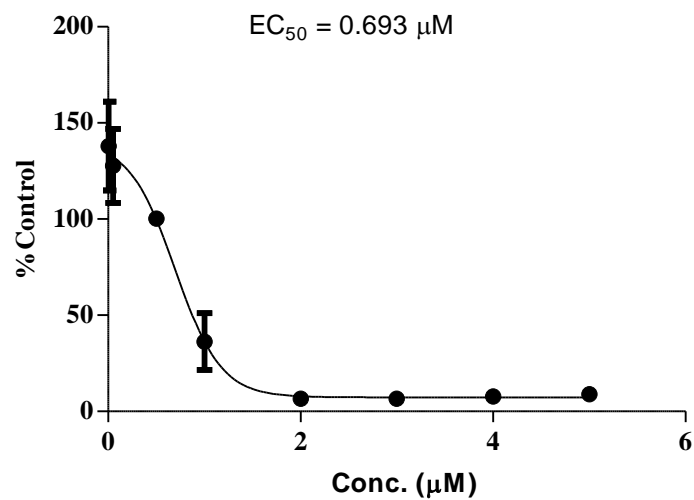


Figure 3.40: The EC₅₀ of the drug encapsulated with hyperbranched polymers

From all the above results, starting from synthesising water soluble hyperbranched polymer, encapsulation studies with model drugs and drug and finally the toxicity test showed the water soluble hyperbranched polymer is a promising candidate as drug delivery system.

Chapter 4: Synthesis and Characterization of Hyperbranched Polyglycidol Conjugated with Poly(ethylene) Glycol and Folic Acid (PG-PEG-Folate)

4.1 Overview and aim

Cancer is a common disease in the modern world. More than one in three people will develop some form of cancer during their lifetime. Diet, lifestyle and environment are major factors that cause this disease. Most drugs for cancer treatment have very poor solubility in water. This, and their instability in a biological environment make it difficult to deliver them to specific sites in safe dosages.³⁶

Camptothecin, **12** (Figure 4.1) has been widely used to treat various types of cancer but can damage DNA, leading to cell destruction. This drug has very low solubility in water and its side effect is inflammation of the urinary bladder. In order to overcome these problems, this drug has been conjugated with liposomes, micelles and emulsions. Cisplatin, **13**, also has some effects when introduced into the human body. The formation of stable DNA-cisplatin complexes, resulting in the formation of a DNA structure that prevents replication.

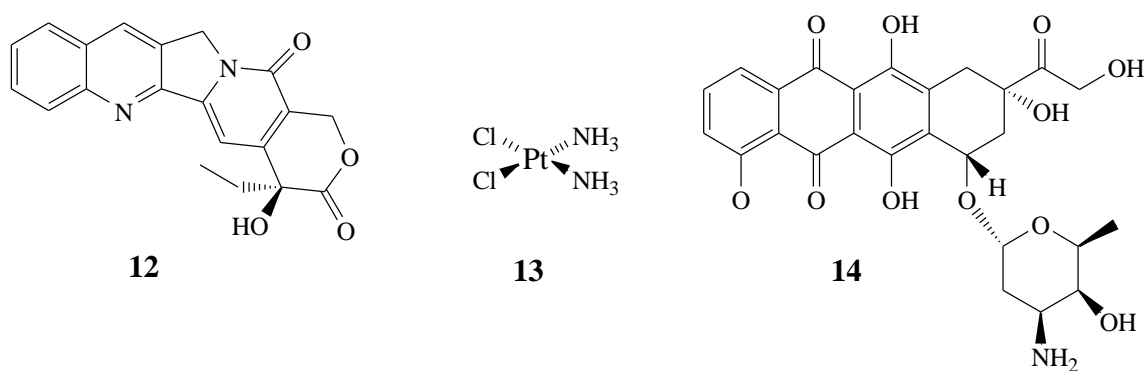


Figure 4.1: Anticancer drugs: Camptothecin (**12**), Cisplatin (**13**) and doxorubicin (**14**)

Another anticancer drug, doxorubicin, **14**, has been widely used to treat leukaemia, Hodgkin's lymphoma and cancers of the bladder, breast, stomach, lung, ovaries and

thyroid. In order to enhance drug solubility in water, cisplatin has been encapsulated with liposomes (trade name Doxil[®]).^{36,69-71}

A major drawback of anticancer drugs is they easily attack healthy cells as well as cancerous cells. However, these harmful side effects can be reduced by developing drug carriers which can take the drug directly to the specific targeted tumour site. Dendritic polymers such as dendrimers and hyperbranched polymers are suitable as potential carriers in drug delivery applications. Apart from drug delivery, these macromolecules can be extended to targeting via functionalisation, as shown in **Figure 4.2**.

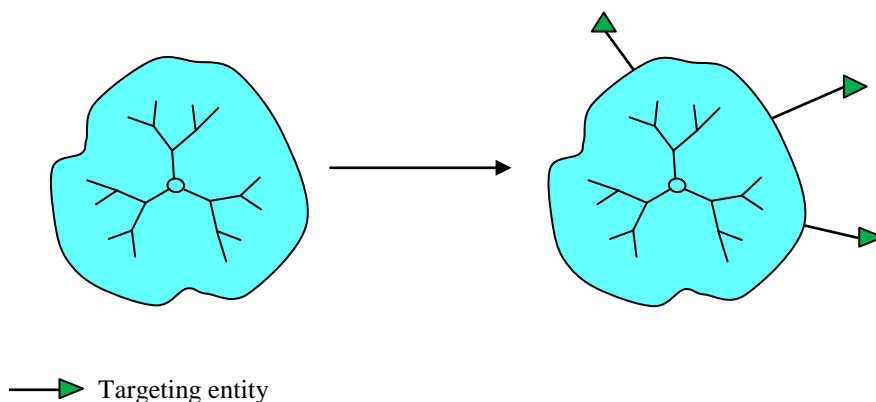
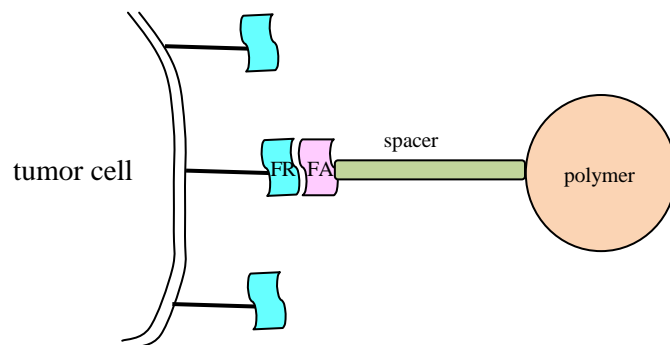


Figure 4.2: Cartoon of dendrimers with targeting entity

In cancer treatment, the folate receptor (FR) has been known to be over-expressed in several human tumours such as in the kidney, breast, lung and brain. FR density also appears to increase with advancing stages of the cancer.⁷²⁻⁸⁰ Exploiting the above-mentioned facts, it is hypothesized that folate conjugation to dendritic polymers could improve the accumulation of drugs at the tumour site and enhanced the possibility of killing the cancer cells.⁸¹ A better picture of the above is depicted in **Figure 4.3** below.



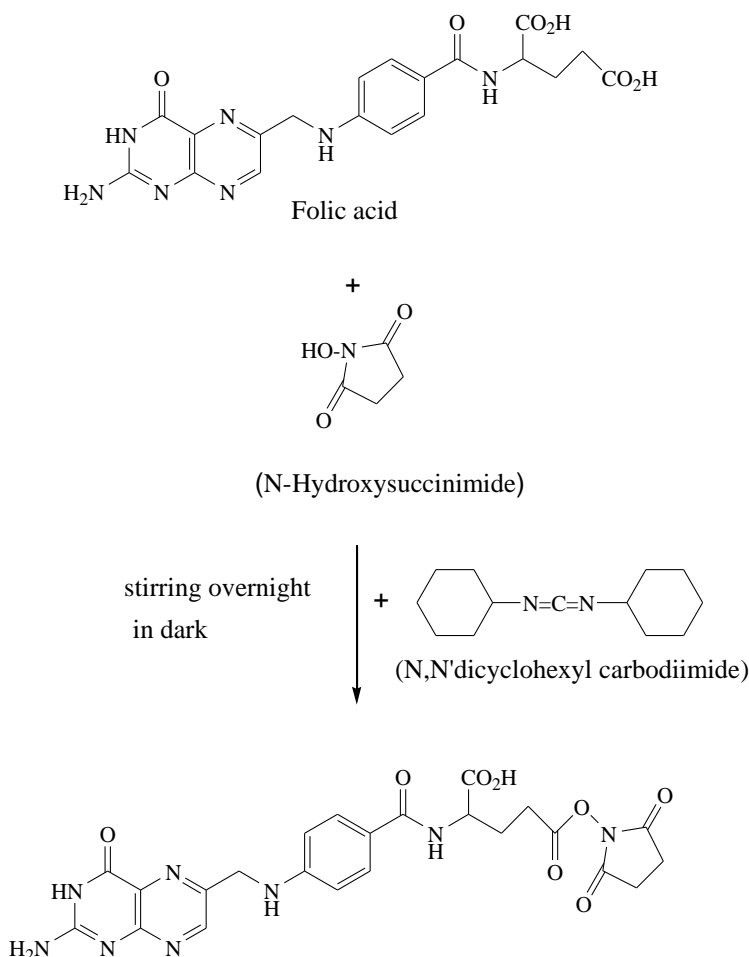
FR – folic receptor
FA – folic acid

Figure 4.3: Schematic functionalisation of folic acid via a spacer with a polymer

In this chapter, the subject will be hyperbranched polymers with the targeting ability of a folate receptor. This can be achieved by conjugating folic acid with hyperbranched polymers via poly (ethylene) glycol as a spacer.

4.2 Results and discussion

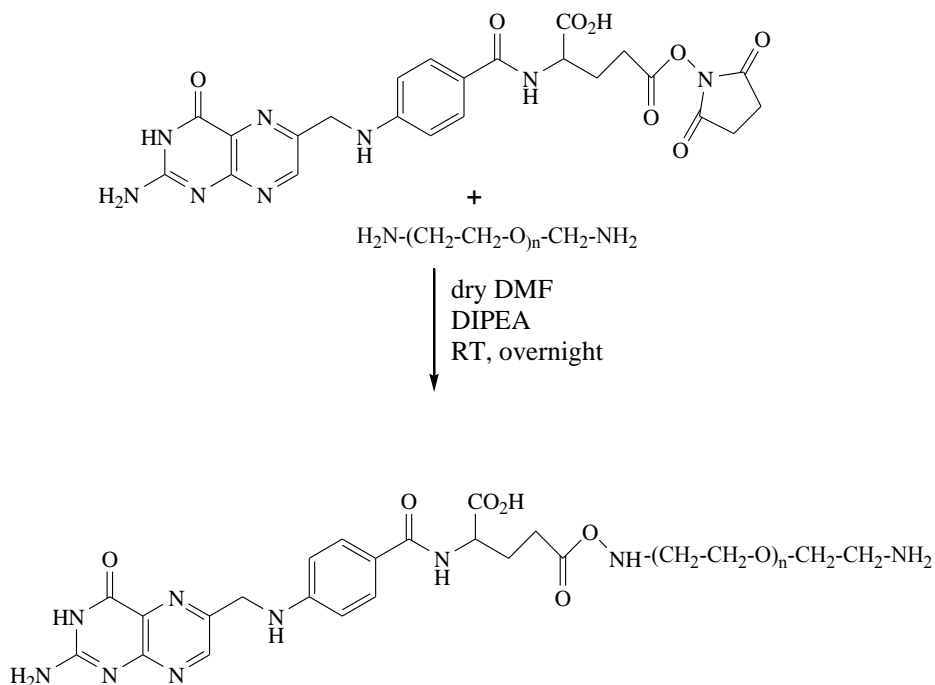
Conjugation of folic acid through a polyethylene glycol (PEG) spacer with hyperbranched polyglycidol (PG) was achieved by employing several steps before the final product was produced. Initially, folic acid was activated by N-hydroxysuccinimide (NHS) to produce an NHS ester of folic acid (FA-NHS) (**Scheme 4.1**).⁸²⁻⁸⁸



The synthesis of folic acid ester was very crucial as this step was very important before polyethylene glycol (PEG) could be conjugated with folic acid. In **Scheme 4.1**, NHS will convert folic acid to an ester compound and NHS is a good leaving group. This leaving group was essential for conjugation with PEG. To the above reaction, N,N'-dicyclohexyl

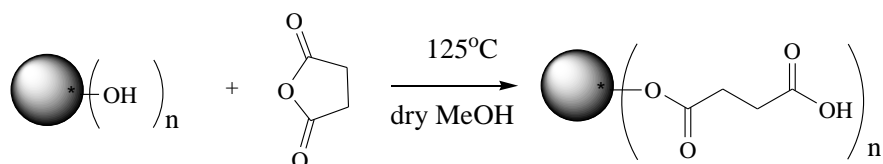
carbodiimide was added as a coupling agent. Such a long period have been used to make these compound and many attempts have been made to get an appropriate method. Several different temperatures were tried, different durations of experiment, modification to the reagent and using different solvents. Through all the experiments, experience was gained in handling the compound. Another challenging step was to reduce DMSO concentration using a very specific apparatus.

Folic acid is known to have a good targeting ligand, and therefore it is suitable for these proposed targeting design. Folic acid can be conjugated with hyperbranched polymers through two approaches: direct and indirect conjugation. In this work, indirect conjugation was chosen, which used a folic acid ester and was then conjugated with poly(ethylene glycol) (PEG)3000 bis amine ($\text{NH}_2\text{-PEG3000-NH}_2$) to produce a conjugated folic acid ester with PEG bis amine as the spacer. The schematic reaction was shown below in **Scheme 4.2**.



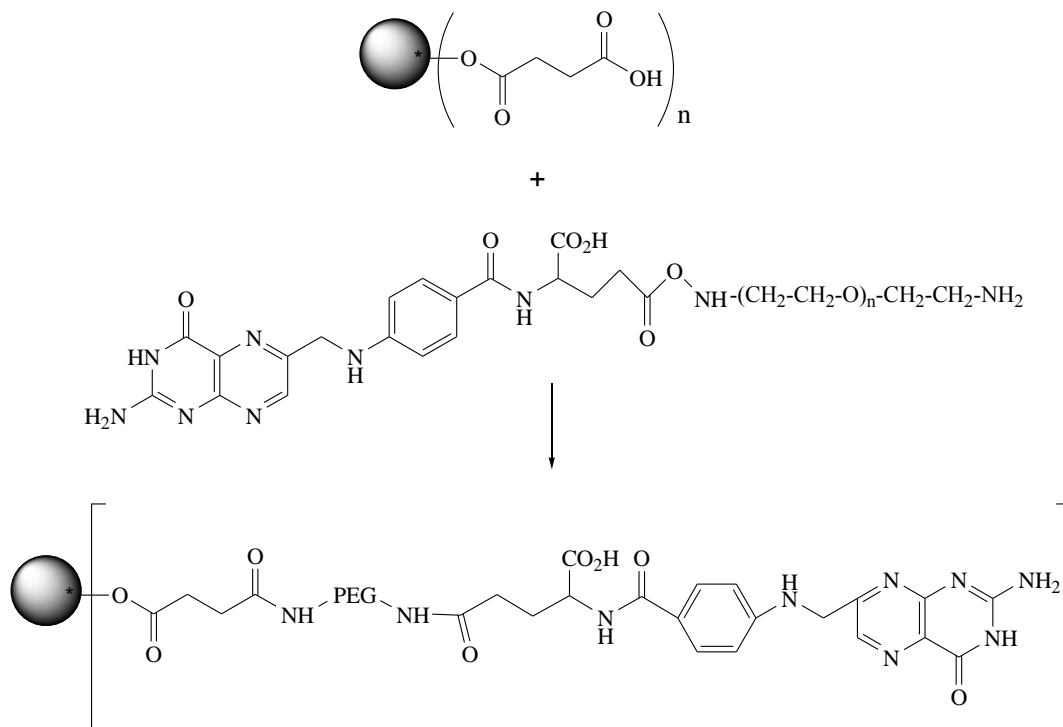
Scheme 4.2 : Synthesis of Folate - PEG-NH₂

Prior to the preparation of the hyperbranched polymer conjugated with folate-PEG-NH₂, it was first activated with succinic anhydride to produce polyglycidol - succinic anhydride (PG-SA) (**Scheme 4.3**).⁸⁹⁻⁹²



Scheme 4.3: Synthesis of PG-SA

The final step was conjugation of PG-SA with folate-PEG-NH₂ to produce polyglycidol-poly (ethylene glycol)-folate (PG-PEG-Folate) shown in **Scheme 4.4**.⁸⁹



Scheme 4.4: Synthesis of PG-Folate-PEG

The above ideas were transferred into actual experiments by combining and/or subtracting ideas taken from the literature, finally, the series of experiments developed listed below :

- Step 1- synthesis of polyglycidol succinic anhydride (PG-SA)
- Step 2- synthesis of folic acid ester (FA-NHS)
- Step 3- synthesis of folate-poly(ethylene glycol) bis amine (Folate-PEG-NH₂)
- Step 4- synthesis of polyglycidol-folate-poly(ethylene glycol) (PG-Folate-PEG)

4.2.1 Step 1: Synthesis and characterization of polyglycidol-succinic anhydride (PG-SA)

Initially, the hydroxyl end group of polyglycidol was converted to a carboxyl end group (PG-SA) (**Scheme 4.3**). This compound was synthesised by dissolving hyperbranched polyglycidol (PG) with dry MeOH, and succinic anhydride was added. This PG was synthesised by ring-opening polymerisation of glycidol as the monomer and p-nitrophenol as the core. The mixture was stirred continually for 48 hours at a temperature of 125 °C. Purification of the product was carried out by precipitation with ethanol three times. The final product was a viscous yellow solid. The product was characterised using ¹H NMR, as shown in **Figure 4.4**. A broad peak was observed in the range of 4.33 – 3.21 ppm, corresponding to the abundance of protons in the polymer backbone of polyglycidol. One broad singlet at 2.54 ppm could be attributed to the α - and β - methylene protons adjacent to the carboxylic group.

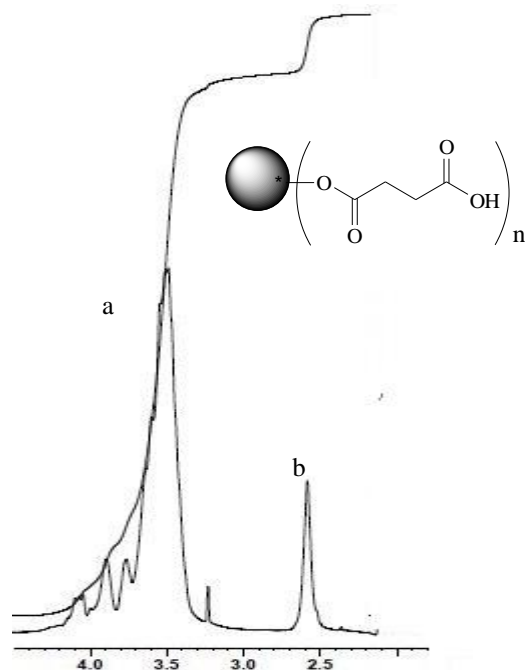


Figure 4.4: ^1H NMR spectrum of PG-SA in D_2O

From the GPC result, the molecular weight (M_n) was 1742 gmol^{-1} . Therefore, by using this information, we could calculate the number of protons exist in the broad peak (a). The degree of polymerization (DP) was determined by dividing the M_n of PG by the molecular weight of glycidol (74.08 gmol^{-1}); the value was 24. As glycidol contains five protons, these value was multiplied by the DP. Thus, an estimated 120 protons existed in (a). These can then be used to calculate the number of protons under peak b. By integrating peaks a and b, the number of protons existing in (b) was calculated to be 12. Therefore, after synthesising PG with succinic anhydride, there were three carboxylic group attached to the surface of the polyglycidol.

This result was supported by ^{13}C NMR where the presence of a carboxylic and ester group was detected at 177.4 and 174.5 ppm respectively. PG-SA was prepared as an intermediate compound before further conjugation with folic acid and poly (ethylene

glycol) as the spacer. Folic acid was first converted into its active compound as described below.

4.2.2 Step 2: Synthesis of folic acid ester (FA-NHS)

A folic acid ester (FA-NHS)(Scheme 4.1) was produced by reacting folic acid with 1,3-dicyclohexylcarbodiimide (DCC) and N-hydroxysuccinimide (NHS) in dry DMSO. The reaction was stirred continually, light protected and left overnight in a nitrogen environment. DCC is a good coupling agent that coupled NHS with carboxylic acid at the end of the folic acid. The above reaction produced dicyclohexylurea (DCU) a side product of DCC. The DCU was filtered and the filtrate was concentrated using vacuum distillation at 40 °C. The solution was precipitated using a mixture of cold acetone:diethyl ether (30:70) three times and dried overnight in a vacuum. The product was a solid yellow powder. The folic acid ester was characterised using ¹H NMR.

Figure 4.5 depicts the NMR spectrum of FA-NHS.

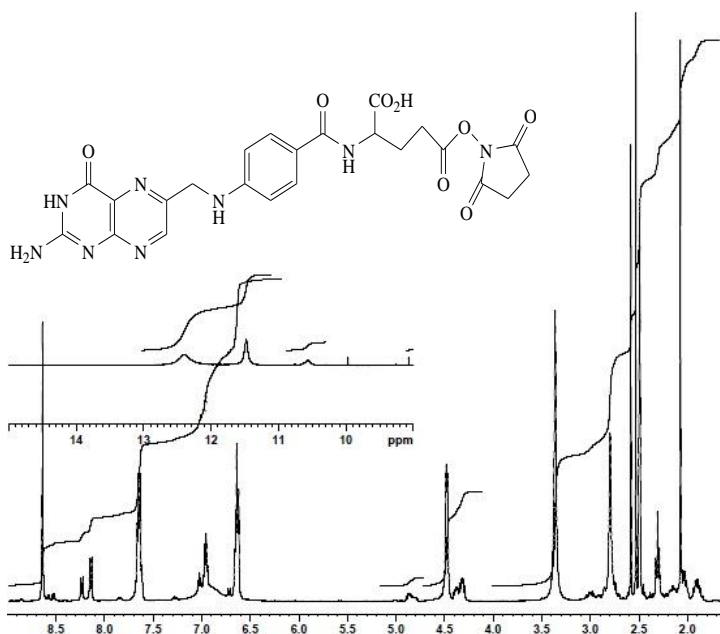


Figure 4.5: ¹H NMR spectrum of FA-NHS in DMSO

The spectrum clearly shows the broad carboxylic peak at 11.52 ppm. The presence of a folate group was observed at 8.65 ppm (pteridine proton), 8.16 ppm (aliphatic amide proton), 7.67 ppm and 6.66 ppm (aromatic proton).⁸⁸ The NHS peak was depicted at 2.81 ppm. Further characterisation using ¹³C showed the presence of a carboxylic and ester peak at 177.4 and 174.5 ppm respectively.

Folic acid contains two carboxylate groups γ and α : the former exhibits much higher reactivity than the latter.⁹³ Therefore, the γ carboxylate position was chosen to couple with NHS to form an ester compound. This ester compound was a good leaving group when reacted with amine. Consequently, the next step involved the conjugation of the activated folic ester with poly (ethylene glycol) bis amine.

4.2.3 Step 3: Synthesis of folate-polyethylene glycol bis amine (Folate-PEG-NH₂)

Folate-PEG-NH₂ was prepared by using an N hydroxysuccinimide ester of folic acid (FA-NHS) from the previous step (**Scheme 4.2**). PEG bis amine (Mw = 3400) and FA-NHS were dissolved separately in dry DMF. After all the reactant was dissolved, the solutions were mixed together and diisopropyl ethylamine was added. The mixture was allowed to react at room temperature for 24 hours in a nitrogen environment. After the reaction was completed, the solvent was reduced using vacuum distillation and finally precipitated in diethyl ether and dried in a vacuum. The final product was a pale yellow solid. The product was confirmed by ¹H NMR as shown in **Figure 4.6**. The presence of a folic acid group was detected at 8.67, 7.63 and 6.67 ppm. The PEG peak was detected at 3.52 ppm. This result was supported by a ¹³C NMR spectrum at 175.2 ppm and 173.3 ppm which represents the carboxylic acid group from folic acid and the amide group.⁸⁸

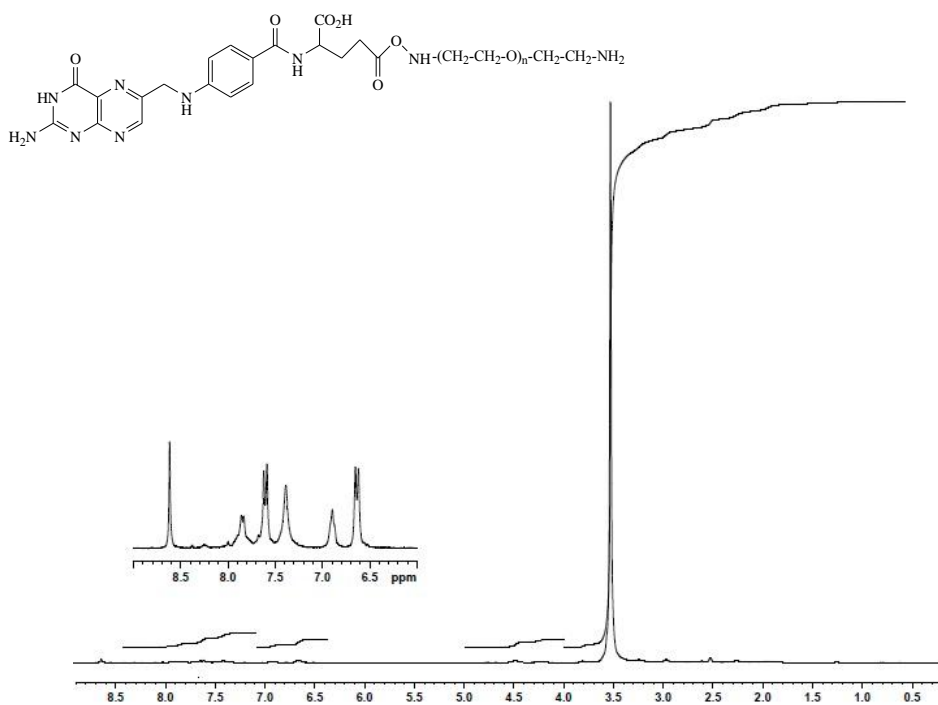


Figure 4.6: ^1H NMR spectrum of PEG-FA in DMSO

In the final step, we conjugated polyethylene glycol with the above targeting moiety to produce a good delivering system. This was done through a synthetic route, described below.

4.2.4 Step 4: Synthesis of polyglycidol-folate-poly(ethylene glycol) (PG- Folate-PEG)

The final product, PG-Folate-PEG, was synthesised using a multi-step reaction. This involves a reaction between PG-SA (**Scheme 4.3**) and Folate-PEG-NH₂ (**Scheme 4.2**). PG-SA was dissolved in DMSO, followed by DCC and pyridine. Folate-PEG-NH₂ was also dissolved in DMSO prior to its addition to the above solution. The mixture was allowed to react at room temperature for 24 hours in a nitrogen environment. After the reaction was completed, the solvent was reduced to half by vacuum distillation; water was added to the sample which was then freeze-dried overnight, yielding a pale yellow powder. The powder was characterised using ^1H NMR, as shown in **Figure 4.7**. The presence of folic acid was detected at 8.70, 7.55 and 6.69 ppm. Recall that in Step 1, the

^1H NMR for PG was observed in the range of 4.33 – 3.21 ppm and the PEG peak at 3.52 ppm (Step 3). Therefore, the broad peak was denoted as PEG overlap with the PG peak.

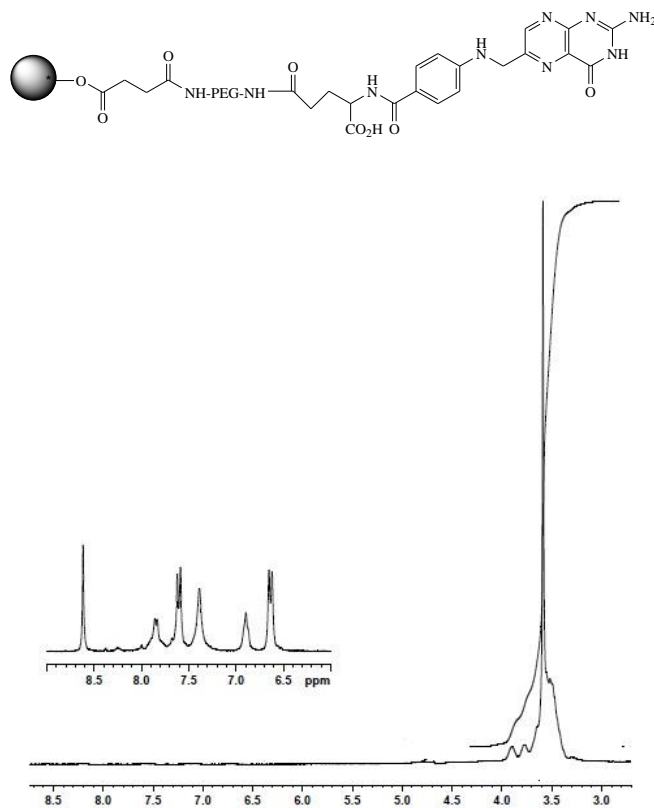


Figure 4.7 : ^1H NMR spectrum of PG-PEG-FA in D_2O

The number of folic acid molecules conjugated to PG can be estimated as follows. From Step 1 we calculated there was three carboxylic acids were attached to the PG surface. Therefore, a three PEG-Folate would be conjugated to the PG end group. If this had happened, it would be expected that the molecule would be much bigger. But, from the GPC result, the M_n was only 2151. A qualitative estimation suggested that only one might be conjugated to the PG (but one is all we need).

Chapter 5: Hydroxyl Terminated PAMAM Dendrimers: Encapsulation Using TCPP and Ibuprofen

5.1 Overview

In the past decade, dendrimers have emerged as promising delivering agents in the pharmaceutical world. These polymers have defined compositions, high molecular mass and a highly branched structure. These tree-like structures were first introduced by Newkome¹³ and Tomalia¹⁴ in 1985. Dendrimer has well defined globular three dimensional architecture in which all chains emerged gradually from core towards the end of the branching point, low polydispersity, and high surface functionality.⁹⁴

With all these attractive properties, dendrimers have become significant candidates as nanodrug vehicles due to their nanostructure and chemical versatility.⁹⁵ Compared to traditional polymeric drug vehicles, dendrimers have several advantages, such as: 1) stable architecture; 2) high density and well-defined surface functionalities, which have multifunctional benefits such as targeting, imaging and killing cells, 3) are monodispersed polymers, which ensure reproducible pharmacokinetics; 4) can easily penetrate through the cell membrane, which enhances cellular uptake of the drug complex or conjugation, and 5) have controlled shapes, which make them suitable for various medical applications.¹⁰⁰

Significantly, dendrimers have proved their ability to enhance the solubility of poorly soluble⁹⁷⁻⁹⁸ drugs and the bioavailability⁹⁹ of drugs. This is due to hydrophobic species inside the dendrimer and the hydrophilic properties at their periphery. The proposed mechanism is a hydrophobic interaction between the drug and the hydrophobic interior, as well as hydrogen bonding and ionic interaction at the surface of the dendrimer.¹⁰⁰ Other factors that contribute to the effectiveness of dendrimer as drug delivery vehicles are dendrimer generation, pH, core, temperature, polymeric architecture and surface functional groups.⁹⁴

5.2 Effect of generation size

Many efforts have been made to study the effect of dendrimer generation on the solubility of hydrophobic drugs. Different generations of both amine and ester terminated dendrimers have proved to increase the solubility of nifedipine several fold (**Figure 5.1**).⁹⁷

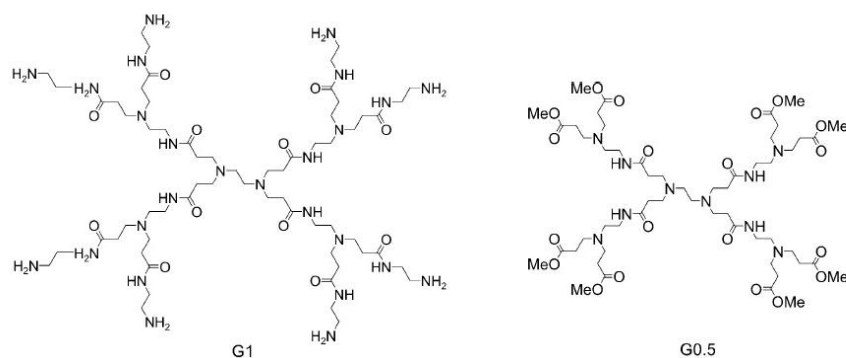


Figure 5.1: Effect of generation size in solubilisation of drugs

For example, the generation 4 of amine, hydroxyl and ester terminated dendrimers can solubilise indomethacin.¹⁰² Another type of dendrimer with a poly(ethylene glycol) core and citric acid as the branching unit also shows that an increase in generation size can solubilise hydrophobic molecules such as pyrene, 5-amino salicylic acid, mefenamic acid and diclofenac.¹⁰³ Different generations of poly(alkyl aryl ether) dendrimers with a phenolic hydroxyl group at the periphery and poly(propylene imine) can increase the solubility of pyrene.^{100,101} Polyamidoamine (PAMAM) dendrimers also showed it can solubilise different non-steroidal anti-inflammatory drug (NSAID). The above examples prove that generation size and concentration plays an important role in NSAID solubilisation.¹⁰⁶

5.3 Effect of pH

Another factor that contributes to drug solubilisation in dendrimers is pH. For instance, the protonation of nitrogen whether inside or at the periphery of PAMAM dendrimers is highly influenced by pH. The solubility of nifedipine in amine terminated G3 PAMAM dendrimer rises linearly with increasing concentration when used at pH 7 and 10 but not at pH 4. This was due to the protonation of tertiary amines in these dendrimers, which created a polarity environment inside the cavities, hence no increase in solubility. In contrast, for ester terminated dendrimers, at pH 4, less nitrogen was protonated; in other words, more tertiary amines were available for hydrogen bonding with drug molecules. At pH 7 (neutral), both primary and tertiary amines are less influenced for protonation compared to pH 4 or 10. As a result, the highest solubilisation effect for nifedipine was achieved at pH 7.¹⁰¹

5.4 Effect of core, polymer architecture and surface functionalities

Different cores for synthesising dendrimers can affect their capability to bind hydrophobic molecules. The basic idea was to have a dendrimer with a hydrophobic core and hydrophilic at the outer shell. For example 3,5-dihydroxy benzyl alcohol was used as the core to build a dendritic unimolecular micelle. Other researcher used 4,4-bis(4-hydroxyphenyl) pentanol as the core to construct the dendrimer. Both dendrimers were used as solubilisation enhancers for pyrene. The solubility of pyrene using the former dendrimer increased to 120 fold whereas the later by 356 fold.¹⁰⁷⁻¹⁰⁸ A bigger core molecule provides larger voids inside the dendritic structure, and these enhance the solubility of the guest molecule.

Different polymer architectures provide different solubilisation effects. The solubilisation effect of Paclitaxel using PEG 400 was compared with poly[oligo(ethylene glycol)methacrylate][poly(OEGMA)], five-arm star-shaped polyOEGMA, and polyglycerol dendrimers with G3, G4 and G5 (**Figure 5.2**).¹⁰⁹

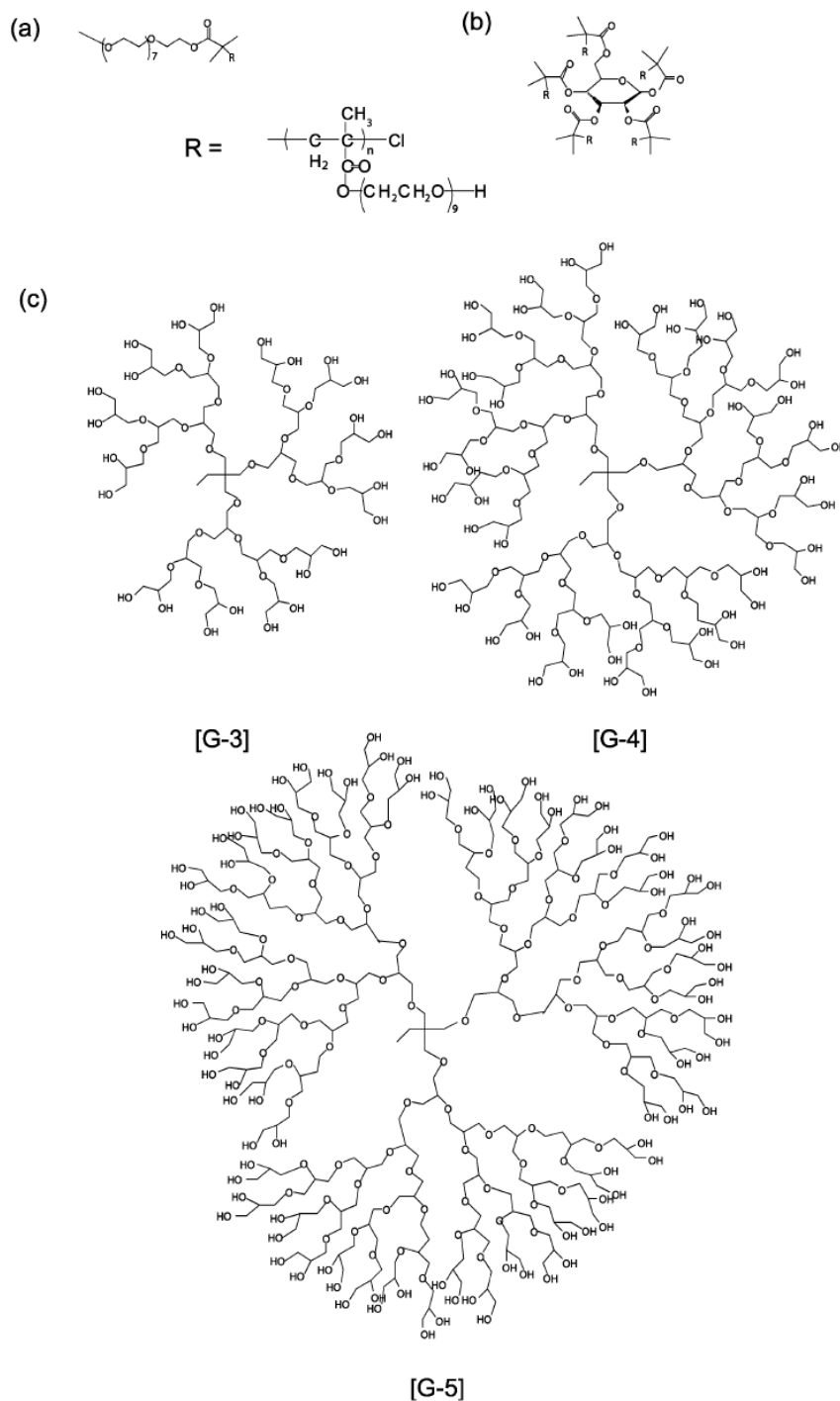


Figure 5.2: Effect of polymer architecture in solubilising paclitaxel, where (a) is poly(OEGMA), (b) is five-arm star-shaped polyOEGMA and (c) are G3, G4 and G5 polyglycerol dendrimers¹⁰⁹

The results showed that the solubility of all polymers increases tremendously compared to PEG 400.¹⁰⁹

Researchers have investigated various techniques and modifications to enable drugs to be delivered to targeted sites. As reviewed above, another modification suitable for this application is to modify the surface functionalities of dendrimers. An ester terminated PAMAM dendrimer was modified to a hydroxyl terminated PAMAM dendrimer using tris(hydroxymethyl amino methane). This method changed the ester termination into three hydroxyl end groups. These can increase the solubility of dendrimers significantly.⁵⁰ Other researchers suggest using PEG to enhance solubility and drug delivery. The use of different PEG arm length also affects the solubility of drugs.¹¹⁰⁻¹¹¹

5.5 Dendrimer toxicity

Dendrimers such as polyamido amine (PAMAM),⁹⁴ as shown in **Figure 5.3**, with an amine group at the periphery can form a stable complex with DNA that can penetrate the cell membrane to release DNA inside the cells.¹¹² Dendrimers have also been shown to be promising drug delivery vehicles for anticancer drugs using specific drugs and treatments at specific targeted cancerous sites.⁹⁷

Although dendrimers have shown a tremendous advantage as drug delivery vehicles, there are certain aspects that cannot be denied, i.e. the toxicity behaviour caused to the cell by the dendrimers. Studies have shown that cationic dendrimers with a NH₂ periphery are toxic to cells. For example, cationic melamine dendrimers,¹¹³ polypropyleneimine (PPI) and poly-L-lysine (PPL)¹¹⁴ show significant toxicity due to their surface cationic groups.

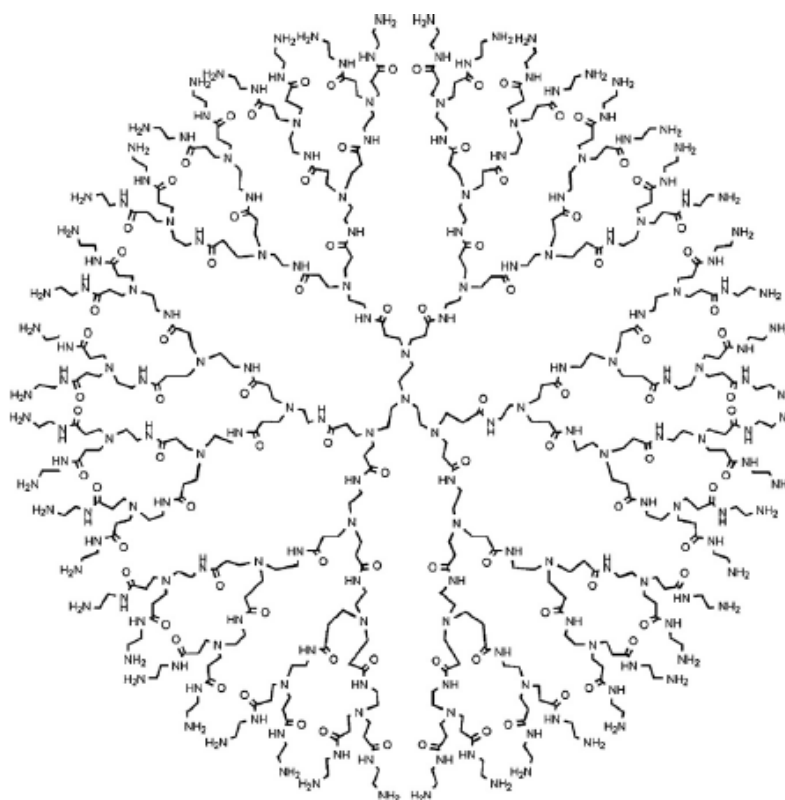


Figure 5.3: PAMAM dendrimer

Due to this toxicity issue, it was believed strongly that dendrimers can be modified to make them non-toxic and water-soluble, thus making them perfect delivering agents. Therefore, this chapter will be discussed on modifications to dendrimers' surface terminal groups.

5.6 Aims

Dendrimers have become promising agents for delivering drugs to specific sites, but there are some studies show that while cationic dendrimers can solubilise the drug, they can be toxic to the cell. As a result, it was believed that water soluble dendrimer may be the best candidates as drug vehicles for transporting drugs to targeted areas.

In this chapter, a comparison of solubilisation enhancement between water soluble hyperbranched polyglycerol with water soluble dendrimer was carried out. This is because they have some similarities in the polymer architecture and ability as drug delivery systems. For this specific study, a similar molecular weight of around 4000 Da will be used for both macromolecules.

Initially, PAMAM dendrimers were synthesised from generation 0.5 to generation 2.5. Water soluble PAMAM dendrimers were then synthesised using an ester terminated of generation 2.5 PAMAM dendrimers with a tris hydroxymethyl amino methane (TRIS) group. The result was the conversion of the ester group into three hydroxyl terminal groups at the surface of the dendrimers.

The synthesised water soluble dendrimers were then compared with water soluble hyperbranched polymers using *p*-nitrophenol as the core. Hyperbranched polymer was synthesised using the anionic polymerisation method using glycidol as the monomer. The core to monomer ratio used for this polymerisation was 1:5.

Both polymers were then encapsulated with model drug and drug, i.e. tetracarboxyphenyl porphyrin (TCPP) and ibuprofen respectively. Both drug and model drug have some solubility in water. Four different concentrations were used in this study; 1.00×10^{-4} M, 2.00×10^{-4} M, 4.00×10^{-4} M and 6.00×10^{-4} M.

Having previously demonstrated the ability of hyperbranched polymers to solubilise both drugs with the above polymer concentrations, a plateau response was revealed. It

was expected that encapsulation with water soluble dendrimers would cause them to behave the same as hyperbranched polymers.

5.7 Results and discussion

5.7.1 Synthesis of PAMAM dendrimers

As previously discussed, PAMAM dendrimer was chosen and the general synthesis of PAMAM dendrimers involved two iterative steps, namely 1) 1,4 Michael addition to produce ester terminated PAMAM dendrimers and 2) amidation to produce amine terminated PAMAM dendrimers or the whole PAMAM generation dendrimers.

1,4 Michael addition utilises the α - β unsaturated carbonyl compound. The carbonyl substituent has an electron-withdrawing effect, which generates a δ positive on the α carbon. This α carbon is stabilised by its resonance. Due to this effect, the β carbon becomes electropositive, therefore making it prone to nucleophilic attack. In this reaction, methyl acrylate acts as α - β unsaturated carbonyl, whereas ethylenediamine is the nucleophile. The mechanism of both steps are illustrated in **Figure 5.4**.

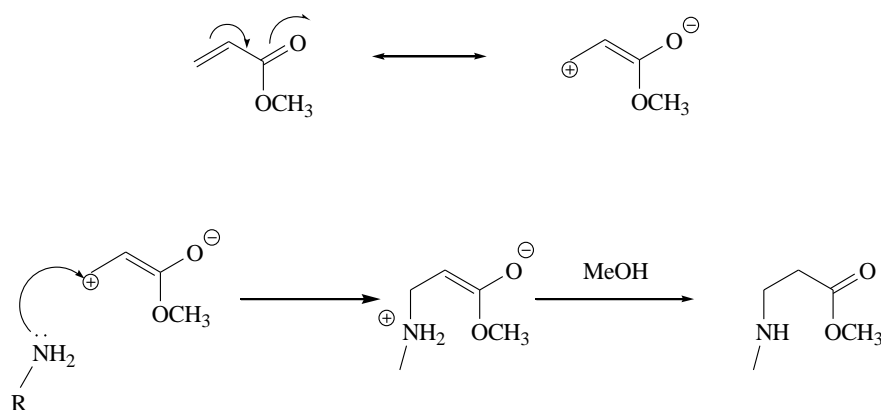


Figure 5.4: The 1,4 Michael addition

The second step is amidation. This step consumes the nitrogen lone pair from ethylene diamine and behaves as a nucleophile, attracting the positive carbonyl carbon from the methoxy group. The mechanism is shown in **Figure 5.5** below.

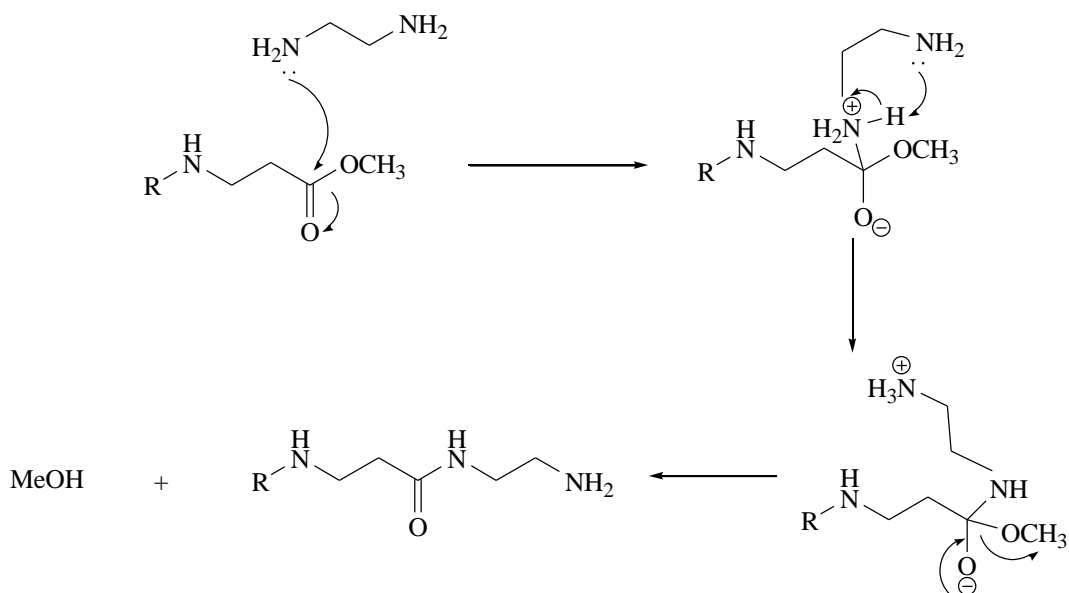


Figure 5.5: The amidation reaction

5.7.2 Synthesis of a G0.5 to G2.5 PAMAM dendrimer

The synthesis of a G0.5 PAMAM dendrimer was achieved by dropwise addition of methyl acrylate to ethylene diamine (EDA) dissolved in methanol at 0°C. This was allowed to return to room temperature and was stirred overnight. Excess ethylene diamine was removed under vacuum. The complete removal of these solvent was monitored using ^1H NMR. The product was a viscous honey yellow oil. This is the result of the Michael addition involving nucleophilic of ethylene diamine acting as the core. The nucleophilic core reacted with four equivalent of methyl acrylates, producing a G0.5 PAMAM dendrimers of four ester terminal group.

This ester terminated intermediate was then dissolved in methanol and added dropwise to a stirred ethylene diamine for thirty minutes at 0 °C. The solution was allowed to come to room temperature and was left for five days. Excess EDA was removed using an azeotropic mixture of toluene and methanol in a 9:1 ratio. Complete removal of EDA was accessed by ^{13}C NMR. The product was a slightly viscous honey yellow oil. This

was the result of the amidation reaction, producing G1.0 PAMAM dendrimer with four amine terminal group. These two steps, the initial Michael addition and amidation, were used iteratively to generate higher generations of dendrimers.

The diamine (G1.0) was dissolved in methanol. Methyl acrylate was then added dropwise to the stirred solution for thirty minutes at 0 °C. The mixture was brought back to room temperature and left overnight. Excess methyl acrylate was removed via a rotary evaporator. The product was a G1.5 PAMAM dendrimer possessing eight ester terminal groups with more viscous oil. The G2.0 PAMAM dendrimer was synthesised using the previous G1.5 dissolved in methanol, and EDA was added dropwise to the solution at 0 °C. The reaction was allowed to rise to room temperature and was then allowed to react for seven days. Purification was done using an azeotropic mixture of toluene and methanol and then the removal of all EDA was confirmed by ¹³C NMR. The oil produced was more viscous, as a result of the dendrimer containing eight amine terminal groups. The reaction from G0.5 to a G2.0 PAMAM dendrimer is shown schematically in **Figure 5.6** below. This schematic reaction, clearly illustrates that the Michael addition (red) and amidation reaction (blue) can be used iteratively to create higher generations of dendrimers.

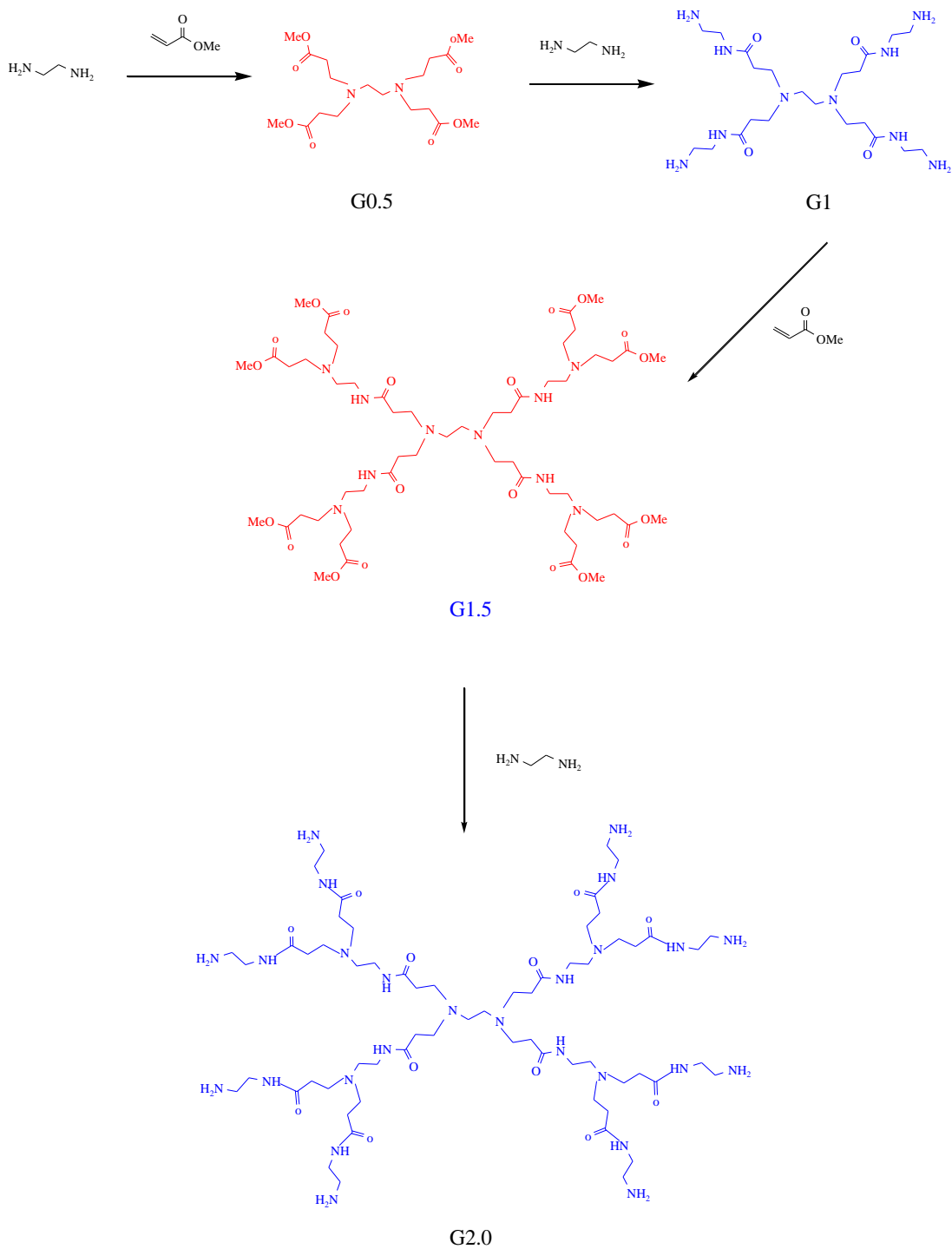


Figure 5.6: Synthesis of PAMAM dendrimer G0.5 to G2.0 showing each Michael addition (red) and amidation step (blue)

To synthesise G2.5 PAMAM dendrimer, the G2.0 PAMAM dendrimer with an amine terminated group was dissolved in methanol. To this stirred mixture, methyl acrylate was added dropwise at 0 °C. The mixture was brought to room temperature and stirred overnight. After the reaction was complete, the excess methyl acrylate was removed using a rotary evaporator. Finally, further removal of solvent was done using a high vacuum pump. A generation 2.5 PAMAM dendrimer with an ester terminal group was produced in the form of viscous yellow oil. A schematic diagram of the reaction from generation 2.0 to 2.5 PAMAM dendrimer is presented below in **Figure 5.7**.

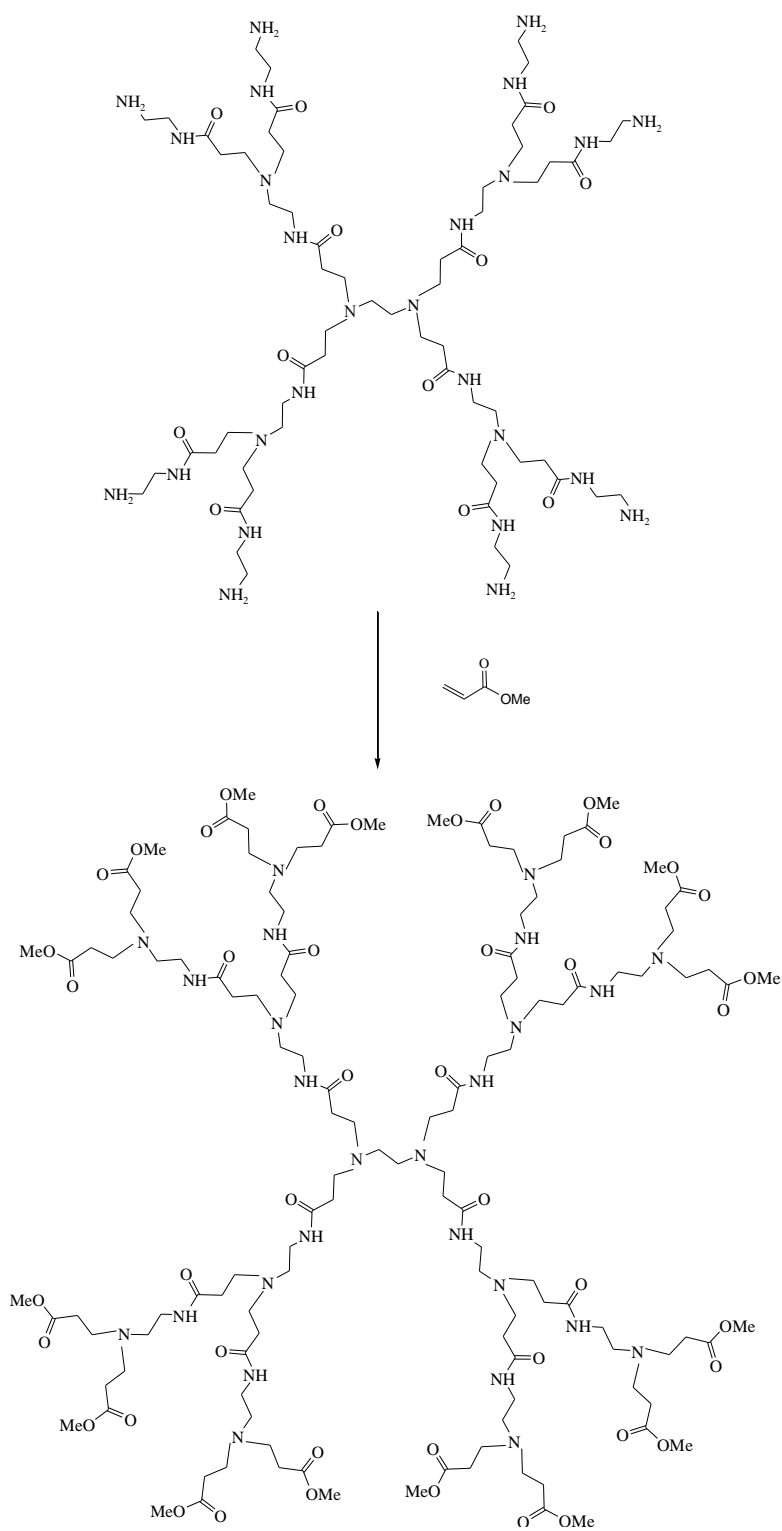


Figure 5.7: Synthesis of PAMAM dendrimer from G2.0 to G2.5

In order to ensure that all the synthesised dendrimers (G0.5 to G2.5) have good agreement with the theory discussed above, several characterisation tools were used, including ^1H and ^{13}C NMR spectroscopy, IR spectroscopy and mass spectrometry. ^1H NMR is a valuable tool for confirming hydrogen abundance and relative population. **Figure 5.8** shows the ^1H NMR for G0.5 with a strong methoxy peak (a) observed at 3.68 ppm. This is the characteristic peak of an ester terminated half generation dendrimer. Two triplets at 2.76 ppm (b) and 2.49 ppm (c) were attributed to the existence of newly formed CH_2 groups and a singlet found at 2.54 ppm (d) indicated the proton from the core (ethylene diamine).

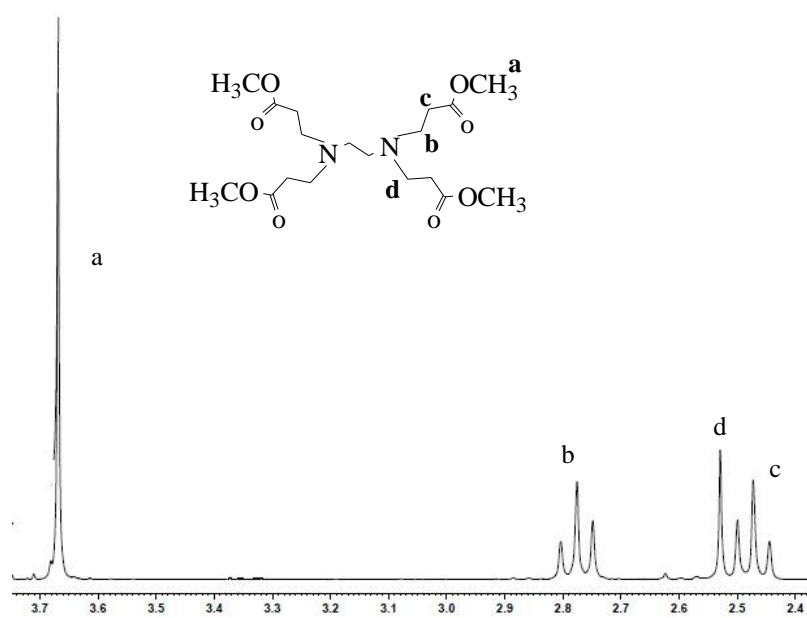


Figure 5.8: ^1H NMR spectrum for G0.5 PAMAM dendrimer in MeOH

The spectra of higher dendrimer generations are more difficult to interpret. This is due to the presence of too many protons. As a result, there were large regions of overlap and broadened triplets and multiplets. These are shown in **Figure 5.9**. On the G2.5 PAMAM dendrimer spectrum, a very strong singlet peak (a) associated with methoxy was observed at 3.66 ppm. There were multiplet at 3.37 ppm (b) and two multiplets

ranging from 2.93 to 2.33 ppm (c) indicating the existence of CH₂ groups in the dendrimer architecture.

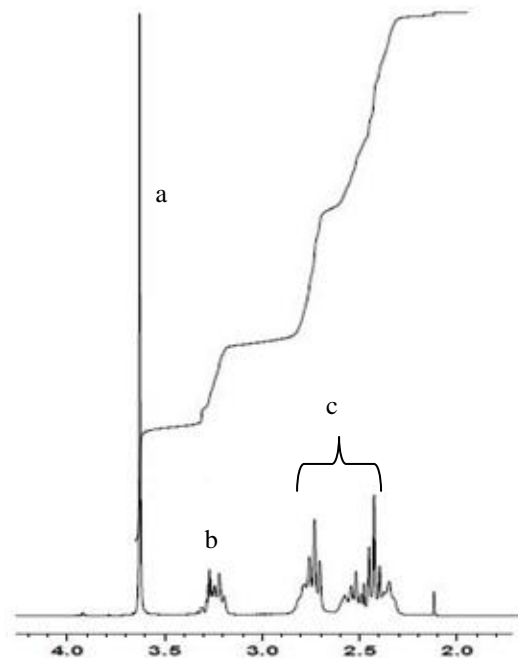


Figure 5.9: ¹H NMR spectrum of a generation 2.5 PAMAM dendrimer

Another characterisation used to confirm the above dendrimer was mass spectroscopy. This showed that the molecular ion peak was almost the same, with the exact molecular weight predetermined from the ideal structure shown in **Table 5.1**. Another interpretation tool used to approve these structure was IR spectroscopy. The spectra showed a significant ester peak at 1730 cm⁻¹ for ester terminated PAMAM dendrimers. For amine terminated PAMAM dendrimers, an amide peak was observed at around 3200 cm⁻¹ and an amide carbonyl peak at 1640 cm⁻¹. Finally, after all the above characterisation was completed, we were confident in the synthetic procedure used to synthesise the generation 2.5 PAMAM dendrimer

Table 5.1: The molecular weight for G0.5 to G2.5 PAMAM dendrimers

PAMAM generation	End group	Molecular formula	MH⁺ peak	Expected Mw
0.5	CO ₂ Me (4)	C ₁₈ H ₃₂ N ₂ O ₈	405	404
1.0	NH ₂ (4)	C ₂₂ H ₄₈ N ₁₀ O ₄	517	516
1.5	CO ₂ Me(8)	C ₅₄ H ₈₈ N ₁₀ O ₂₀	1206	1196
2.0	NH ₂ (8)	C ₆₂ H ₁₂₈ N ₂₆ O ₁₂	1468	1428
2.5	CO ₂ Me(16)	C ₁₂₄ H ₂₂₄ N ₂₆ O ₄₄	4130	2805

5.7.3 Purification of the PAMAM dendrimer

The half generation PAMAM dendrimer underwent Michael addition reaction and the excess methyl acrylate used was easily removed because of the high volatility of the compound. The removal was easily done using rotary evaporator. However, for an amidation step, the ethylenediamine (EDA) is not easily removed and therefore affects the following synthetic procedure. Incomplete removal of EDA can behave as a new initiator core, which will react to form undesired by-products. This abnormality is illustrated in **Figure 5.10** below:

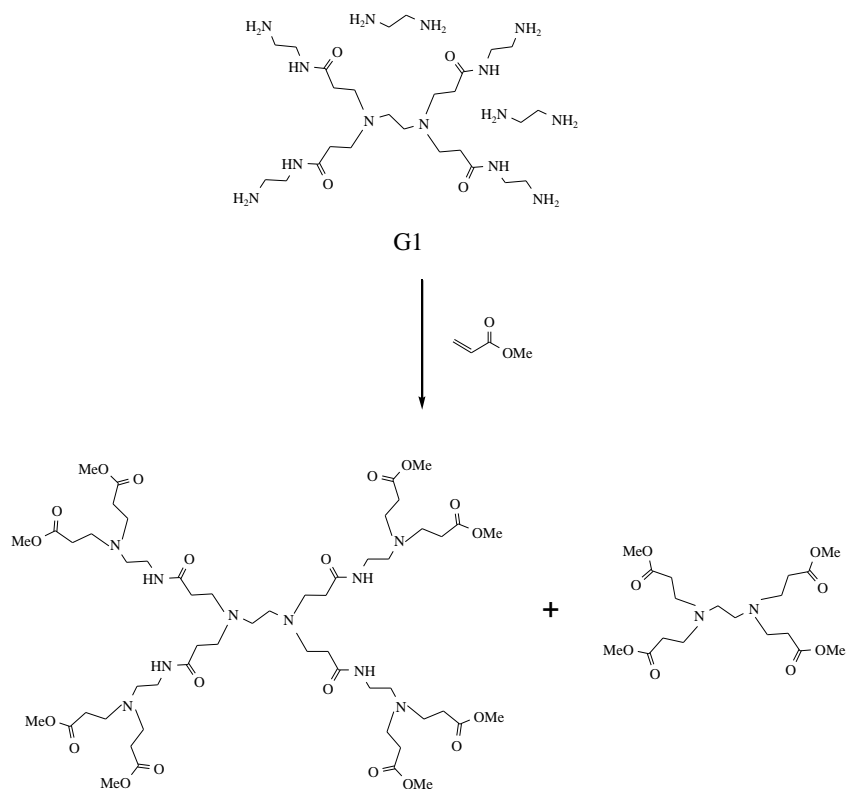


Figure 5.10: Incomplete removal of EDA and their by-products

The by-products were G1.5 and G0.5, which were generated together. If these occurred, these two different generation PAMAM dendrimers were extremely difficult to remove due to their structural and physical similarity to the desired dendrimer. Consequently, these would lead to substantial broadening of the molecular weight distribution.

The efficient way to eradicate EDA was by washing repeatedly with an azeotropic mixture. This mixture was a combination of toluene and methanol with a 9:1 ratio. The G1.0 PAMAM dendrimer was added with the above solution and placed in a rotary evaporator. How this azeotropic solution works is explained below. The G1.0 PAMAM dendrimer possesses four amine terminated surface groups. EDA forms hydrogen bond, which is strongly bound to the amine terminal group. In order to prevent this occurrence, something must be incorporated into the solution to bind with the hydrogen bonding

sites. Methanol is a good competitor for these sites, but has the limitation of a low boiling point. Upon evaporation, the concentration decreases, meaning it is removed from the binding sites, which EDA will then occupy. By using an azeotropic solution, methanol can be a good competitor, as toluene will increase the azeotropic solution boiling point and facilitate the removal of EDA.

The complete removal of methyl acrylate was confirmed using ^1H NMR. Methyl acrylate vinyl groups usually appeared at around 5-6 ppm. However, for EDA, ^{13}C NMR was used, and the EDA peak was easily visualised at 43.6 ppm.

Consequently, the following discussion will focus on synthesising water soluble PAMAM dendrimers which contained 48 hydroxyl groups at the periphery.

5.7.4 Synthesis of PAMAM dendrimer with 48 hydroxyl groups

A further reaction using the G2.5 PAMAM dendrimer to generate a hydroxyl terminated dendrimer was performed. Tris(hydroxymethyl) aminomethane (TRIS) and anhydrous potassium carbonate were dissolved in dry DMSO. To this suspension, PAMAM generation 2.5 dissolved in dry DMSO was added. The mixture was allowed to react for 72 hours at 50 °C under nitrogen conditions. The solution was then filtered and the solvent removed using vacuum distillation at 40°C. Finally, a small amount of water was added, followed by acetone to precipitate the product. A pale yellow viscous oil was collected. The reaction mechanism indicating the conversion of PAMAM generation 2.5 to a hydroxyl terminated dendrimer is shown in **Figure 5.11**.

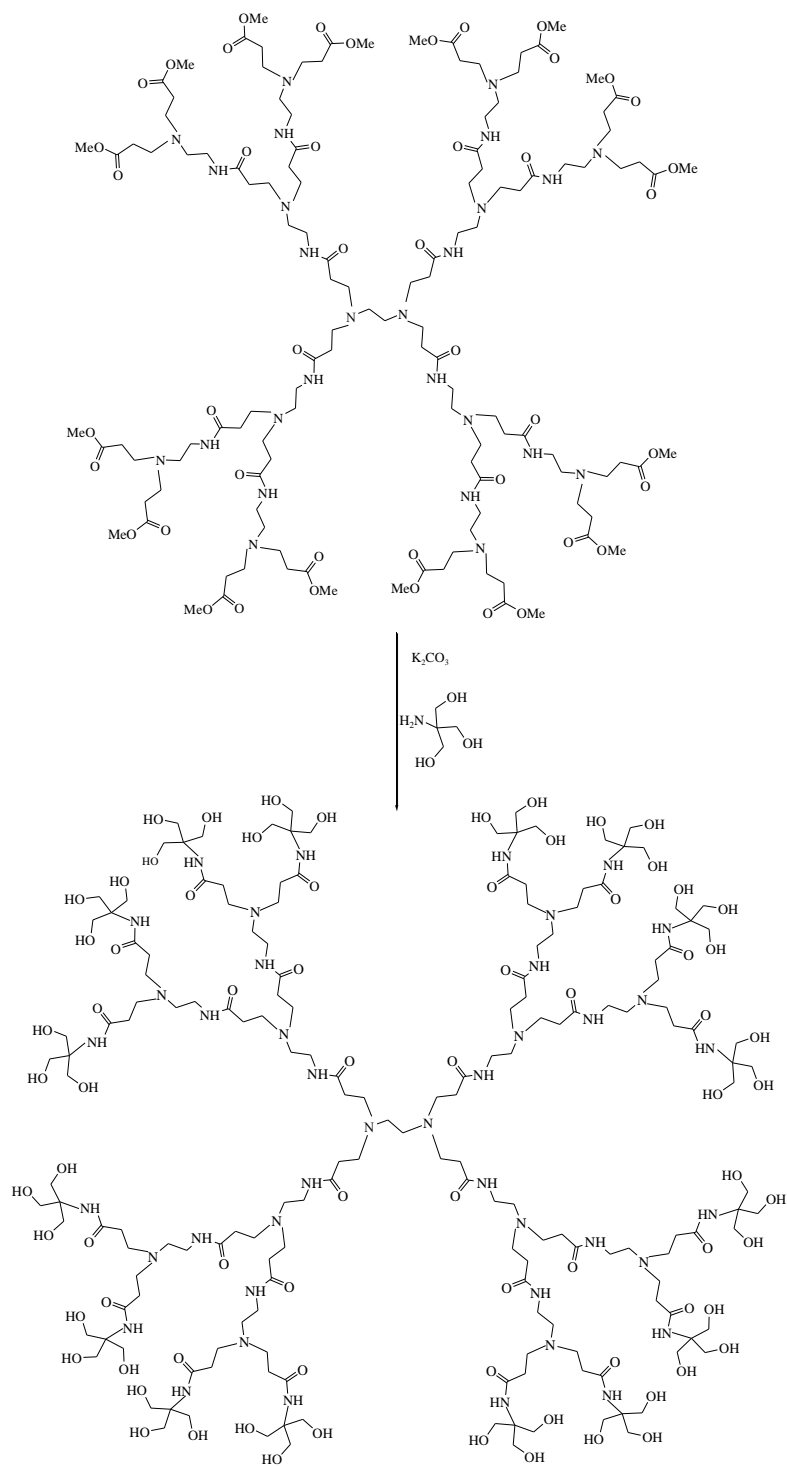


Figure 5.11: Synthesis of a generation 2.5 PAMAM dendrimer into a hydroxyl terminated PAMAM dendrimer

To prove the above compound was successfully synthesised, the product was characterised using ^1H NMR, ^{13}C NMR and mass spectroscopy. The proton peaks associated with methylene protons adjacent to the terminal hydroxyl groups were seen at 3.64 ppm. A series of broad multiplets was observed in conjunction with the CH_2 peaks in the dendrimer architecture. The carbonyl peaks at 174.4 ppm and 175.4 ppm indicated the interior amide and exterior amide respectively.⁵⁰ The methyl group was completely removed from the ^{13}C NMR spectra. Mass spectrometry revealed a molecular ion of 4130. Further characterisation using IR showed an OH broad band at 3303 cm^{-1} and amide carbonyl at 1657 cm^{-1} . As expected, the hydroxyl terminated PAMAM dendrimer was soluble in water.

5.7.5 Encapsulation of hydrophobic molecules with water soluble PAMAM dendrimer

In this study, two hydrophobic molecule were used, namely ibuprofen and tetracarboxyphenyl porphyrin (**Figure 5.12**). The properties of both molecules have been extensively discussed in **Chapter 3**.

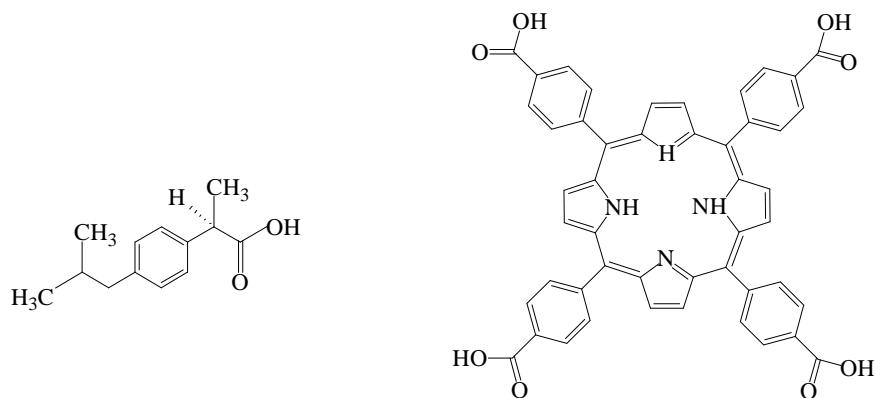


Figure 5.12: Molecules used in complex forming

Encapsulation was carried using four different concentrations, i.e. $1.00 \times 10^{-4}\text{ M}$, $2.00 \times 10^{-4}\text{ M}$, $4.00 \times 10^{-4}\text{ M}$ and $6.00 \times 10^{-4}\text{ M}$, of PAMAM dendrimers with 48 OH terminal

groups. Dendrimers and guest molecules were dissolved separately in methanol and then mixed together. The methanol was then removed using a rotary evaporator giving a dendrimer/guest molecules co-precipitate. Finally TRIS buffer (pH 7.4 with 0.1M) was added. All insoluble substances were filtered prior to UV measurement.

5.7.5.1. Encapsulation of ibuprofen with water soluble PAMAM dendrimers

The first drug used was ibuprofen with molecular weight of 206.28 g mol⁻¹ and its characteristic peak detected at $\lambda_{\text{max}} = 222$ nm. This drug has some solubility in water (less than 1 mg/ml~less than 4.80 x 10⁻³ M). After encapsulation, the peak observed was too strong and therefore it was diluted 50 fold. The initial concentration was calculated by dividing the absorbance by the extinction coefficient (ϵ) of ibuprofen. The extinction coefficient value was obtained graphically from a Beer Lambert plot at 8387.5 M⁻¹ cm⁻¹. It was then multiplied by 50 to get the concentration.

In order to know exactly how much ibuprofen was encapsulated inside the dendrimer, ibuprofen was freshly dissolved in water and filtered. The solution was measured using UV-Vis spectrophotometer and the value obtained was 2.68 x 10⁻⁴ M. These amount was then subtracted from the initial results. The results are tabulated in **Table 5.2** below.

Table 5.2: Ibuprofen concentration in solution and encapsulated ibuprofen with dendrimer

Dendrimer concentration (x 10 ⁻⁴ M)	[Ibuprofen] (x 10 ⁻⁴ M)	[Ibuprofen] encapsulated inside dendrimer* (x 10 ⁻⁴ M)
Without polymer	2.68	0.00
1.00	5.78	3.10
2.00	7.18	4.50
4.00	8.54	5.86
6.00	9.91	7.23

* *concentrations of encapsulated ibuprofen after deduction of freshly soluble material 2.68 x 10⁻⁴ M*

The effect of dendrimer concentration on the solubility of ibuprofen in the presence of water soluble PAMAM dendrimers is shown in **Figure 5.13**. The solubility of ibuprofen in water was 2.68×10^{-4} M. It was observed that the solubility of ibuprofen was significantly improved by the PAMAM dendrimer. The solubility increased up to the highest concentration of dendrimer used, which was 6.00×10^{-4} M. The increase in solubility of ibuprofen was presumably attributed to the internal cavities inside the water soluble PAMAM dendrimer interacting with the ibuprofen. Furthermore, there were tertiary amines inside the cavities which could interact with ibuprofen by hydrogen bond formation.⁹⁴

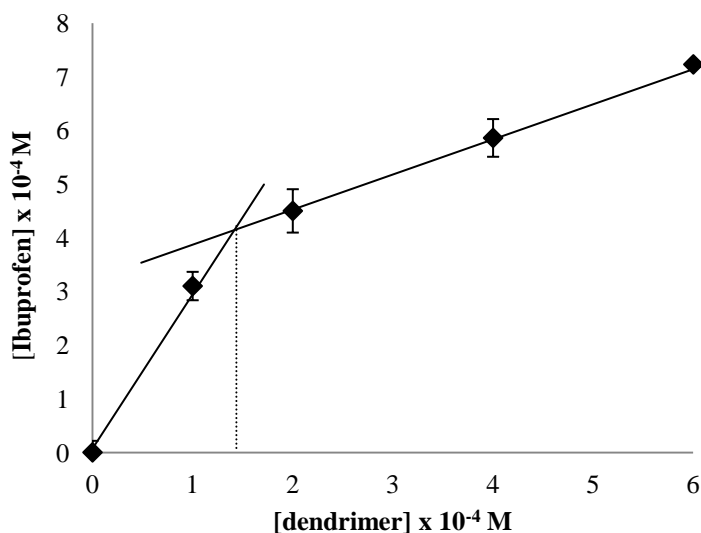


Figure 5.13: Increased ibuprofen solubility with increased concentration of water soluble dendrimer

If considered carefully, the graph increase was not linear. For example, for polymer concentration of 1.00×10^{-4} M, the solubility was 3.10×10^{-4} M, we should predicted that for polymer concentration of 2.00×10^{-4} M, the ibuprofen solubility should be around 6.00×10^{-4} M, but it not happened. When we looked at polymer concentration of 4.00×10^{-4} M the ibuprofen concentration should be around 12.00×10^{-4} M, but it only increased up to 5.86×10^{-4} M. The ideal situation is demonstrated in the cartoon in **Figure 5.14** below.

The figure below showed the ideal situation, where, when one polymer can encapsulated 3 guest molecules, therefore for four polymers, they can encapsulated twelve guest molecules.

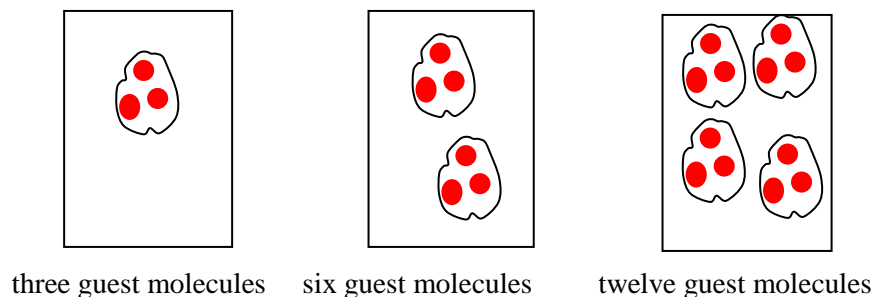


Figure 5.14: Expected model of encapsulated ibuprofen within dendrimers

However, the graph in **Figure 5.13** showed that the ibuprofen concentration was initially increased and plateaued at dendrimer concentration of 6.00×10^{-4} M. At this stage, it was decided to investigate the possible aggregation behaviour of the dendrimers at higher concentration. It was reported that amine terminated dendrimers aggregate around 10^{-3} - 10^{-6} M and the OH terminated dendrimers aggregate around 10^{-4} - 10^{-6} M.¹¹⁵ The onset of aggregation, known as critical aggregation or micelle concentration (CMC), is often accompanied by a direct change in solution properties. It was almost certain aggregation has occurred in the dendrimers. On examining the ibuprofen concentration versus dendrimer concentration plot, it was clearly shown a prominent break in linearity observed at 1.5×10^{-4} M. This is the beginning of aggregation in dendrimers.¹¹⁶

Loading per mole ibuprofen inside dendrimer was determined by dividing the concentration of ibuprofen by the concentration of dendrimer. For dendrimer concentration of 1.00×10^{-4} M, loading per mole ibuprofen was three. For the next discussion, a bigger molecule was used for encapsulation study, which was TCPP.

5.7.5.2 Encapsulation of TCPP with water soluble PAMAM dendrimers

The second drug molecule used was tetracarboxyphenyl porphyrin (TCPP). This molecule is bigger than the ibuprofen molecule. We used the same encapsulation

method as before with four different dendrimer concentrations. The absorbance of the solution was too strong, thus it was diluted 100 fold. The concentration was calculated by dividing the absorbance by extinction coefficient (ϵ) value of TCPP which was $3.30 \times 10^5 \text{ M}^{-1} \text{ cm}^{-1}$. The value was then multiplied by 100. In order to know the value of TCPP encapsulated in the dendrimer, the value was deducted from the value of TCPP dissolved in water. This experiment was done by dissolving excess TCPP in water, and any undissolved TCPP was filtered off. The solution was then assessed by UV-Vis spectrophotometer with a value of $0.72 \times 10^{-4} \text{ M}$. This value was then deducted with the concentration of TCPP in solution. From these results, we also can calculate loading per mole TCPP inside the dendrimer. These value was obtained by dividing the TCPP concentration by the dendrimer concentration. All datas are tabulated in **Table 5.3** below.

Table 5.3: TCPP concentration in solution and encapsulated TCPP in dendrimer

[Dendrimer] ($\times 10^{-4} \text{ M}$)	[TCPP] ($\times 10^{-4} \text{ M}$)	[TCPP] encapsulated inside dendrimer* ($\times 10^{-4} \text{ M}$)
Without polymer	0.72	0.00
1.0	1.85	1.13
2.0	2.42	1.70
4.0	3.09	2.37
6.0	4.40	3.68

* *concentrataion of encapsulated TCPP after deduction with $0.72 \times 10^{-4} \text{ M}$*

From the above results, the effect of different concentrations of dendrimers on the solubility of TCPP can be clearly seen. It was observed that the solubility of TCPP increased linearly until polymer concentration of $2.00 \times 10^{-4} \text{ M}$ and plateaued at the highest dendrimer concentration of $6.00 \times 10^{-4} \text{ M}$, as shown in **Figure 5.15**.

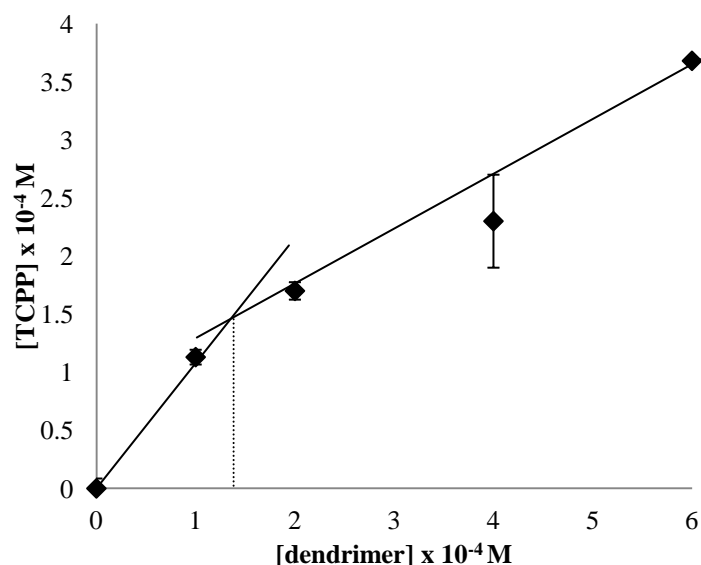


Figure 5.15: Increased solubility of TCPP with increased concentration of water soluble dendrimers

It was postulated that the proposed mechanism was due to the hydrophobic bonding of drug molecules inside the cavity of the dendrimers. Another factors that presumably contributed to the increased solubility was the internal amide inside the cavities, which may interact with TCPP to form hydrogen bonds.⁵⁰ As previously discussed, the TCPP solubility increased after encapsulation with dendrimers, however, the increment was not linear. It was clearly demonstrated that the dendrimers aggregated at higher concentration. From **Figure 5.15** the dendrimer started aggregating at dendrimer concentration of 1.5×10^{-4} M. Loading per mole TCPP for dendrimer concentration of 1.00×10^{-4} M was one. This might be because the TCPP molecule was big and only one molecule could solubilised inside the dendrimer hydrophobic voids.

From the encapsulation studies of both molecules, it was clearly observed that the solubility increased with an increased in dendrimer concentration. The following section will compare the solubility behaviour between water soluble PAMAM dendrimers and water soluble hyperbranched polymers.

5.7.6 Comparison of the effect of PAMAM dendrimers and hyperbranched polymers on the solubility enhancement of ibuprofen and TCPP

This section specifically compares the solubilisation behaviour of hyperbranched polymers and OH terminated dendrimers. Both macromolecules are soluble in water. Comparisons were made using the same drug molecules, concentrations, method and similar molecular weight. We envisaged that the 48 OH terminal group was suitable in this study because the molecule was not very big and was less expensive than other bigger dendrimer molecules. The results for both complex formations are shown in **Figure 5.16** and **5.17**:

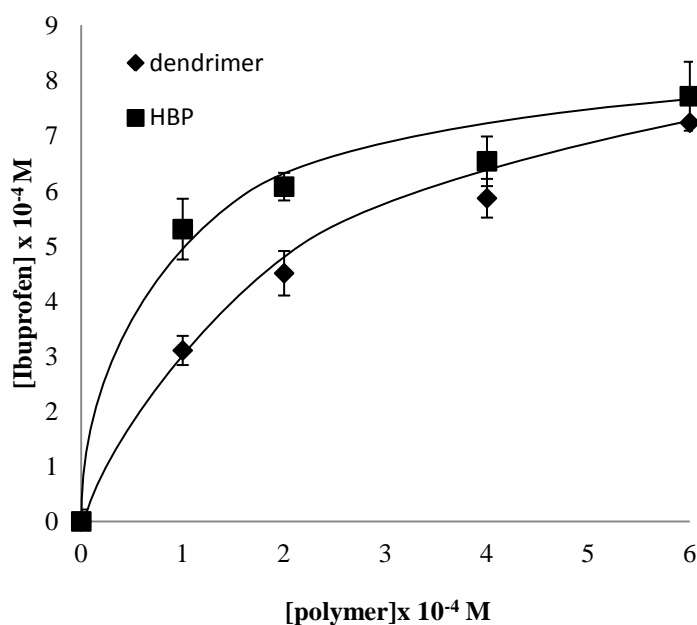


Figure 5.16: Encapsulation of ibuprofen using water soluble hyperbranched polymers and dendrimers

The above graph shows the encapsulation of ibuprofen using water soluble hyperbranched polymers and dendrimers. Ibuprofen has some solubility in water at 2.63×10^{-4} M. After encapsulation with hyperbranched polymer at a concentration of 1.00×10^{-4} M, the solubility increased to 5.30×10^{-4} M whereas with the dendrimer, the solubility increased to 3.01×10^{-4} M. Both polymers showed increased solubility after

encapsulation. The graph trend line, both polymers showed a linear responds at polymer concentration of 2.00×10^{-4} M and became plateaued at polymer concentration of 6.00×10^{-4} M.

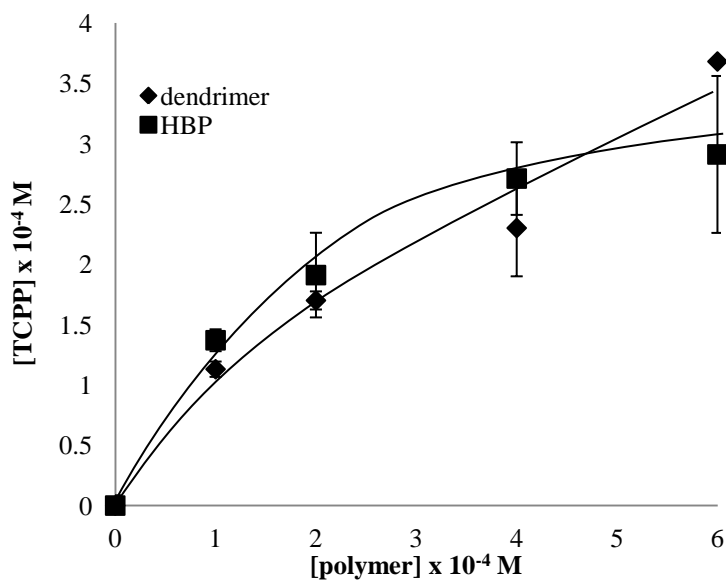


Figure 5.17: Encapsulation of TCPP using both polymers

Figure 5.17 shows the encapsulation studies of TCPP encapsulated with both polymers. For both polymers, the solubility rose linearly at polymer concentration of 2.00×10^{-4} M and plateaued at polymer concentration of 6.00×10^{-4} M. The above graphs also showed that the solubilisation of the hyperbranched polymers were better than the dendrimers. It was postulated that the plateaued trend line of the polymers might be due to the aggregation of polymers at higher concentration.

Chapter 6: Conclusion

Most new drugs developed by the pharmaceutical industry are not beneficial to the patient because of their poor solubility. There is an urgent need to develop a delivery agent which will enhance the solubility of drugs. Over the past decades, many drug carriers have been developed including linear polymers, block copolymers and dendrimers. In this study, water soluble hyperbranched polymers were chosen because they can be prepared using one-pot synthesis and are very cost-effective.

Water soluble hyperbranched polymers with a *p*-nitrophenol core and glycidol monomer were synthesised using anionic ring-opening polymerisation. These polymers have a hydrophobic interior and are hydrophilic at the surface. Five different molecular weights were prepared using different core to monomer ratios which were 4000 Da, 8500 Da, 12500 Da, 27500 Da and 50000 Da. For each molecular weight, four different concentrations which were 1.00×10^{-4} M, 2.00×10^{-4} M, 4.00×10^{-4} M and 6.00×10^{-4} M were prepared.

These water soluble hyperbranched polymers were used to solubilise several hydrophobic molecules. The molecules used were naphthalene, tetracarboxyphenyl porphyrin, ibuprofen and anti-prion drug. The results clearly demonstrated that hyperbranched polymers are capable of solubilising hydrophobic molecules. For a lower concentration of polymers, solubility increased linearly with the concentration of hydrophobic molecules. However, at a higher polymer concentration, the concentration of hydrophobic molecules plateaued. This was due to the aggregation of the polymers. When this occurred, only a small number of guest molecules were able to diffuse inside the cavity of the hyperbranched polymer. It was concluded that the optimum concentration of model drugs (naphthalene and TCPP) and drug (ibuprofen) used was in the range of 2.00×10^{-4} M and 4.00×10^{-4} M. The highest polymer molecular weight which give optimum effect of solubilisation is 12500 Da. The final hydrophobic molecule used was anti-prion drug which was insoluble in water. The results showed

that the hyperbranched polymers increased the solubility of the drug. A cytotoxicity test showed that the hyperbranched polymers were not toxic to the SMB cell.

In order to make the hyperbranched polymers suitable for targeting specific sites, we conjugated folic acid at the surface of the hyperbranched polymers through PEG as the spacer. After a lot of discussion and experimentation, several steps were developed to produce hyperbranched polymers conjugated with folic acid through poly(ethylene) glycol as the spacer:

- Step 1 – synthesis of polyglycidol succinic anhydride (PG-SA)
- Step 2 – synthesis of folic acid ester (FA-NHS)
- Step 3 – synthesis of folate-poly(ethylene glycol) bis amine (Folate-PEG-NH₂)
- Step 4 – synthesis of polyglycidol-folate-poly(ethylene glycol) (PG-Folate-PEG)

The first step was to convert the OH surface of the PG functional group to a carboxylate group (PG-SA). The second step was preparation of the folic acid ester (FA-NHS) followed by conjugation of the PEG spacer (Folate-PEG). The final step was conjugation of PG-SA with Folate-PEG to produce PG-PEG-Folate. The macromolecule is suitable for targeted cancer treatment.

Dendrimers are unique synthetic macromolecules that have attracted much attention as drug delivery systems. We therefore made a comparison between dendrimers and hyperbranched polymers as solubilising enhancers for hydrophobic molecules. Different generations (G0.5 to G2.5) of PAMAM dendrimers were synthesised using two iterative steps, i.e. Michael addition and amidation. For dendrimers that underwent the Michael addition reaction, ester-terminated PAMAM dendrimers were produced. The amidation reaction produced amine-terminated PAMAM dendrimers.

In order to make these dendrimers suitable for drug delivery, the G2.5 amine-terminated PAMAM dendrimers were converted to hydroxyl-terminated PAMAM dendrimers. This was achieved by introducing TRIS to the dendrimers, and each ester terminal group was converted to three hydroxyl groups at the surface of the PAMAM dendrimers.

These water-soluble PAMAM dendrimers then underwent an encapsulation study with ibuprofen and TCPP. The results clearly demonstrated that the dendrimers easily increased the solubility of both molecules. The dendrimer shown to aggregate at the concentration of 1.5×10^{-4} M. We then compared the solubility enhancement behaviour of hyperbranched polymers and dendrimers. For this investigation, we used a similar molecular weight of 4000 Da for both polymers. The result showed for both polymers, the drug molecule concentration increased and plateaued at a higher polymer concentration. From the result, it was demonstrated that hyperbranched polymers have more solubilisation effect than dendrimers for both ibuprofen and tetracarboxyphenyl prophyrin.

For future works, further investigation should be carried out including drug release study, toxicity test, particle size analysis and degradation studies.

Chapter 7: Experimental

7.1 General Description of Chemicals and Instrumentation

Solvents and reagents

All chemicals and reagents were obtained from commercial supplier (Sigma Aldrich, BDH Chemicals) and freshly used.

Nuclear magnetic resonance spectroscopy (NMR)

All sample were characterized via ^1H and ^{13}C NMR which was recorded at 250 MHz and 63 MHz on a Bruker AC and were referenced internally to residual proton signals of the deuterated solvent. The spectra were analysed using Bruker 1D Win-NMR, version 6.2.0.0.

Fourier transform infrared spectroscopy (FTIR)

FTIR spectroscopy was performed using Perkin Elmer Spectrum RX FT-IR System in the range of 700 to 4000 cm^{-1} .

Gel permeation column (GPC)

Aqueous GPC data was performed using Millipore Waters Lambda-Max 481 LC spectrometer with a LMW/HMW column. The eluent used was $\text{NaNO}_3/\text{NaH}_2\text{PO}_4$ at pH 7. Calibration was done using polyethylene glycol-polyethylene oxide standards (Mn 220-1, 1,000,000 Da). The molecular weights were reported relative to these standard. Raw data obtained was further analysed using cirrus GPC online software.

UV-vis spectroscopy

The absorbance was recorded using Specord S 600 machine and analysed using WINASPECT spectroanalytical software.

Mass spectroscopy

Two types of equipment used to determined the mass, depending on the molecular weight of sample. Lower molecular weight (2-800 Da), Electrospray Ion Mass Spectrometry (ESI) was used and recorded using Micromass Prospec spectrometer. Molecular weight of more than 800 Da, Matrix Assisted Laser Desorption Ionisation Time of flight (MALDI-TOF) spectrometry was used. The experiment was done using dithranol or dihydroxy benzoic acid matrices on Bruker III mass spectrometer.

7.2 Synthesis of hyperbranched polymers

General synthesis of hyperbranched polymers

All chemical used were purchased from Sigma-Aldrich UK and used as received. Polymerization was carried out in three neck round bottom flask equipped with mechanical stirrer and fitted with a condenser under nitrogen atmosphere. Para-nitrophenol was dissolved in certain amount of diethylene glycol dimethyl ether at 50 °C. After all core was dissolved, the temperature was increased to 90 °C and NaH was added. Various amount of glycidol was added using mechanical pump for 12 hours and then left for further 5 hours. Then, the reaction was allowed to cool at room temperature and the solvent was poured off. The product which was a brown polymer, was dissolved in methanol and then precipitated in 400 ml of acetone. The mixture was left for an hour and the solvent was disposed. This method was repeat twice.

Synthesis of polyglycerol using 1:5 ratio

The general scheme above was used to synthesise the polymer. *p*-nitrophenol (200.00 mg, 1.44 mmol), diethylene glycol dimethyl ether (20 ml), sodium hydride (11.52 mg, 0.48 mmol) and glycidol (530.00 mg, 7.19 mmol). The product (200.25 mg, 31% by mass) was brownish viscous polymer and dried in vacuum oven overnight.

^1H NMR (D_2O , 250 MHz) $\delta_{\text{H}} = 3.35\text{-}4.56$ (b, polymer backbone), 2.16 (s, OH), ^{13}C NMR (D_2O 250 MHz) $\delta_{\text{H}} = 62.4, 70.8, 78.3$; FTIR (cm^{-1}) 3362 (OH), 2891 (CH_2 , CH); GPC (Mn) 4000, (Mw) 7200, PD = 1.8

Synthesis of polyglycidol using a 1:10 ratio

The general scheme above was used to synthesise the polymer. The reaction used para-nitrophenol (210.00 mg, 1.44 mmol), diethylene glycol dimethyl ether (20 ml), sodium hydride (11.52 mg, 7.00 mmol), glycidol (1.18 g, 15.10 mmol). The product (400.20 mg, 30 % by mass) was brownish viscous polymer and dried in vacuum oven overnight.

^1H NMR (D_2O , 250 MHz) $\delta_{\text{H}} = 3.3\text{-}4.0$ (b, polymer backbone), 2.22 (s, OH), ^{13}C NMR (D_2O , 250 MHz) $\delta_{\text{H}} = 62.3, 70.9, 78.6$; FTIR (cm^{-1}) 3361 (OH), 2870 (CH_2 , CH); GPC (Mn) 8500, (Mw) 17000, PD = 2.0

Synthesis of polyglycidol using a 1:25 ratio

The general scheme above was used to synthesise the polymer. The reaction used para-nitrophenol (200.00 mg, 1.44 mmol), diethylene glycol dimethyl ether (20 ml), sodium hydride (11.52 mg, 0.48 mmol), glycidol (2.66 g, 35.97 mmol). The product (400.35 mg, 15% by mass) was brownish viscous polymer and dried in vacuum oven overnight.

^1H NMR (D_2O , 250 MHz) $\delta_{\text{H}} = 3.39\text{-}4.28$ (b, polymer backbone), 2.19 (s, OH), ^{13}C NMR (D_2O , 250 MHz) $\delta_{\text{H}} = 63.2, 71.2, 79.2$; FTIR (cm^{-1}) 3366 (OH), 2868 (CH_2 , CH); GPC (Mn) 12500, (Mw) 28750, PD = 2.3

Synthesis of polyglycidol using a 1:50 ratio

The general scheme above was used to synthesise the polymer. The reaction used para-nitrophenol (200.00 mg, 1.44 mmol), diethylene glycol dimethyl ether (20 ml), sodium hydride (11.52 mg, 7 mmol), glycidol (5.52 g, 74.62 mmol). The product (500.36 mg, 9 % by mass) was brownish viscous polymer and dried in vacuum oven overnight.

^1H NMR (D_2O , 250MHz) $\delta_{\text{H}} = 3.32\text{-}4.15$ (b, polymer backbone), 2.19 (s, OH), ^{13}C NMR (D_2O , 250MHz) $\delta_{\text{H}} = 62.3, 70.6, 78.9$; FTIR (cm^{-1}) 3361 (OH), 2860 (CH_2 , CH); GPC (Mn) 27500, (Mw) 96250, PD = 3.5

Synthesis of polyglycidol using a 1:100 ratio

The general scheme above was used to synthesise the polymer. The reaction used para-nitrophenol (210.00 mg, 1.44 mmol), diethylene glycol dimethyl ether (20 ml), sodium hydride (11.52 mg, 7 mmol), glycidol (11.18 g, 151.08 mmol). The product (500.36 mg, 4 % by mass) was brownish viscous polymer and dried in vacuum oven overnight.

^1H NMR (D_2O , 250 MHz) $\delta_{\text{H}} = 3.33\text{-}4.23$ (b, polymer backbone), 2.15 (s, OH), ^{13}C NMR (D_2O , 250 MHz) $\delta_{\text{H}} = 62.5, 71.3, 78.5$; FTIR (cm^{-1}) 3365 (OH), 2860 (CH_2 , CH); GPC (Mn) 50000 (Mw) 300000, PD = 6.0

Synthesis of tetracarboxyphenyl porphyrin (TCPP)

The synthesis was done by mixing propionic acid (250 ml) and 4-carboxybenzaldehyde (8.25 g, 54.95 mmol) in a three neck round bottom flask fitted with a condenser. The reaction mixture was heated until reflux and pyrrole (3.70 ml, 55.14 mmol) was added to the reaction via syringe. Refluxing was continued approximately for 1 hour with stirring. The product was separated from the reaction by hot filtration and washed with dichloromethane. TCPP obtained was washed with cold methanol and the solid purple filtrate was collected and dried under vacuum. Yield : 4.00 g; 2%) ^1H NMR (DMSO, 250 MHz), δ_{H} 13.32 (s, 4H, COOH), 8.86 (s, 8H, pyrrolic- β -CH), 8.23 (q, 16H, phenylic CH), -2.95 (s, 2H, NH), ^{13}C NMR (DMSO, 250 MHz) δ 167.4, 127.9, 40.1, 39.8, 39.4, 39.1, 38.8, 38.5., FTIR ν_{max} (cm^{-1}): 2626, 2725, 1683, 1602, 1463, 1377, UV/vis (MeOH) λ_{max} : 418.0, 515.0, 547.5, MH^+ (ESI-MS) = 791 (calculated 791 g mol^{-1}), $\text{C}_{48}\text{H}_{30}\text{N}_4\text{O}_8$, Elemental analysis, C: 67.69%, H: 4.27%, N: 5.52%, O: 22.52% (calculated C: 72.9%, H: 3.82%, N: 7.09%, O:16.19%)

Beer-Lambert experiment for naphthalene, ibuprofen and tetracarboxyphenyl porphyrin

10.00 mg of each compound was dissolved in methanol (1 L). The absorbance of all samples were measured using UV spectrophotometer at their characteristic wavelength (naphthalene: 219 nm, ibuprofen: 222 nm, TCPP: 415 nm) with methanol as reference. Further dilution was made up using a 100 ml volumetric flask. 10 ml of stock solution was taken out and the flask was filled to the mark with methanol and swirled to mix.

These steps were repeated a few times until a graph indicating absorbance versus concentration could be plotted.

Beer-Lambert of anti-prion drug

The above experiment was conducted by dissolving 10.00 mg of the drug and dissolved in 1L methanol. The absorbance was recorded at 325 nm was measured using UV-Vis spectrophotometer with methanol as reference. Further dilutions were conducted using 100 ml volumetric flask. The steps were repeated a few times until a graph indicating absorbance versus concentration could be plotted.

7.2.1 General procedures for encapsulation studies

Preparation of four different concentration from different molecular weights

Four different concentration ie 1.00, 2.00, 4.00 and 6.00 ($\times 10^{-4}$) M of hyperbranched polymers were prepared.

Molecular weight of 4000

4.00 mg, 8.00 mg, 16.00 mg and 24.00 mg of the polymer was dissolved in 10 ml of methanol to make of the above concentrations.

Molecular weight of 8500

8.50 mg, 17.00 mg, 34.00 mg and 60.00 mg of the polymer was dissolved in 10 ml of methanol to make the above concentrations.

Molecular weight of 12500

12.50 mg, 24.00 mg, 50.00 mg and 75.00 mg of the polymer was dissolved in 10 ml of methanol to make the above concentrations.

Molecular weight of 27500

27.50 mg, 55.00 mg, 110.00 mg and 165.00 mg of the polymer was dissolved in 10 ml of methanol to make the above concentrations.

Molecular weight of 50000

50.00 mg, 100.00 mg, 200.00 mg and 300.00 mg of the polymer was dissolved in 10 ml of methanol to make the above concentrations.

Preparation of 0.01M buffer solution

12.1 g of tris(hydroxymethyl) aminomethane was dissolved in 1 L of deionised water to make the concentration of 0.1 M

Encapsulation of naphthalene with hyperbranched polymers

100.00 mg of naphthalene, was dissolved in 10 ml of methanol in a vial. The solution was added to each polymer solution prepared. The solution was physically mixed for 5 minutes and the solvent was removed under vacuo. Then, 10 ml of buffer solution was added to the sample. The sample was repeated at least two times. The absorbance of all samples were recorded at their characteristic wavelengths.

Encapsulation of ibuprofen with hyperbranched polymers

100.00 mg of ibuprofen, was dissolved in 10 ml of methanol in a vial. The solution was added to each polymer solution prepared. The solution was physically mixed for 5 minutes and the solvent was removed under vacuo. Then, 10 ml of buffer solution was added to the sample. The sample was repeated at least two times. The absorbance of all samples were recorded at their characteristic wavelengths.

Encapsulation of TCPP with hyperbranched polymers

100.00 mg of TCPP, was dissolved in 10 ml of methanol in a vial. The solution was added to each polymer solution prepared. The solution was physically mixed and the solvent was removed under vacuo. Then, 10 ml of buffer solution was added to the sample. The sample was repeated at least two times. The absorbance of all samples were recorded at their characteristic wavelengths.

Encapsulation of anti-prion drug with hyperbranched polymers

10.00 mg of hyperbranched polymer and 5.00 mg of anti-prion drug were dissolved in 10 ml of methanol in different vial. Both solutions were added together and physically mixed for 5 minutes and the solvent was removed under vacuo. Then, 10 ml of distilled water was added to the sample. The absorbance was recorded at its characteristic wavelength.

7.2.2 Cytotoxicity Studies

Cytotoxicity evaluation for hyperbranched polymer and encapsulated anti-prion drug with hyperbranched polymer

Cytotoxicity study of hyperbranched polymer with four different molecular weight ie 4000 Da, 8500 Da, 12500 Da and 50000 Da was conducted against SMB cell line using MTT assay. The SMB cells were grown in medium 199 Eagle salts supplemented with 10% newborn calf serum, 5% foetal calf serum and 5% penicillin-streptomycin at 10ml/L and allowed to grow for 24 hours at 37°C under 5% CO₂ in air and 95% humidity. Different concentrations of hyperbranched polymers ie 100 µM, 500 µM and 1000 µM were added to the cell and incubated for 5 days at 37°C. For the measurement of cell viability, 10 µl of 5 mg/ml of MTT solution was added into 96 well plates for 2 hours at 37 °C . After treatment, the medium was removed and 30 µL of acidic

isopropanol was added to each well to extract the formazan dye out from the cell wall, which produced a purple colour. The absorbance of the dye was measured at its characteristic wavelength at 570 nm with reference at 690 nm.

7.3 Functionalisation of hyperbranched polymer with folic acid and PEG spacer

Synthesis of polyglycidol-succinic acid (PG-SA)

To a two neck round bottom flask was added PG (500.00 mg, 0.12 mmol) and dissolved in dry methanol (75 ml). After all PG was dissolved, succinic anhydride (1.58 g, 15.78 mmol) was added and the flask was evacuated and filled with nitrogen gas. The mixture was refluxed for 48 hours at 125 °C, using a drying tube. Then, the solution was removed in half and the remained, was precipitated in acetone (400 ml). This step was repeated three times and the precipitated was filtered and dried in vacuum oven overnight. The product was viscous dark yellow solid. Yield=1.00 g, 48%. ¹H NMR (D₂O, 250 Mhz): δ_H = 8.25 (s, 2H, nitrophenol), 7.25 (s, 2H, nitrophenol), 4.33 – 3.21 (b, polymer backbone), 2.54 (s, 16H, succinic acid, CH₂). ¹³C NMR (D₂O, 250 Mhz): δ_c = 177.4, 174.5, 79.4, 68.8, 60.7, 29.0, GPC (aqueous) : Mn = 1714

Synthesis of folic acid ester (FA-NHS)

Folic acid (1.00 g, 2.26 mmol) was dissolved in 10 ml of dry DMSO and was activated by 1,3-dicyclohexylcarbodiimide (DCC) (500.00 mg, 2.42 mmol) for two hours at room temperature. N-hydroxysuccinimide (300.00 mg, 2.60 mmol) was dissolved separately in 2 ml dry DMSO and was added to the solution above. The mixture was stirred in light protected container for 24 hours at room temperature under nitrogen environment. After 24 hours, the solution was filtered and the filtrate solvent was concentrated by half using vacuum distillation at 40 °C. The solution was precipitated in the mixture of acetone : diethyl ether (30 : 70 v/v ratio) and followed by filtration. The precipitate was washed with 100 ml of mixture of acetone : diethyl ether (30 : 70 v/v ratio) and diethyl ether (3 x 100 ml) and vacuum dried overnight. The product was solid yellow powder (1.00 g, 60%). ¹H NMR (DMSO, 250 Mhz): δ_H = 11.52 (broad, 1H, COOH), 8.65 (d, *J*=8.00, 1H, CH), 8.16 (d, *J*=8.00, 1H, NH), 7.67 (t, *J*= 8.00, 1H, CH), 6.97 (t, *J* = 8.00, 1H, NH), 6.66 (t, *J*= 8.00, 1H, CH), 4.85 (m, 2H, NH₂), 4.53 (s, 1H, CH), 2.81 (m, 4H, NHS hydrogen), 2.34 (m, 2H, CH₂), 2.11 (m, 2H, CH₂). ¹³C NMR (DMSO, 250 Mhz): δ_c = 174.4, 173.2, 154.2, 128.4, 121.7, 52.2, 40.1, 39.3, 30.8, 26.4. MH⁺ (ESI-MS) = 539 (calculated 538 gmol⁻¹), C₂₃H₂₂N₈O₈, Elemental analysis, C: 51.78%, H: 5.10 %, N:19.20%, O: 23.92% (calculated C: 51.30%, H: 4.12%, N: 20.81%, O:23.77%)

Synthesis of folate-polyethylene glycol bis amine (Folate-PEG-NH₂)

Polyethylene glycol bis amine (300.00 mg, 0.10 mmol) was dissolved in 5 ml dry DMF. Folic acid ester (100.00 mg, 0.18 mmol) was dissolved in 2 ml dry DMF separately and

was added to the above solution. Then, diisopropyl ethylamine (100.00 mg, 0.77 mmol) was added and the mixture was stirred at room temperature for 24 hours under nitrogen condition. The volume of the solution was reduced using vacuum distillation and was precipitated with diethyl ether. The precipitated was washed with diethyl ether for three times and dried under vacuum. The product obtained was solid yellow powder. (0.15 g, 30%). ^1H NMR (DMSO, 250Mhz): $\delta_{\text{H}} = 8.67$ (s, 1H), 7.63 (d, 2H), 6.67 (d, 2H), 3.52 (PEG), ^{13}C NMR (DMSO, 250 Mhz): $\delta_{\text{C}} 175.2, 173.3, 70.2$, MALDI –TOF MS : 3151

Synthesis of polyglycidol-folate-polyethylene glycol (PG- Folate-PEG)

PG-SA (100.00 mg, 0.05 mmol) was dissolved in 3 ml dry DMSO and was activated by dicyclohexylcarbodiimide (DCC)(150.00 mg, 0.072 mmol) in dry DMSO (3 ml) in the presence of pyridine (5.8 μl , 0.072 mmol). Then folate-PEG-NH₂ (300.00 mg, 0.08 mmol) was dissolved in 3 ml dry DMSO and was added to the above solution. The reaction was stirred overnight at room temperature in N₂ atmosphere. After the reaction complete, the solvent was evaporated and distilled water added to the sample. The remaining yellow solution was freeze dried overnight. The product was pale yellow solid (150.00 mg, 27%). ^1H NMR (DMSO, 250Mhz): $\delta_{\text{H}} = 8.70$ (s, 1H), 7.55 (s, 1H), 6.69 (s, 1H), 4.69 (s, 2H), 4.96 – 3.24 (polyglycidol backbone), 2.63 (s, 4H), 1.65 (broad, 2H), 1.20 (broad, 3H). ^{13}C NMR (DMSO, 250 Mhz): $\delta_{\text{C}} 175.3, 173.8, 72.1, 69.5, 62.54$, GPC (Mn) 2151

7.4 Comparison between PAMAM dendrimer and hyperbranched polymer

Synthesis of G0.5 PAMAM dendrimer holding 4 methyl ester terminal groups

Methyl acrylate (25.1g, 0.29 mol) was added dropwise for 30 minutes to a solution of EDA (2.56 g, 43.00 mmol) dissolved in methanol (20 ml) at 0 °C in a 500 ml round bottom flask. The reaction was stirred overnight at room temperature. Excess methyl acrylate was removed in vacuo and placed under high vacuum for a few hours. The product was yellow honey oil (13.5g, 48%). ^1H NMR (MeOD, 250 Mhz): $\delta_{\text{H}} = 3.68$ (s, 12H, CH_3), 2.76 (t, 8H, $\text{NCH}_2\text{CH}_2\text{C}=\text{O}$), 2.54 (s, 4H, $\text{NCH}_2\text{CH}_2\text{N}$), 2.49 (t, 8H, $\text{OC}=\text{OCH}_2$). ^{13}C NMR (MeOD, 250 Mhz): 171.8, 47.1, 32.2, FTIR λ_{max} : 3283 (amide, NH), 2974 (CH-sp²), 1730 (ester carbonyl), 1640 (amide carbonyl), 1534 (amide NH bend), 1464 (CH₂ bend) cm^{-1} . MALDI –TOF MS : 405

Synthesis of G1.0 PAMAM dendrimer holding 4 amine terminal groups

The ester intermediate PAMAM G0.5 dendrimer (6.70 g, 17.00 mol) was dissolved in methanol (50 ml) and added dropwise to EDA (48.90 g, 0.82 mol), in a round bottom flask (500 ml) at 0 °C. The reaction was kept stirring for 5 days. Purification was done using 9:1 (toluene : methanol) azeotropic solution and followed by washing with methanol. The mixture was then underwent rotary evaporation and placed under high vacuum. The product was a viscous yellow/brown oil (5 g, 8.99%). ^1H NMR (MeOD, 250 Mhz): $\delta_{\text{H}} = 4.93$ (s, 4H, NH), 3.69(s, 8H, NH_2), 3.33-3.27 (mm, 16H, H_2NCH_2 +

CH₂NH), 2.81-2.41 (m, 20H, C=OCH₂CH₂ + NCH₂CH₂N). ¹³C NMR (MeOD, 250 Mhz): 173.7, 51.0, 49.9, 48.2, 38.1, 33.3, FTIR λ_{max}: 3280 (amide, NH), 2987 (CH), 1634 (amide carbonyl), 1544 (amide NH bend), 1438 (CH₂ bend) cm⁻¹. MALDI –TOF MS : 517(MH⁺)

Synthesis of G1.5 PAMAM dendrimer holding 8 methyl ester terminal groups

The diamine intermediate PAMAM G1.0 dendrimer (2.50 g, 4.80 mol), was dissolved in methanol (50 ml) and placed into round bottom flask (500 ml). Methyl acrylate (7.30 g, 85.00 mmol), was added drop wise to the solution for 30 minutes at 0 °C. The solution was left stirring for 24 hours at room temperature. Excess methyl acrylate was removed via rotary evaporator. The solution was then placed under high vacuum for a few days to remove traces of reagent yielding 3.20 g, (72 %). ¹H NMR (MeOD, 250 Mhz): δ_H = 4.91 (s, 4H, NH), 3.69 (s, 24H, CH₃), 3.39-3.21(m, 24H, NHCH₂ + NHCH₂CH₂CHNCH₂), 2.87-2.35 (mm, 44H, NCH₂CH₂N + NCH₂CH₂C=ONH + NHCH₂CH₂N + CH₃OC=OCH₂). ¹³C NMR (MeOD, 250 Mhz): 173.3, 173.2, 52.4, 50.7, 49.8, 49.1, 37.1, 32.2, 31.9, FTIR λ_{max}: 3231 (amide, NH), 2952 (CH), 1640 (amide carbonyl), 1592 (amide NH bend), 1431 (CH₂ bend) cm⁻¹. MALDI –TOF MS : 1430(MH⁺)

Synthesis of G2.0 PAMAM dendrimer holding 8 amine terminal groups

EDA (51.20 g, 0.85 mol), was added dropwise to a stirred solution of the ester terminated intermediate produced from previous step (6.60 g, 5.50 mmol) in methanol (30 ml) at 0 °C. The reaction was stirred for 7 days. The solution was then washed with azeotropic mixture of 9:1 toluene: methanol for excess EDA removal. The left over solvent was then removed under vacuo. The product was yellow honey/brown viscous oil (7.10 g, 90 %). ¹H NMR (MeOD, 250 Mhz): δ_H = 4.92 (s, 4H, NH), 3.65(s, 8H, NH₂), 3.40-3.20 (m, 24H, NHCH₂CH₂N + NH₂CH₂CH₂NH), 2.89-2.26 (mm, 76H, NH₂CH₂CH₂NH + NCH₂CH₂C=O + NCH₂CH₂NH + NCH₂CH₂N). ¹³C NMR (MeOD, 250 Mhz): 172.3, 50.7, 48.3, 46.1, 40.2, 35.8, 32.0, 31.8, FTIR λ_{max}: 3280. (amide, NH), 2987 (CH), 1634 (amide carbonyl), 1544 (amide NH bend), 1438 (CH₂ bend) cm⁻¹. MALDI –TOF MS : 517(MH⁺)

Synthesis of G2.5 PAMAM dendrimer holding 16 methyl ester terminal groups

The generation 2.0 amine terminated PAMAM dendrimer (1.25 g, 0.87 mmol) was dissolved in 30 ml methanol and methyl acrylate (2.80 g, 0.03 mol) was added dropwise for at least 30 minutes in ice bath (0 °C) and stirred for two days at room temperature. The solvent and methyl acrylate were removed under vacuo and then put in high vacuum for a few days. The product was honey yellow viscous oil (1.8 g, 73.5%). ¹H NMR (MeOD, 250 Mhz): δ_H = 3.68 (s, 48H, CH₃), 3.37 (m, 12H, NHCH₂CH₂N), 2.93-2.33 (mm, 152H, OC=OCH₂CH₂N + NCH₂CH₂NH + NHC=OCH₂CH₂N + NCH₂CH₂N). ¹³C NMR (MeOD, 250 Mhz): 173.2, 173.3, 52.4, 50.8, 49.1, 48.3, 37.2, 33.1, 32.2, FTIR λ_{max}: 3283 (amide, NH), 2974 (CH-sp²), 1730 (ester carbonyl), 1640 (amide carbonyl), 1534 (amide NH bend), 1464 (CH₂ bend) cm⁻¹. MALDI –TOF MS : 3242(MH⁺)

Synthesis of PAMAM dendrimer with 48 hydroxyl terminal group

The PAMAM dendrimer with generation 2.5 (1.00 g, 0.37 mmol) was dissolved in dry DMSO (5 ml) and this solution was added to a stirred suspension of tris(hydroxymethyl) aminomethane (750.00 mg, 6.05 mmol) and anhydrous potassium carbonate (850 mg, 6.05 mmol), in dry DMSO (15 ml). The solution was stirred for 72 hours at 50 °C under nitrogen environment. The solution was filtered and the solvent was removed by half using vacuum distillation at 40 °C. The viscous yellow oil was dissolved in small amount of water, followed by precipitation using acetone. These step was repeated three times before the product was dried overnight in vacuum oven. The final product was pale yellow oil. (1.3g, 60%). ¹H NMR (D₂O, 250 Mhz): δH = 3.64 (s, 96H, CH₂OH), 2.21 – 3.26 (164H, broad series of multiplets, remaining CH₂). ¹³C NMR (D₂O, 250 Mhz): 175.4, 174.4, 62.0, 60.5, 51.8, 48.8, 38.4, 37.1, 33.1, FTIR λ_{max}: 3303 (broad, OH), 1657 (amide carbonyl) cm⁻¹. MALDI –TOF MS :4130.

Encapsulation of PAMAM dendrimer with 48 hydroxyl terminal group with TCPP and ibuprofen

PAMAM dendrimer with 48 OH hydroxyl terminal group (10.00 mg, 0.002 mmol) was dissolved in methanol (10 ml). Access TCPP and ibuprofen was dissolved separately in methanol (10 ml). After all polymer dissolved, both drugs were added and physically mixed for 5 minutes. All solvent was removed under vacuo and buffer solution was added (10 ml). The solution was filtered and UV measurement was conducted. λ_{max} for TCPP = 415nm and ibuprofen = 222 nm

Chapter 8: References

1. W. D. Callister Jr, *Materials Science and Engineering: An Introduction*, 5th Ed, John Wiley, **2000**, pg 30.
2. Qiu L. Y.; Bae Y. H. *Pharm. Res.*, **2006**, 23,1-30.
3. Pushkar S.; Philip A.; Pathak K.; Pathak D., *Indian J. Pharm. Educ. Res.*, **2006**, 40 (3), 153-158.
4. Muhammad I.; Mathies S., *Ind. Eng. Chem. Res.*, **2010**, 49,1169-1196.
5. Pete G.; PhD Thesis, University of Sheffield, 200.
6. Turk H.; Shukla A.; Paula C. A. R.; Rehage H.; Haag R., *Chem. Eur. J.*, **2007**, 13, 4187-4196.
7. Voit B., *J. Polym. Sci. Part A: Polym. Chem.*, **2005**, 43, 2679-2699.
8. Voit B., *C.R. Chemie*, **2003**, 6, 821-832.
9. Haag R.; Stumbe J. F.; Sunder A.; Frey H.; Hebel A., *Macromolecules*, **2000**, 33, 8158-8166.
10. Indah N. K.; Ling H.; Jurgen P. R.; Haag R., *Macromol. Rapid Commun.*, **2010**, 31, 1516-1520.
11. Sunder A.; Michael K., Hanselmann R.; Mulhaupt R.; Frey H., *Angew. Chem. Ind. Ed.*, **1999**, 38, 3552-3555.
12. Egon B.; Winfried W.; Vögtle F. *Synthesis* **1978** (2): 155–158
13. Newkome G. R.; Yao Z.; Baker G. R.; Gupta V. K., *J. Org. Chem.* **1985**, 50, 2003-4.
14. Tomalia D. A.; H. Baker, Dewald J.; Hall M.; Kallos G.; Martin S.; Roeck J.; Ryder J.; Smith P.; *Macromolecules* **1986**, 19, 2466-8.
15. Hawker C. J.; Frechet J. M. J., *J. Am. Chem. Soc.* **1990**, 112, 7638-47.
16. T. M. Miller, T. X. Neenan, *Chem. Mater.* **1990**, 2, 346
17. Konkolewicz D.; Monteiro M. J.; Perrier S.; *Macromolecules*, **2011**, 44, 7067-7087.
18. Matthews O. A.; Shipway A. N.; Stoddart J. F., *Prog. Polym. Sci.*, **1998**, 23, 1-56.
19. Miller T. M.; Neenan T. X.; Zayas R.; Bair H. E., *J. Am. Chem. Soc.*, **1992**, 114 (3), 1018–1025.
20. Yates C. R.; Hayes W., *Europ. Polym. J.*, **2004**, 40,1257-1281.
21. Voit B., *Journal of Polymer Science: Part A: Polymer Chemistry*, **2000**, 38, 2505-2525.
22. Jikei M.; Kakimoto M.A., *Prog. Pol. Sci.*, **2001**, 26, 1233.
23. Suzuki M.; Ii A.; Saegusai T., *Macromolecules*, **1992**, 25,7071-7072.
24. Sunder A.; Hanselmann R.; Frey H.; Mulhaupt R., *Macromolecules*, **1999**, 32, 4240-4246.
25. M. Liu, N. Vladimirov, J. M. J. Frechet, *Macromolecules* **1999**, 32, 6881-6884

26. Schappacher M.; Deffieux A.; Putaux J. L.; Viville P.; Lazzaroni R., *Macromolecules*, **2003**, *36*, 5776-5783.
27. Hoste K.; Winne K. D.; Schacht E., *Int. J. Pharm.*, **2004**, *277*, 119–131.
28. Roßler A.; Vandermeulen G. W. M.; Klok H., *Adv. Drug Deliv. Rev.*, **2001**, *53*, 95–108.
29. Brigger I.; Catherine D.; Couvreur P., *Adv. Drug Deliv. Rev.*, **2002**, *54*, 631–651
30. Panyam J.; Labhasetwar V., *Adv. Drug Deliv. Rev.*, **2003**, *55*, 329–347.
31. Haag R.; Kratz F.; *Ang. Chem. Int.*, **2006**, *45*, 1198-1215.
32. Maeda H., *Adv. Drug Deliv. Rev.*, **1991**, *6*, 181-202.
33. Nori A., Kopec̣ek J., *Adv. Drug Deliv. Rev.*, **2005**, *57*, 609– 636.
34. Liggins R.T.; Burt H.M.; *Adv. Drug Deliv. Rev.*, **2002**, *54*, 191-202.
35. Kumar N.; Ravikumar M. N.V.; Domb A.J., *Adv. Drug Deliv. Rev.*, **2001**, *53*, 23-44.
36. Pechar M.; Ulbrich K.; Ubr V.; Seymour L. W.; Schacht E. H., *Bioconj. Chem.*, **2000**, *11*, 131-139.
37. Svenson S., *Eur. J. Phar. Biopharm.*, **2009**, *71*, 445-462.
38. Wolinsky J. B.; Grinstaff M. W., *Adv. Drug Deliv. Rev.*, **2008**, *60*, 1037-1055.
39. Gudag S.; Khandare J.; Staples S.; Matherly L. H.; Kannan R.M., *Bioconj Chem.*, **2006**, *17*(2), 275-283.
40. Grayson S. M.; Godbey W.T.; *J. Drug. Target.*, **2008**, *16*, 329.
41. Jevprasesphant R.; Jalal R.J.; Attwood D.; Penny J.; McKeown N.B.; D'Emanuele A., *Int J Pharm* **2003**, *252*, 263-266.
42. Jang W. D.; Selim K.M. K.; Lee C. H.; Kang I. K.; *Prog. Polym. Sci.*, **2002**, *32*, 1-23.
43. Malik N.; Wiwattanapatapee R.; Klopsch R., Lorenz K.; Frey H.; Weener J.W., *J. Contr. Rel.*, **2000**, *65*, 133-148.
44. Duncan R.; Izzo L., *Adv. Drug Deliv. Rev.*, **2005**, *57*, 2215-2237..
45. Veronese F.M.; Schiavon O.; Pasut G.; Mendichi R.; Andersson L.; Tsirk A.; Ford J.; Wu G.; Kneller S.; Davies J.; Duncan R.; *Bioconj. Chem.*, **2005**, *15*, 775-784.
46. Sunder A.; Mülhaupt R.; Frey H.; *Macromolecules*, **2000**, *33*, 309–314.
47. Sunder A.; Hanselmann R.; Frey H.; Mülhaupt R., *Macromolecules*, **1999**, *32* (13), 4240–4246.
48. Kubisa P., *J. Polym. Sci. Part A: Polym. Chem.*, **2003**, *41*, 458-468.
49. Malmstruem. E.; Johansson M.; Hult A., *Macromolecules*, **1995**, *28*, 1698-1703.
50. Beezer A.E.; King A.S.H.; Martin I.K., Mitchel J.C.; Twyman L.J.; Wain C.F.; *Tetrahedron*, **2003**, *59*, 3873-3880.
51. Robertson C.A., Hawkins E. D.; Abrahamse H., *J. Photochem. Photobiol.: B. Biol.*, **2009**, *96*, 1-8.
52. Mitton D., Ackroyd R., **2008**, *5*, 103-111.
53. Tian Y.Y.; Wang L.L.; Wang W., *Laser Phys.*, **2008**, *1*, 1119-1123.
54. Juarranz A.; Jaen P.; Sanz-Rodriquez F.; Cueves J.; Gonzales S., *Clin. Transl. Oncol*, **2008**, *10*, 148-154.

55. Kojima C.; Toi Y.; Harada A.; Kono K., *Bioconj. Chem.*, **2007**, *18*, 663-670.
56. Chatterjee D. K.; Fong L. S.; Zhang Y., *Adv. Drug Del. Rev.*, **2008**, *60*, 1627–1637.
57. Nishiyama N.; Jang W. D.; Kataoka K., *New J. Chem.*, **2007**, *31*, 1074–1082.
58. Cl E.; Snyder J. W.; Ogilby P. R.; Gothelf K. V., *Chem. Bio. Chem.*, **2007**, *8*, 475 – 481.
59. Roby A.; Erdogan S.; Torchilin V. P., *Eur. J. Pharm. Biopharm.*, **2006**, *62*, 235–240.
60. Bae Y. H.; Park K.; *J. Controlled Released*, 2011, *153*, 198-205
61. Grobmeyer S.R.; Moudgil B.M., *Cancer Nanotechnology: Methods and Protocol*, Springer Science, 2010, pg. 25-37
62. Iyer A. K.; Khaled G.; Fang J.; Maeda H.; *Drug Disc. Today*, **2006**, *11*, 812-818.
63. Maeda H.; Wu J.; Sawa T.; Matsumura Y.; Hori K., *J. of Control Released*, **2000**, *6*, 271-284.
64. Ermias D. B., *Annu. Rev Microbiol*, **1999**, *53*, 383-314.
65. Ermias D. Belay, Lawrence B. S., *Annu. Rev. Public Health*, **2005**, *26*, 191-212.
66. Collinge J., *Lancet*, **1999**, *354*, 317-323.
67. Mossman T., *J. Immun. Met.* **1983**, *65*, 55-63.
68. Alexander B.; Browse D. J.; Benjamin I.S., *J Pharmacol Toxicol Methods*, **1999**, *41*, 55-58.
69. Hatefi A.; Amsden B., *Pharm. Res.*, **2002**, *19*, 1389-1399.
70. Malik N.; Evagorou E.G.; Duncan R., *Anticancer Drugs*, **1999**, *10*, 767-776.
71. Kojima C.; Kono K.; Maruyama K.; Takagishi T., *Bioconj Chem.*, **2000**, *11*, 910-917.
72. Kamen B. A.; Smith A. K. *Adv. Drug Delivery Rev.* **2004**, *56*, 1085-1097.
73. Yang Y.Y.; Wang Y.; Powell R.; Peggy C., *Clinical and Experimental Pharmacology and Physiology*, **2006**, *33*, 557–562.
74. Kwon T. H.; Sohn M. H.; Kim S.L.; Jeong H. J.; Kim E. M.; Lee C. M.; *Korean Med. Sci.*, **2007**, *22*, 405-11.
75. Jaracz S.; Chen J.; Kuznetsova L. V.; Ojima I., *Bioorg. Med. Chem.*, **2005**, *13*, 5043–5054.
76. Hilgenbrink A. R.; Low P. S., *J. Pharm. Sci.* **2005**, *94*, 2135-2146.
77. Leamon C. P.; Reddy J. A., *Adv. Drug Delivery Rev.*, **2004**, *56*, 1127-1141.
78. Hagner N.; Joerger M., *Cancer Manag Res.*, **2010**, *2*, 293–301.
79. Kukowska-Latallo J. F.; Candido K.A.; Cao Z.; Nigavekar S. S.; Majoros I.J.; Thomas T. P.; Balogh L. P.; Khan M. KB.; Aker J. R. Jr., *Cancer Res*, **2005**, *15*, 5317.
80. Elnakat, H.; Ratnam M., *Adv. Drug Delivery Rev.* **2004**, *56*, 1067-1084.
81. Leamon C. P.; Low P. S., *Drug. Disc. Today*, **2001**, *6*, 44-51.
82. Zheng Y.; Song X.; Darby M.; Liang Y.; He L.; Cai Z.; Chen Q.; Bi Y.; Yang X.; Xu J.; Li Y.; Sun Y.; Lee R. J.; Hou S.; *J. Biotech*, **2010**, *145*, 47-53.
83. Zhang Y.; Sun Y.; Xu X.; Zhang X.; Zhu H.; Huang L.; Qi Y.; Shen Y. M.; *J. Med. Chem.*, **2010**, *53*, 3262-3272.

84. Dhar S.; Liu Z.; Thomale J.; Dai H.; Lippard S. J., *J. of Am. Chem. Soc.*, **2008**, *130*, 11467-11476.
85. Singh P.; Gupta U.; Asthana A.; Jain N. K., *Bioconj. Chem.*, **2008**, *19*, 2239-2252.
86. Pinhassi R.I.; Asssraf Y. G.; Farber S.; Stark M.; Ickowicz D.; Drori S.; Domb A. J.; Liney Y. D., *Biomacromolecules*, **2010**, *11*, 294-303.
87. Aronov O.; Horowitz A. T.; Gabizon A.; Gobson D., *Bioconj Chem.*, **2003**, *14*, 563-574.
88. Anbharasi V.; Cao N.; Feng S. S., *J. of Biomed. Mat. Res.*, **2010**, *94A*, 3, 730-742.
89. Tziveleka L.; Christina K.; Sideratou Z.; Tsiourvas D.; Paleos C. M., *Macrom. Biosci*, **2006**, *6*, 161-169.
90. Yoo H. S.; Park T.G., *J. Controlled. Rel.*, **2004**, *96*, 273-283.
91. Prabakaran M.; Grailer J. J.; Pilla S.; Steeber D. A.; Gong S.; *Biomaterials*, **2009**, *30*, 3009-3019.
92. Chen S.; Zhang X. Z.; Cheng S. X.; Zhuo R. X.; Gu Z. W., *Biomacromolecules*, **2008**, *9*, 2578-2585
93. Kono K.; Liu M.; Fréchet J. M. J., *Bioconj. Chem.*, **1999**, *10*, 1115-1121.
94. Jain K.; Kesharwani P.; Gupta U.; Nain N.K., *Int. J. of Pharm.*, **2010**, *394*, 122-142.
95. M.R. Anupe.; M. K. Rangaramanujam.; D. A. Tomalia., *Drug Discovery Today*, **2010**, *15*, 171-185.
96. Yang K.; Weng L.; Cheng Y.; Zhang H.; Zhang J.; Wu Q.; Xu T., *J. Phy. Chem.*, **2011**, *115*, 2185-2195.,
97. N. K. Jain.; U. Gupta.; *Expert Opin. Drug Metabol. Toxicol.*, **2008**, *4*, 1035-1052
98. Yiyun, C.; Tongwen, X.; Rongqiang, F., *Eur. J. Med. Chem.* **2005**, *40*, 1390-1393.
99. Emmanuele A.; Jevprasesphant R.; Penny R., Atwood. D., *J Controlled Release.*, **2004**, *95*, 447-453.
100. Aulenta F.; Hayes W.; Rannard S., *Eur. Polym. J.*, **2003**, *39*, 1741-1771.
101. Devarakonda B.; Hill R. A.; Villiers M. M., *Int. J. Pharm.*, **2004**, *284*, 133-140.
102. Chauhan A. S.; Sridevi S.; Chalasani K. B.; Jain A. K.; Jain S. K.; N.K Jain,
103. Diwan P. V., *J. Controlled Release*, **2003**, *90*, 335-343.
104. Namazi H.; Adeli M., *Biomaterials*, **2005**, *26*, 1175-118.
105. Kaanumalle L. S.; Nithyanandhan J.; Pattabiraman M.; Jayaraman N.; V. Ramamurthy B., *J. Am. Chem. Soc.*, **2004**, *126*, 8999-9006.
106. Pistolis G.; Malliaris A., *Langmuir*, **2002**, *18*, 246-251
107. Yiyun C.; Tongwen X., *Eur. J. Med. Chem.*, **2005**, *40*, 1188-1192.
108. Hawker C. J.; Wooley K.L.; Frechet. J. J. M., *J. Chem. Soc. Perkin Trans.*, **1993**, *1*, 1287-1295.
109. Liu M.; Kono K.; Frechet J. J. M., *J. Controlled Release*, **2000**, *6*, 121-131.
110. Ooya T.; Lee J.; Park K., *J. Controlled Release*, **2003**, *93*, 121-127.

111. Kojima C.; Kono K.; Maruyama K.; Takagishi T., *Bioconj. Chem.*, **2000**, *11*, 910-917.
112. Sideratuo Z.; Tsiourvas D.; Paleos C. M., *J. Colloid. Inter. Science*, **2001**, *242*, 272-276.
113. Christine D.; Uchegbu I. F.; Shazlein A. G., *Adv. Drug. Deliv. Rev.*, **2005**, *57*, 2177-2202.
114. Perumal O. P.; Inapagolla R.; Sujatha K.; Rangaramanujam M. K., *Biomaterials*, **2008**, *29*, 3469-3476.
115. Chen .T.; Neerman M. F.; Parrish A. R.; Simanek E. E., *J. Am. Chem. Soc.*, **2004**, *126*, 10044–10048.
116. L.J. Twyman, PhD Thesis, Univ. of Kent, 1995.
117. Amy S. H. K.; Martin I. K.; Lance J. T., *Polym. Int.*, **2006**, *55*, 798-807.